



On Large Scales, Universe is Homogeneous & Isotropic

...The Cosmological *prayer*

(c.f. Shepard's prayer)

True / False...?

...What is the Convergence Scale?

TBD...

(...Also a conclusion!)

Hans **Böhringer**, Peter **Schücker** MPE, D

Doug **Burke** CfA, USA

Sarah **Brough** Swinburne, Aus

Chris **Collins**, Phil **James** Liverpool JMU, UK

Bob **Mann** Edinburgh, UK

Marc **Seigar** UC Irvine, USA

1: Reference
Frames/Flows

Outline

2: Frighten you...

- Introduction – gEs, Properties, Traditional Cosmological Test Particles...
- Reference Frames & “Streaming Motions” / “(Bulk) Cosmic Flows”; (R-F); P-P; H-C; GA; LP
- Photometry; X-ray Selection & Coincidence
- cD Halos / ICL?
- Summary/Conclusions

3: Reassure you

4: gEs special(?)

Introduction:

Properties of gEs / BCGs / BCMs /
cDs; Role as Cosmological Test
Particles



Giant Ellipticals

- Highest ranked, large giant/supergiant ellipticals located exclusively in regions of high galaxy density
- “*Cluster Giant Ellipticals (gE)*”
- “*X-ray Centroid Coincident Cluster Giant Ellipticals*”
- “Brightest Cluster Galaxy/Member” (BCG/BCM) *candidates; cD-galaxies...*

STRUCTURE OF BRIGHTEST CLUSTER MEMBERS. II.

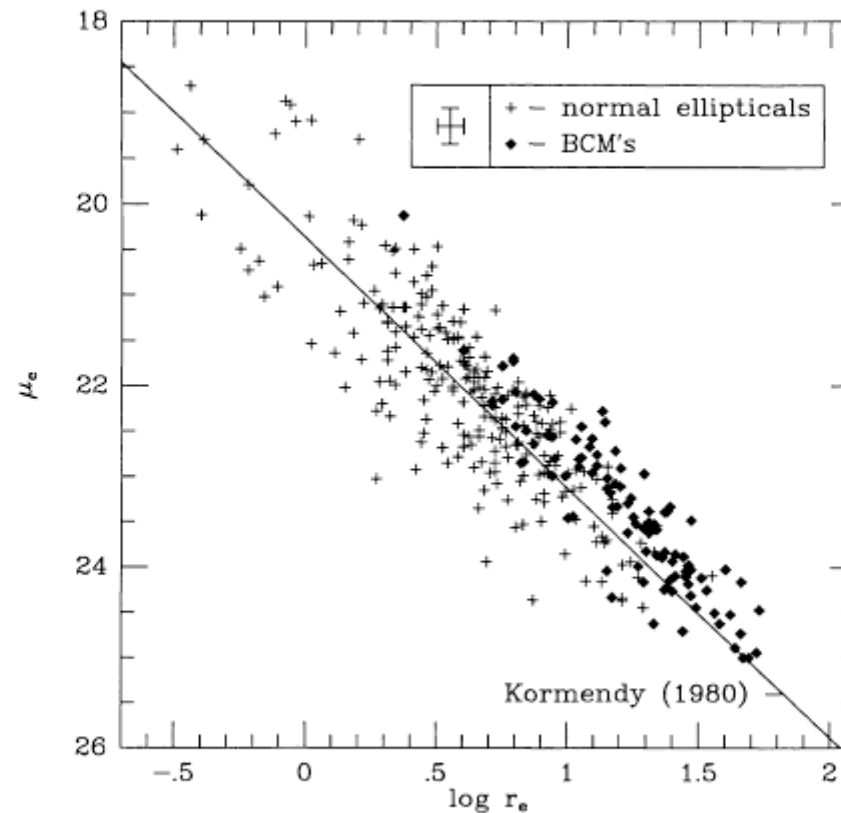


FIG. 4.—Effective surface brightness (μ_e) versus effective radius (r_e) from $r^{1/4}$ fits. The relation for normal ellipticals from Kormendy (1980) is also shown. Enlarged radii for BCMs are evident from the fact that 87% of these objects lie to the right of the relation, whereas the normal ellipticals scatter evenly. A typical error bar is displayed at the top.

the observations from Paper I combined with the results from Malumuth (1983) begin to define a very clear trend of structural parameters which distinguish BCMs from other bright ellipticals of similar luminosities.

The first difference is that BCMs have enlarged characteristic radii when compared with ellipticals of similar luminosity (see Fig. 6, Paper I). This is displayed in Figure 4, where over 87% of the BCMs lie above the relation of Kormendy (1980), yet the normal ellipticals are scattered evenly around this line.

normal ellipticals. In this study, the term “diffuse” is meant to signal the enlarged radii and shallow profile slope producing a large extended galaxy to the eye. There is no distinction between D- and cD-type profiles with respect to profile slope. There is also no apparent correlation between the presence of companions and shallow profiles.

It should be noted that the deviations of BCM structure from that of normal ellipticals is not a luminosity effect of the type used to explain variations in normal elliptical structure

Another interesting result from examination of the N -body merger remnant profiles is that they are to a large extent $r^{1/4}$ in shape. This is not a surprising result, since the simulations of Villumsen (1982) and May and van Albada (1984) also produce merger remnants which are $r^{1/4}$ in shape. This general trend in the profiles from theoretical studies has led many of the above authors to conclude that the $r^{1/4}$ law is a natural density relation that follows from a system which is disrupted and then is allowed to relax. The observations of this paper support this hypothesis, since the dominance of the $r^{1/4}$ relation at the bright end of the sample is quite prominent. The above statement may overgeneralize the evidence of mergers, since several other detailed CCD surface photometry studies (Lauer 1986; Djorgovski 1985) argue against any

which are assumed to form by a process not directly related to mergers. In this diagram there is the suggestion of a break in the trend of brighter galaxies, with larger values of r_e around the $M_V = -21$ point. This break is also at the same point found by Davies *et al.* (1983), where the kinematics of ellipticals change from rotators for the faint ellipticals to being supported by anisotropic velocity distributions. The break was also suggested by the different (L, r) -relations found by Kormendy (1977) and Strom and Strom (1979). Kormendy's sample was concerned with bright ellipticals and hence found a shallower relation than the seven-cluster sample of Strom and Strom, which measured a large number of faint ellipticals. An analysis of bright ellipticals by Romanishin (1986) also found a relation similar to Kormendy's; therefore, the

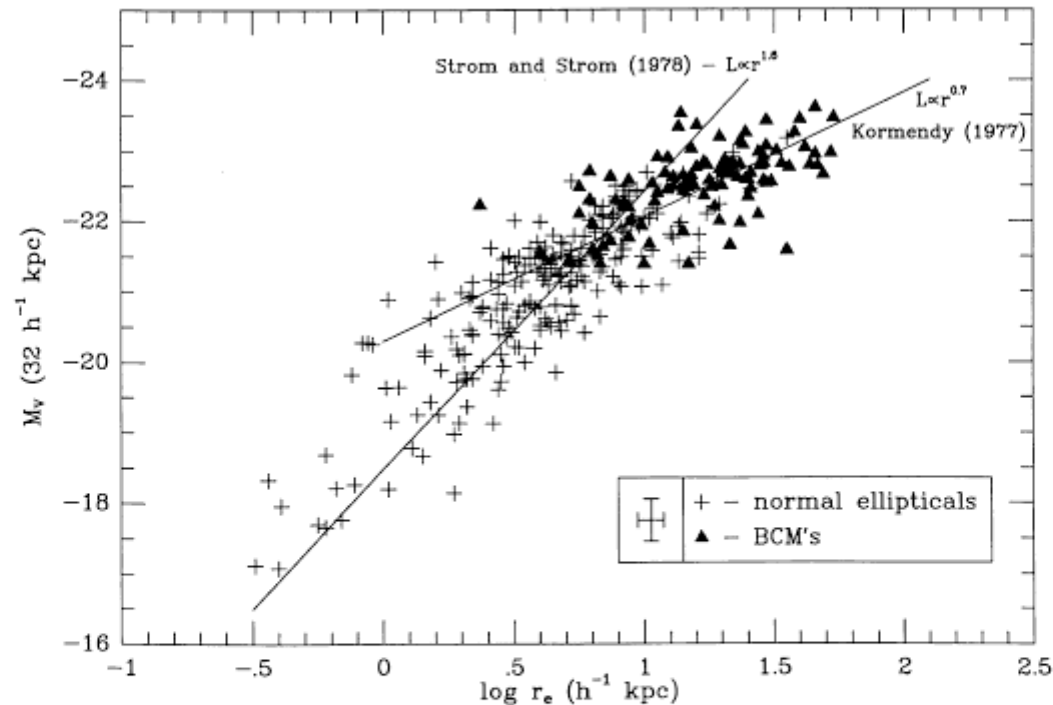


FIG. 8.—Magnitude ($M_{32 \text{ kpc}}$) vs. radius (r_e) diagram. The two relations from Strom and Strom (1979) (dominated by faint ellipticals) and Kormendy (1977) (dominated by bright ellipticals) are also shown. The BCMs are expected to deviate from the relation as a result of their enlarged radii. However, the bright isolated ellipticals also follow the Kormendy relation above $M_V = -21.5$. This break is near the same magnitude where Davies *et al.* (1983) determined that the internal kinematics of ellipticals changes from rotational support to anisotropic velocity support.

different relations for faint and bright ellipticals are not an effect of two different authors and procedures. It should be noted that the isolated ellipticals of this sample are also $r^{1/4}$, and any merger explanation for their shape must assume a runaway merger scenario as proposed by Carnevali, Cavaliere, and Santangelo (1981) in order to reduce the original cluster to one member. Mergers of bright ellipticals may also be primordial, that is, mergers of large protogalactic clouds in order to form anisotropic distributions, rather than mergers between systems in a recent epoch. At the very least, the break in Figure 8 reflects the change in the kinematics of bright ellipticals in their structure.

e) Cluster Properties

If mergers are responsible for BCMs, then it has been shown by several authors (Malumuth and Richstone 1984; see references therein) that this growth will be at the expense of fainter members. The galaxy with the highest probability of being accreted will be near slow-moving ellipticals, which, given some mass segregation in clusters, should be among the higher ranked galaxies. Hence, as the luminosity of the first-ranked member grows, the luminosity of the second- and third-ranked members should decrease (actually it is the ranking that changes, since the second- and third-rank members are consumed). This hypothesis can be tested by plotting the luminosity of the BCM against the difference in the luminosities of the BCM and the second-ranked galaxy, shown in the top panel of Figure 9. M_1 is the total integrated magnitude of the galaxy excluding the luminosity from cD envelopes (assumed not to be related to merger effects; see subtraction method in Paper III). The trend of increasing BCM luminosity with increasing difference between the BCM and the second-ranked member is presented as evidence for dynamical evolution in this sample. There is a well-known selection effect of picking the brightest member of any sample for comparisons in ranking (Malumuth and Richstone 1984);

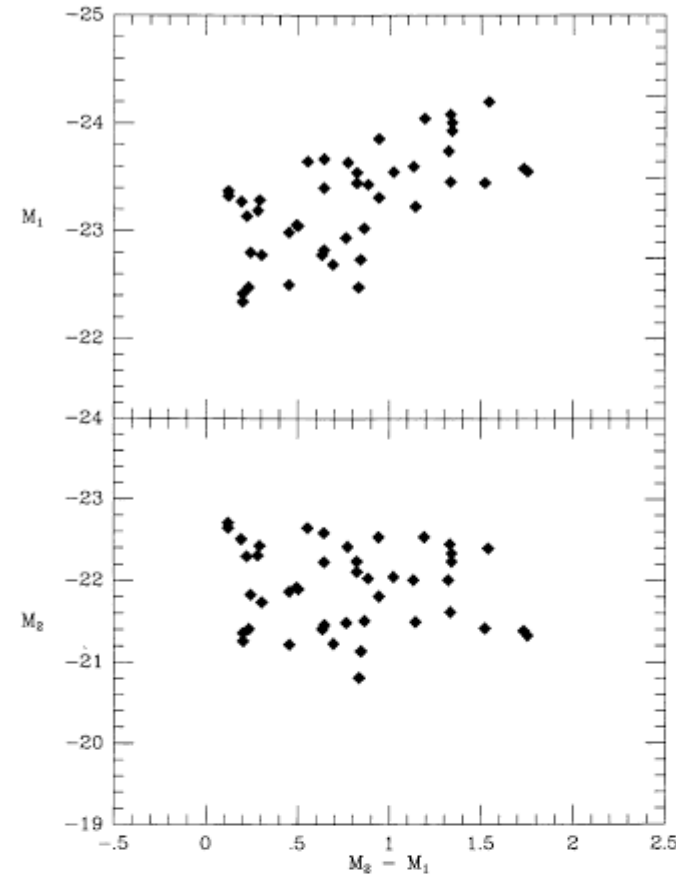


FIG. 9.—Magnitudes of the first- and second-rank galaxies (M_1, M_2) in each cluster versus the difference in their magnitudes ($M_2 - M_1$). Dynamical evolution would imply that the luminosity of the BCMs increases at the expense of lesser cluster members, as seen with the positive correlation in the top panel. This correlation is not a selection effect, since there is no corresponding anticorrelation in the M_2 vs. $M_2 - M_1$ diagram of the bottom panel. These plots compare favorably with the cluster evolution simulations of Malumuth and Richstone (1984) (see their Fig. 7).

Properties of Giant Ellipticals:

- Occupy preferential regions in fundamental plane
- 1st ranks c.f. lower ranks
- Small dispersion in absolute aperture magnitudes: r_e , σ , $\langle\mu\rangle_e \rightarrow 21\%$ (Oegerle & Hoessel 1991); $M-\alpha \rightarrow 17\%$ (Hoessel 1980; Lauer & Postman 1994; Collins & Mann 1997)

c.f. SN ~ 16%

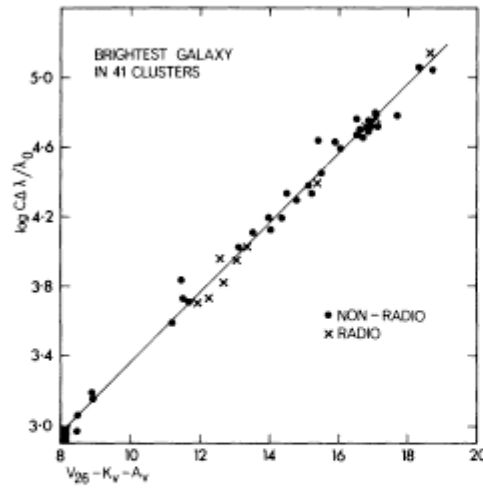


FIG. 2

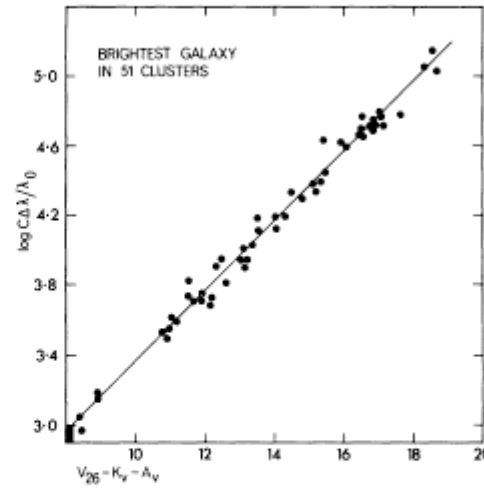


FIG. 3

FIG. 2.—The Hubble diagram for first-ranked galaxies in 41 clusters from the data of table 2. *Abscissa*, the corrected V_c magnitude; *ordinate*, the logarithmic redshift. The box in the lower left is the approximate interval within which Hubble established the redshift-distance relation in 1929. A line of slope 5, required by all homogeneous models in the $z \rightarrow 0$ limit, is fitted to the data in zero point only. It is equation (4) of the text.

FIG. 3.—Same as fig. 1, with data from table 3 added to those of table 2.

**Traditional use in standard
Cosmological tests...**

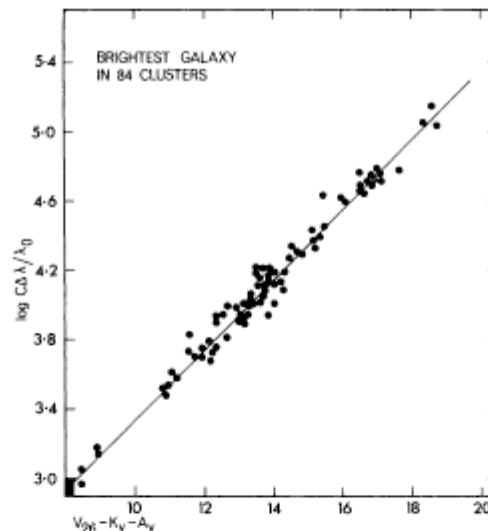


FIG. 4.—Same as fig. 1 for the combined data of tables 2, 3, and 4

**...renaissance as probes of
velocity fields...**



Lynden-Bell et al 1988 ApJ 326,19

Great Attractor...

Controversial: scale



Independent Sample?

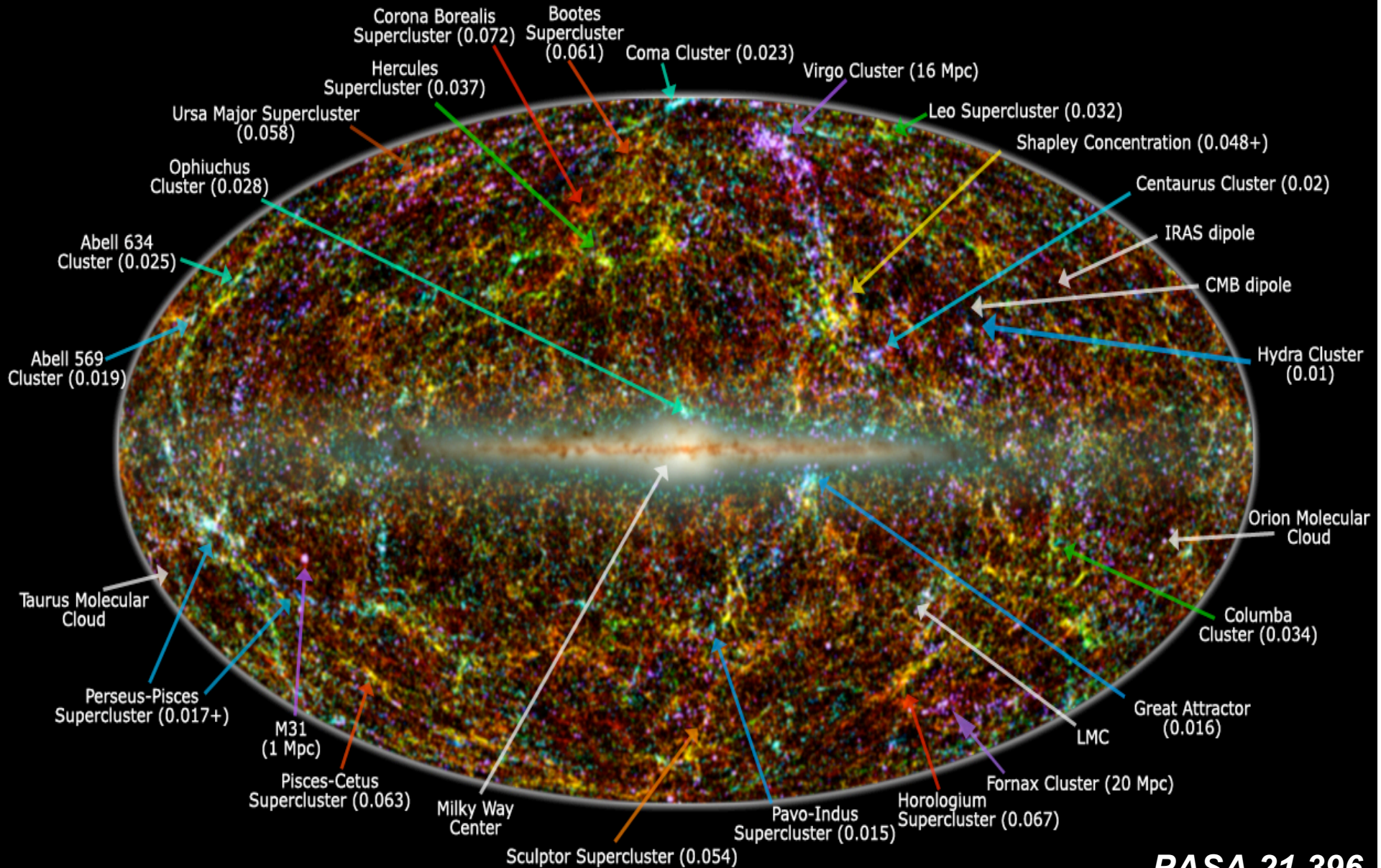


Tested & re-tested

Technique?

...A Fairy Tale, complicated & obscure..?

Large Scale Structure in the Local Universe

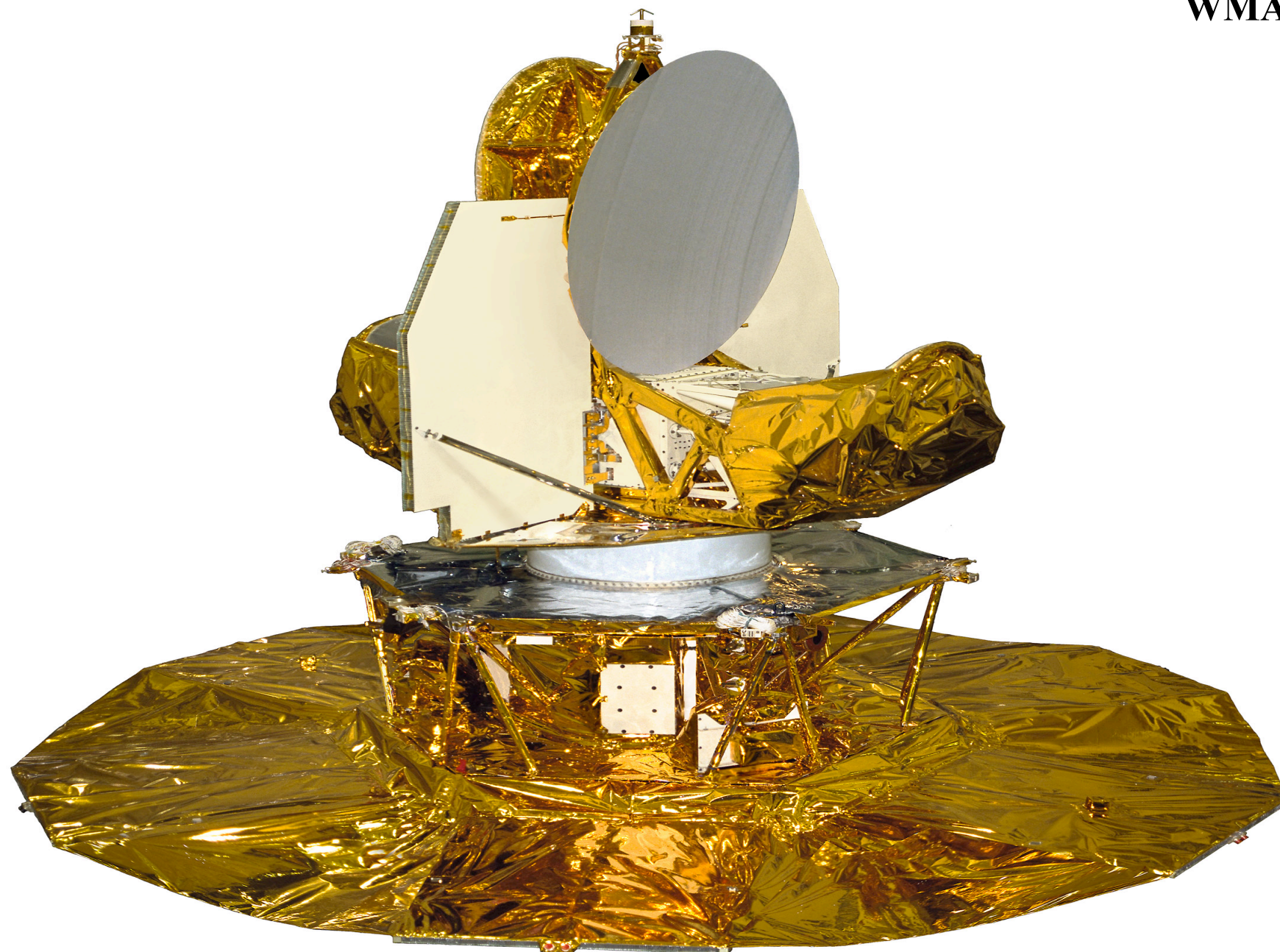


PASA 21,396

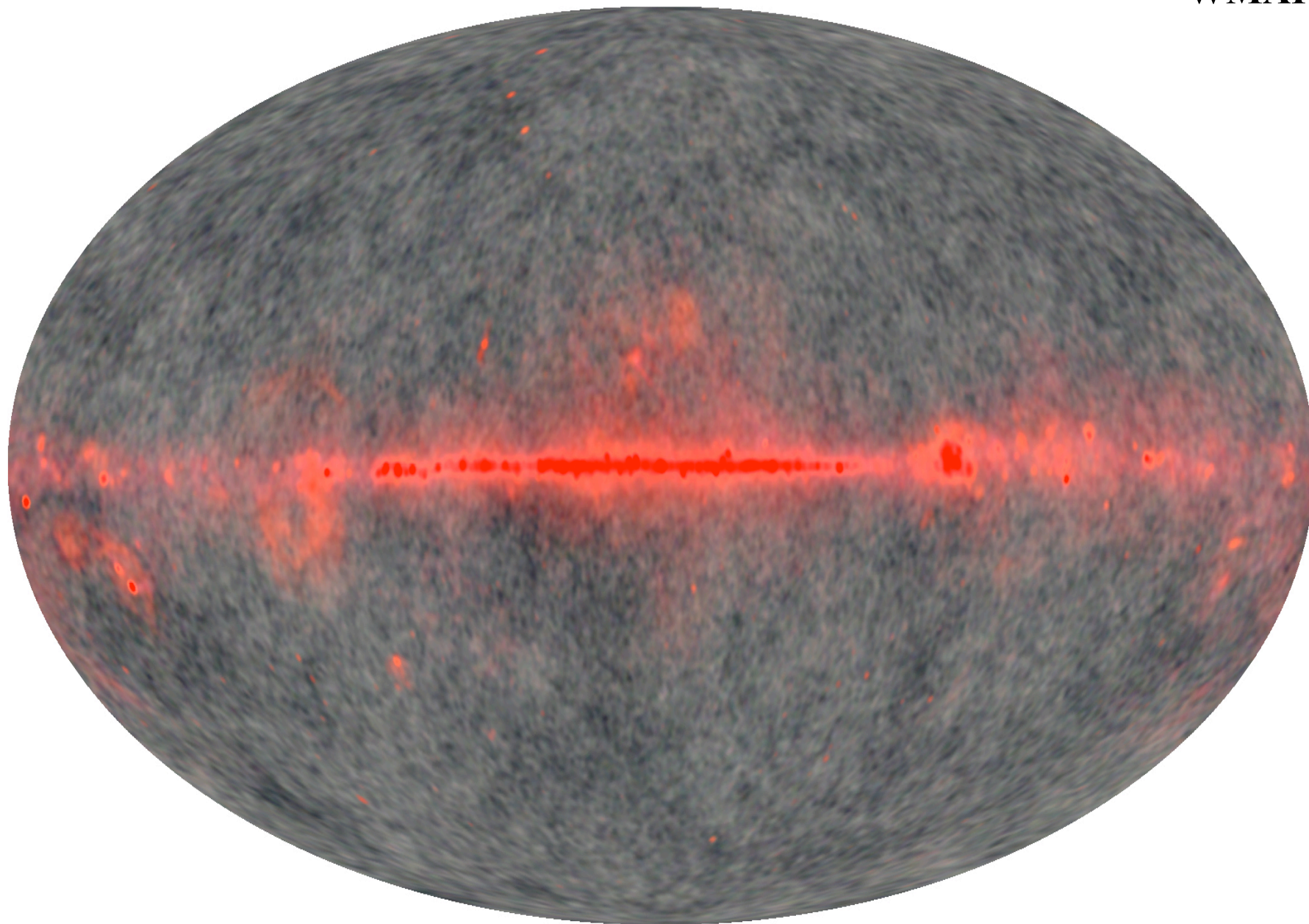
Legend: image shows 2MASS galaxies color coded by redshift (Jarrett 2004); familiar galaxy clusters/superclusters are labeled (numbers in parenthesis represent redshift).
Graphic created by T. Jarrett (IPAC/Caltech)

Reference Frames & “Streaming Motions” / “(Bulk) Cosmic Flows” ...

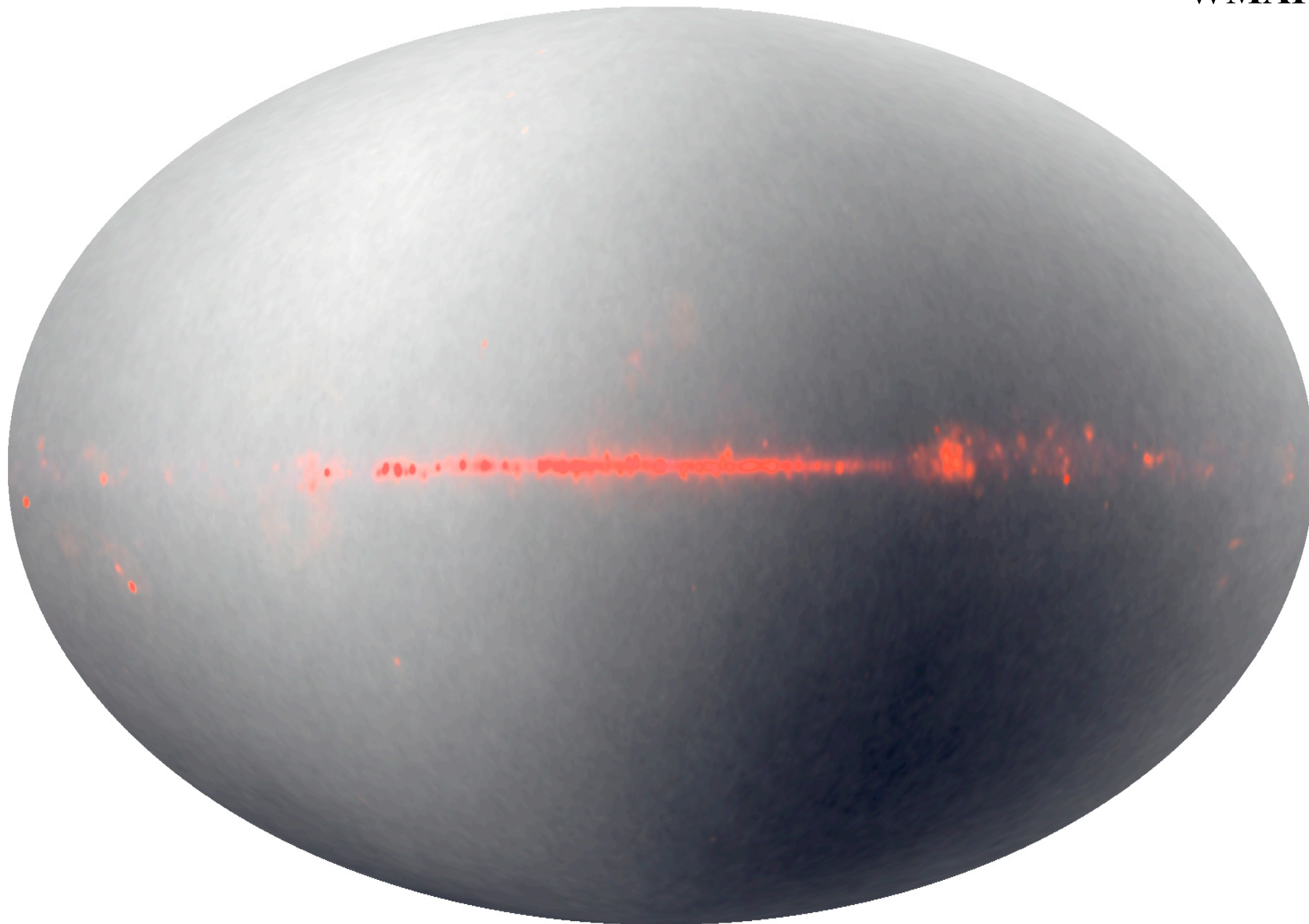
WMAP



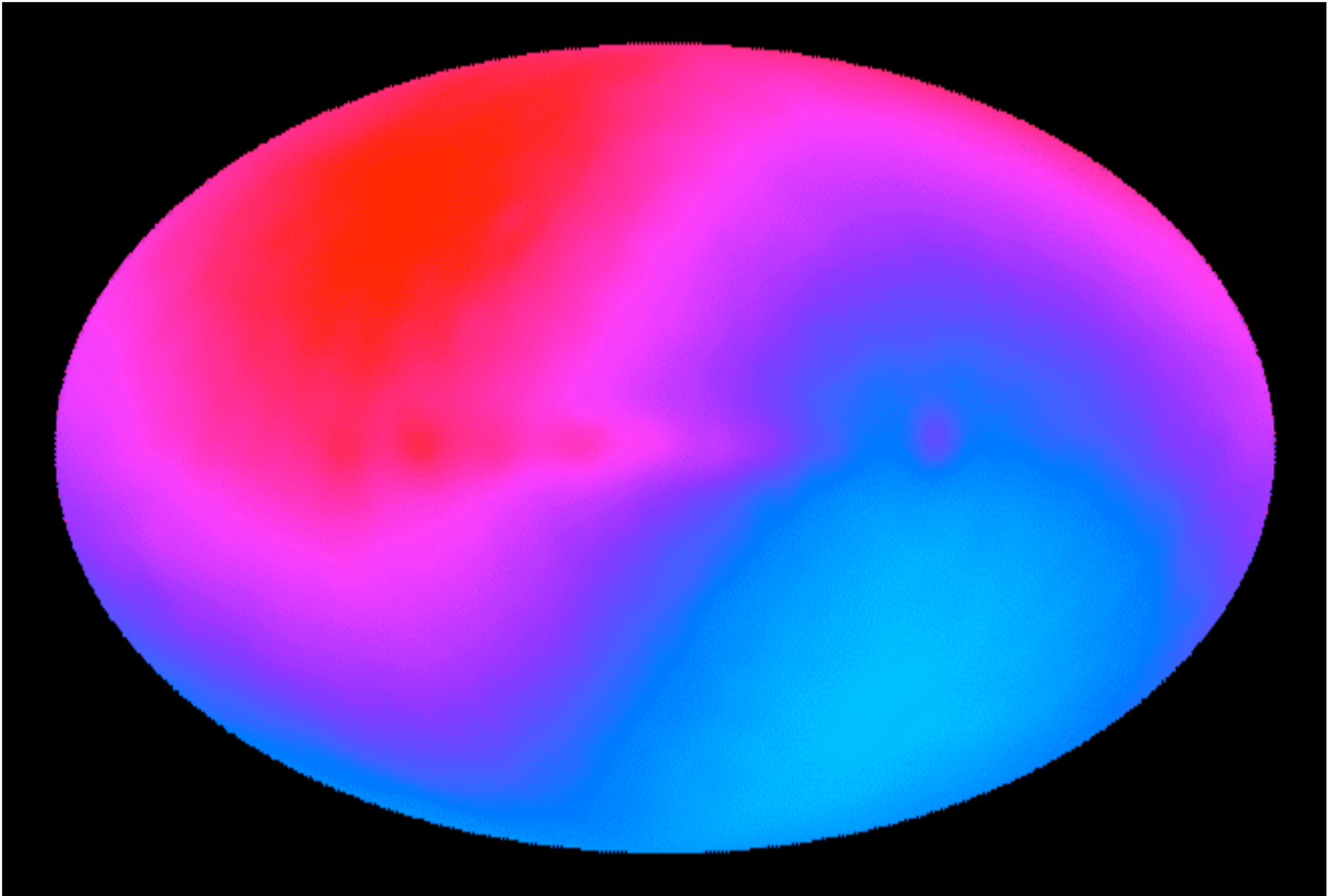
WMAP



WMAP







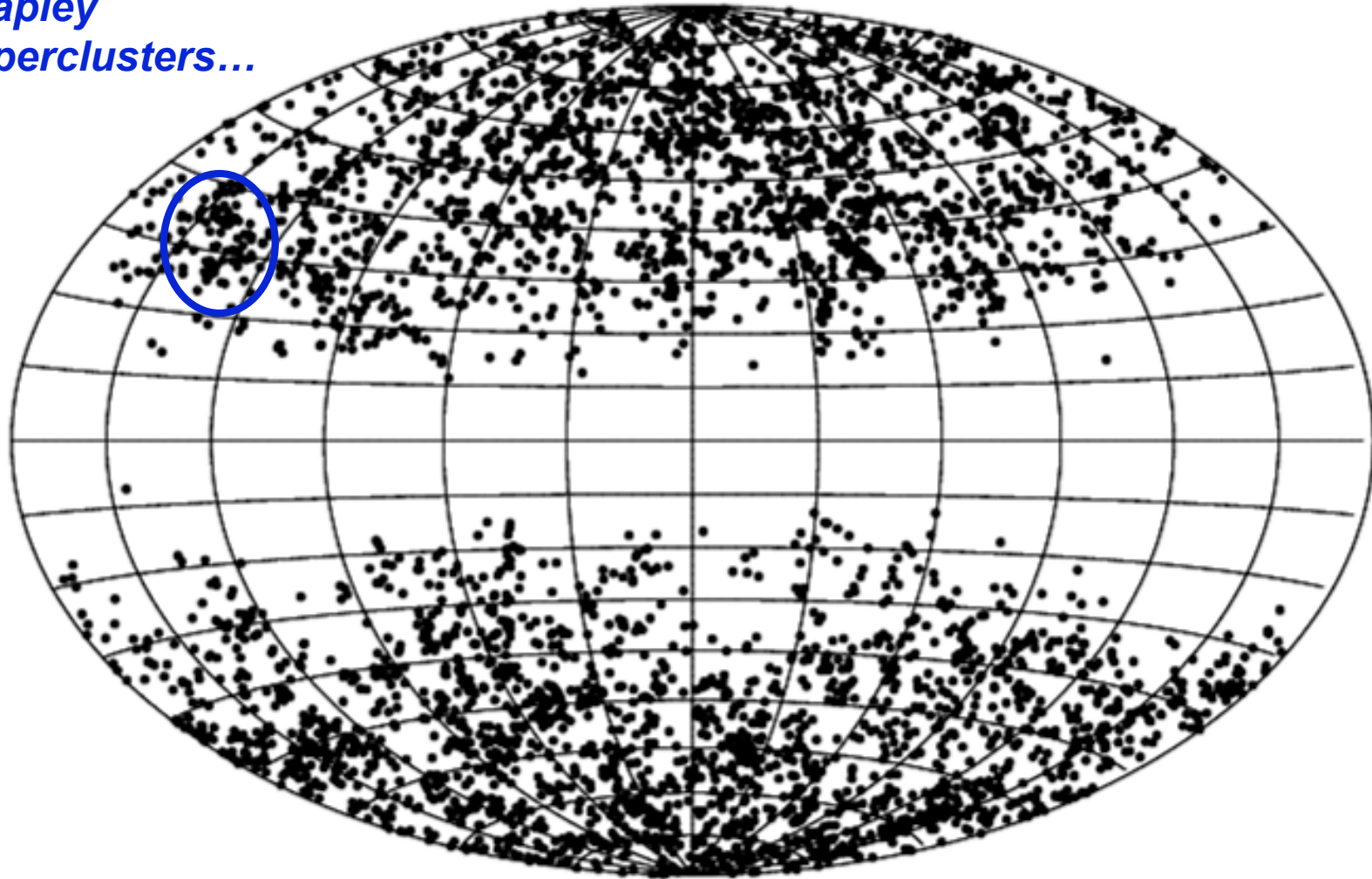
The *CoBE* DMR result dominated by CMB dipole ± 0.001 K. A reference frame.



Coma Cluster (APOD 2006-03-21)

Abell (1958) and Abell, Corwin and Olowin (1989) clusters

*Hydra-Centaurus &
Shapley
Superclusters...*




Conventional Aitoff projection, Galactic coordinates ($\alpha=12^h$ $\delta=0^\circ$)


- Compare redshift independent distance with redshift \rightarrow velocity residual, δV

- $\delta V = (V_{cosmic} + V_{galaxy} + V_{peculiar} + \dots)$

Random



Random



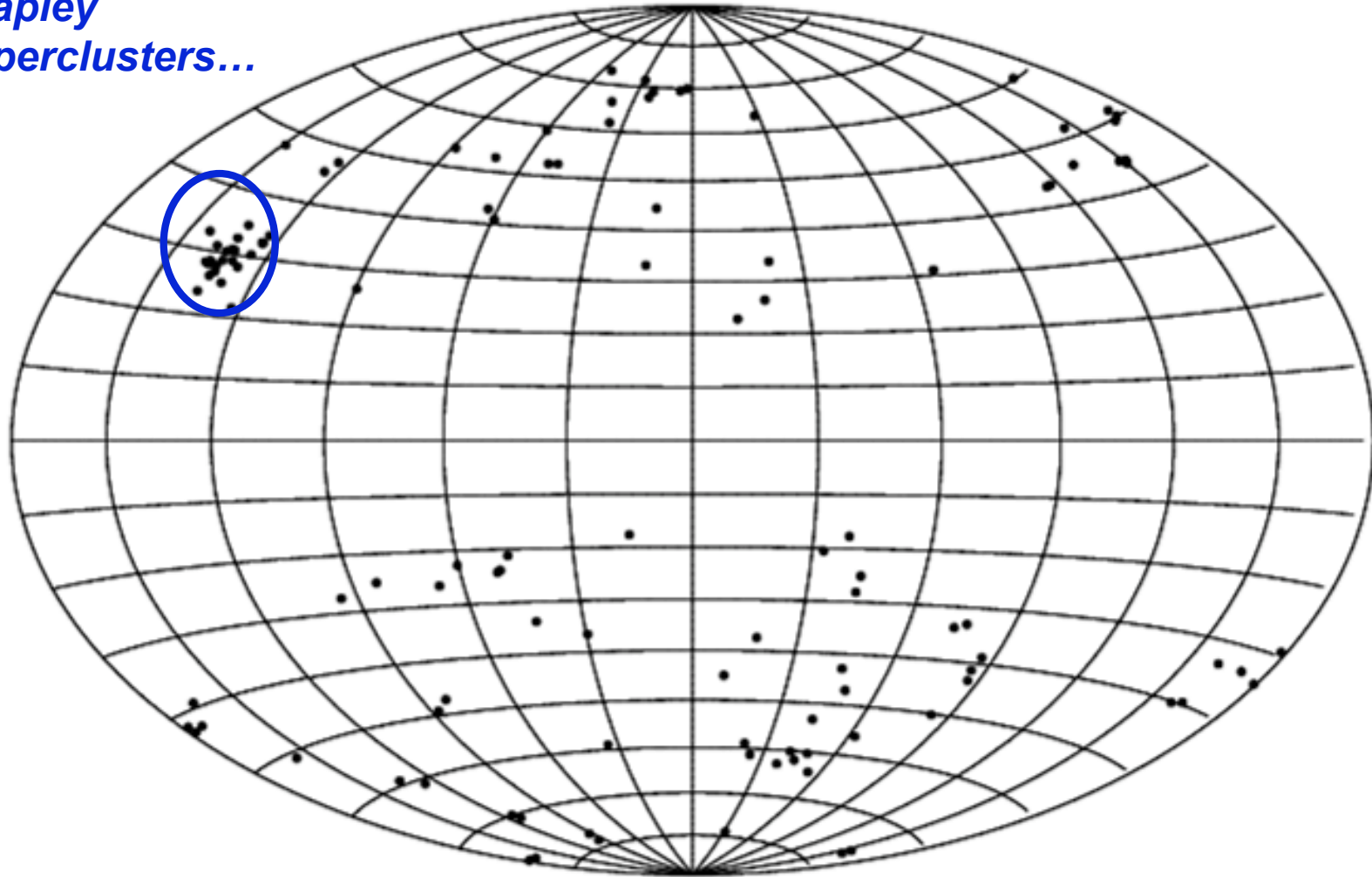
Allow a Coherent component!



- $\delta V \rightarrow \delta M$

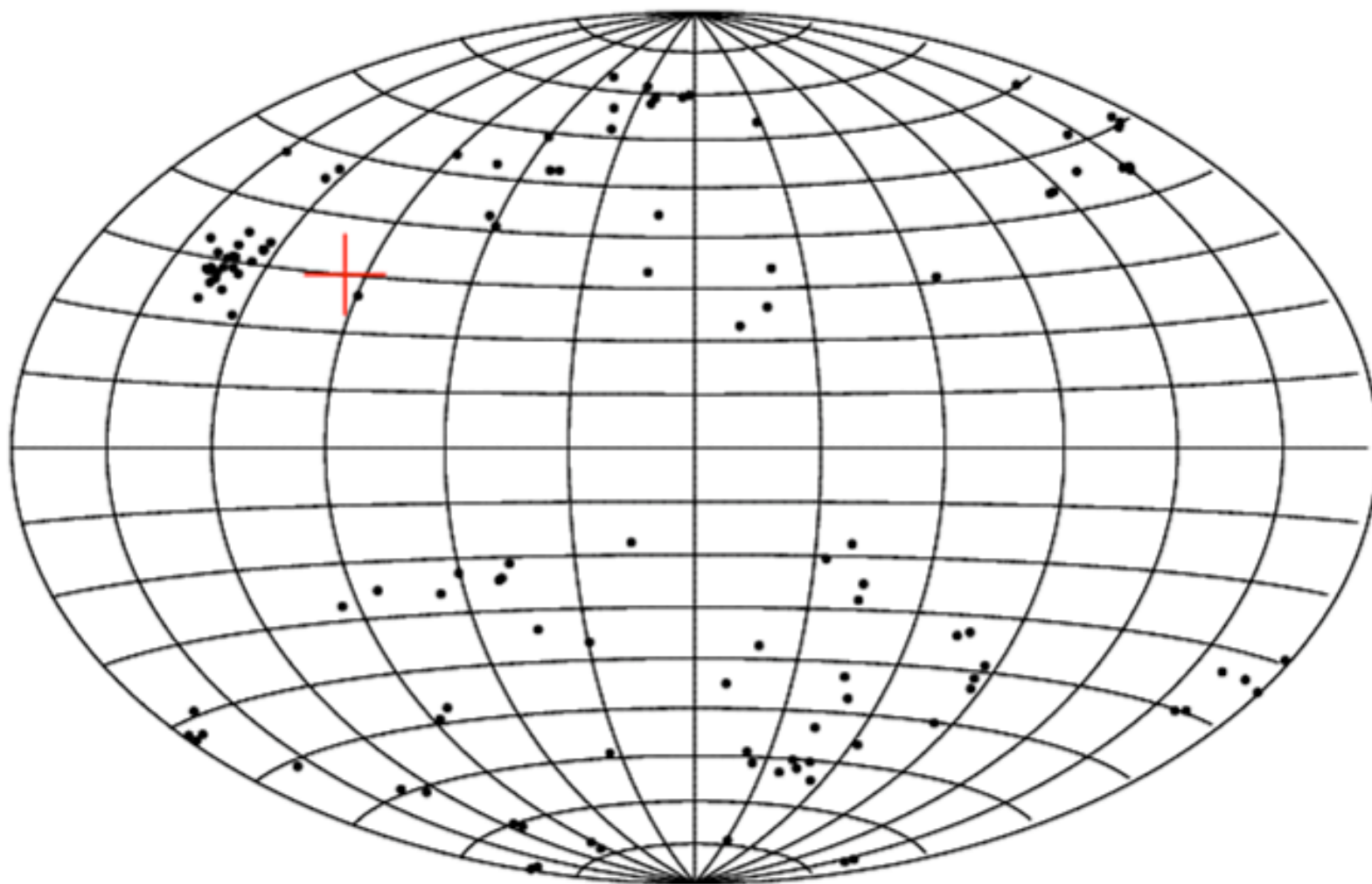
Lauer & Postman (1994) *ACIF* clusters

**Hydra-Centaurus &
Shapley
Superclusters...**



Conventional Aitoff projection, Galactic coordinates ($\alpha=12^h$ $\delta=0^\circ$)

Lauer & Postman (1994) *ACIF* clusters



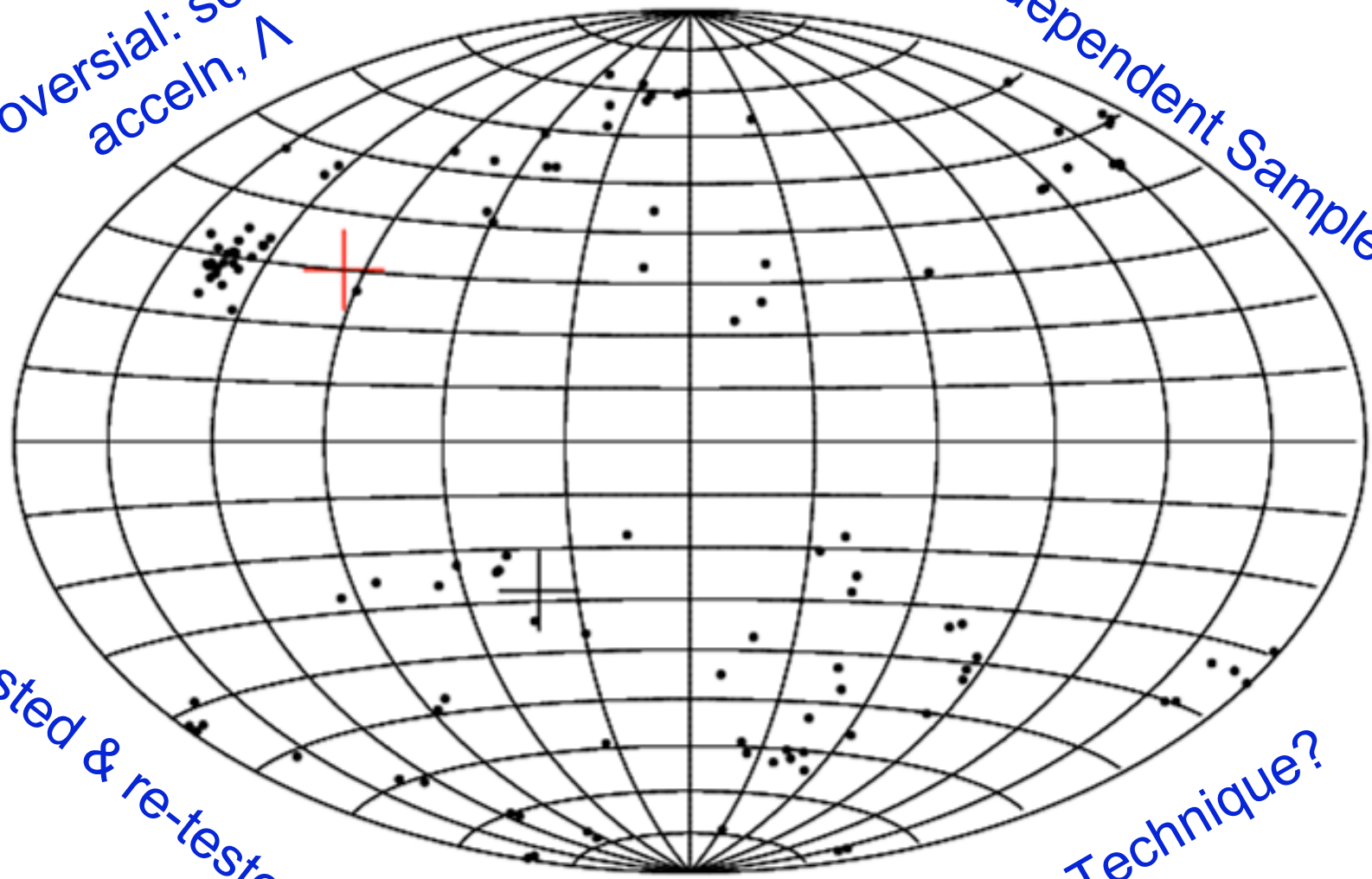
Conventional Aitoff projection, Galactic coordinates ($\alpha=12^h$ $\delta=0^\circ$)

Controversial: scale, H_0 ;
acceln, Λ

Lauer & Postman (1994) *ACIF* clusters

+ CMB Hot Pole
+ Apex of LG w.r.t *ACIF*

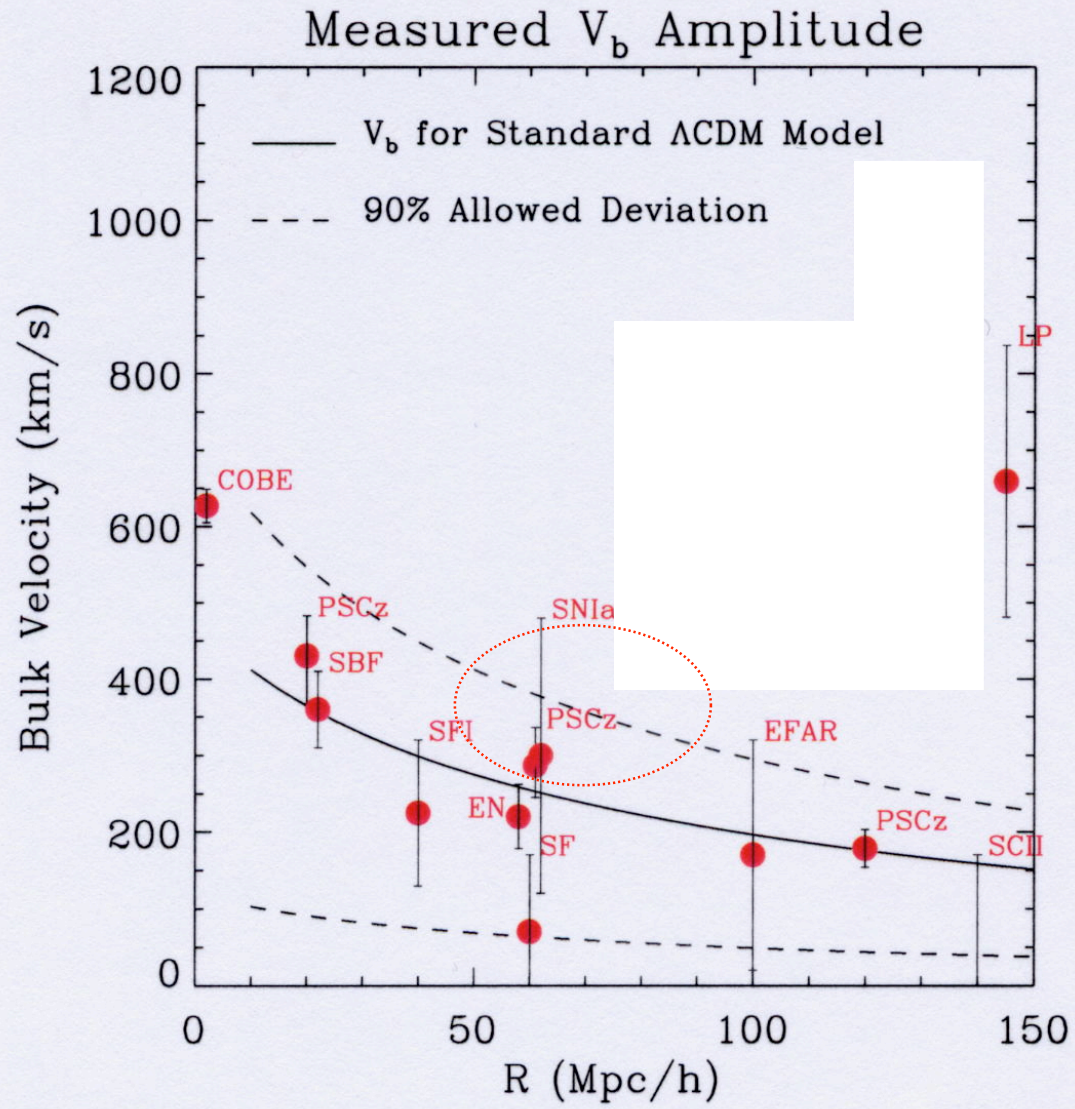
Independent Sample?



Tested & re-tested

Technique?

Conventional Aitoff projection, Galactic coordinates ($\alpha=12^h$ $\delta=0^\circ$)





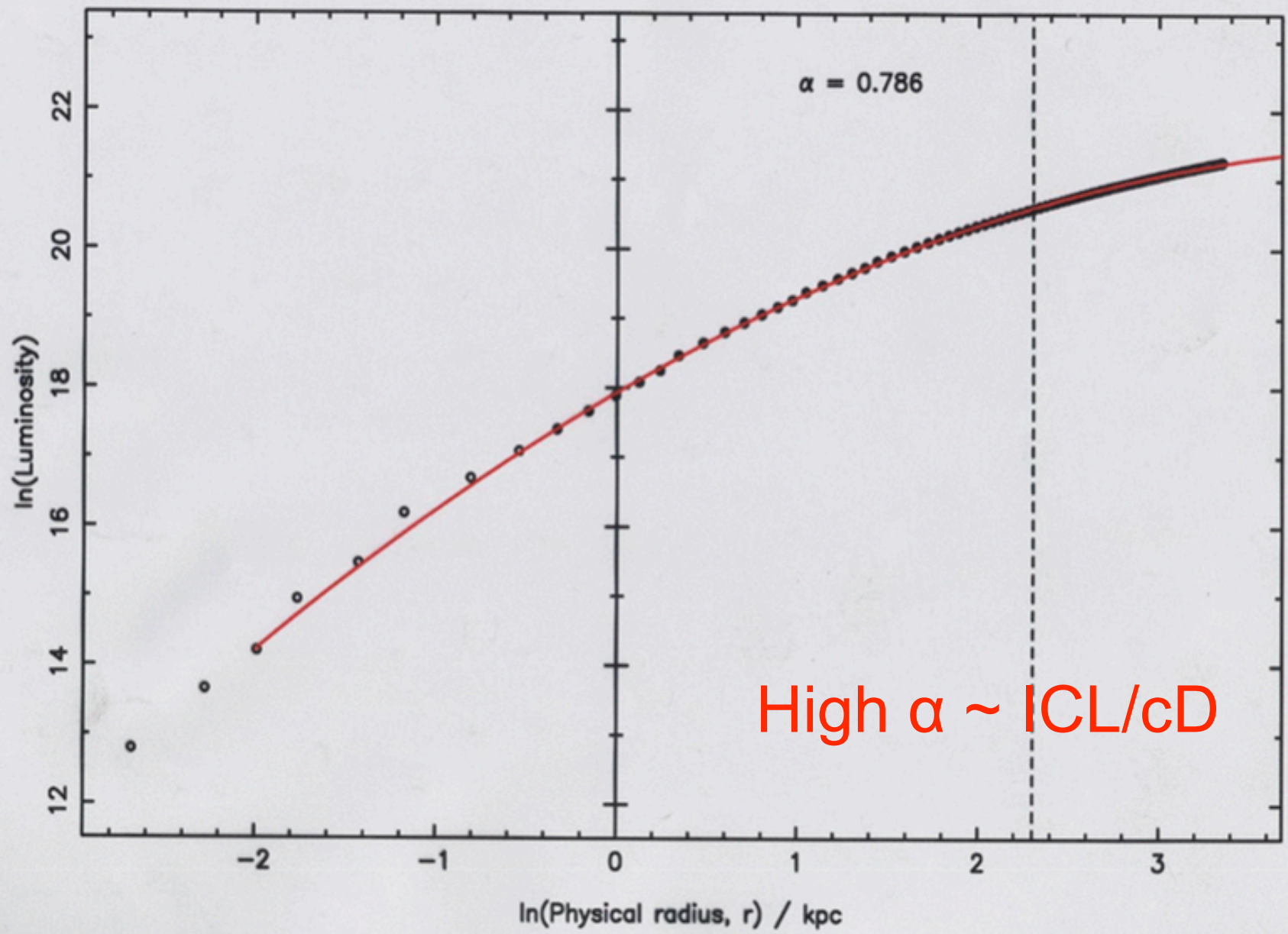
Relative Distance Indicator

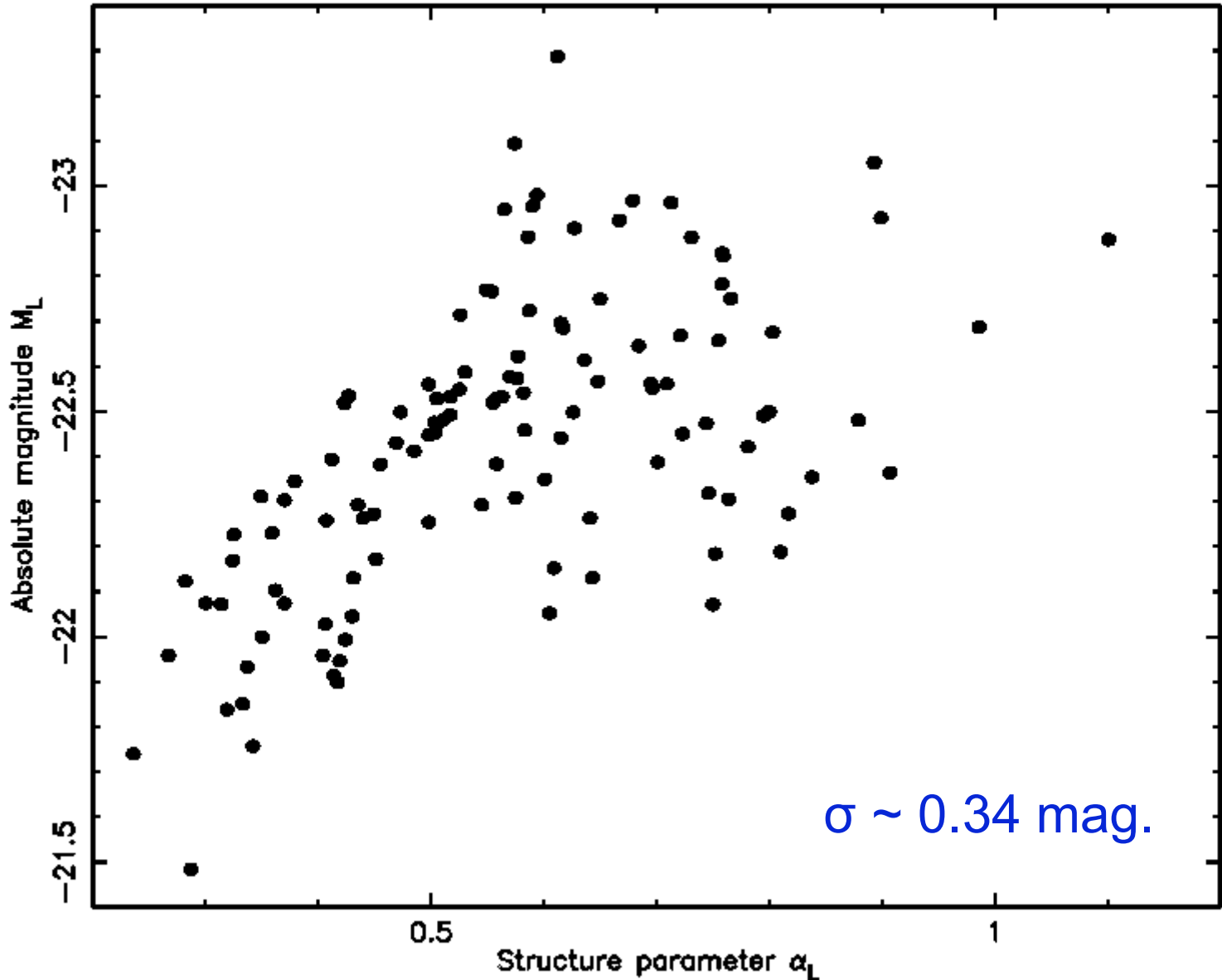
- Structure Parameter (Hoessel 1980 ApJ 241, 493):

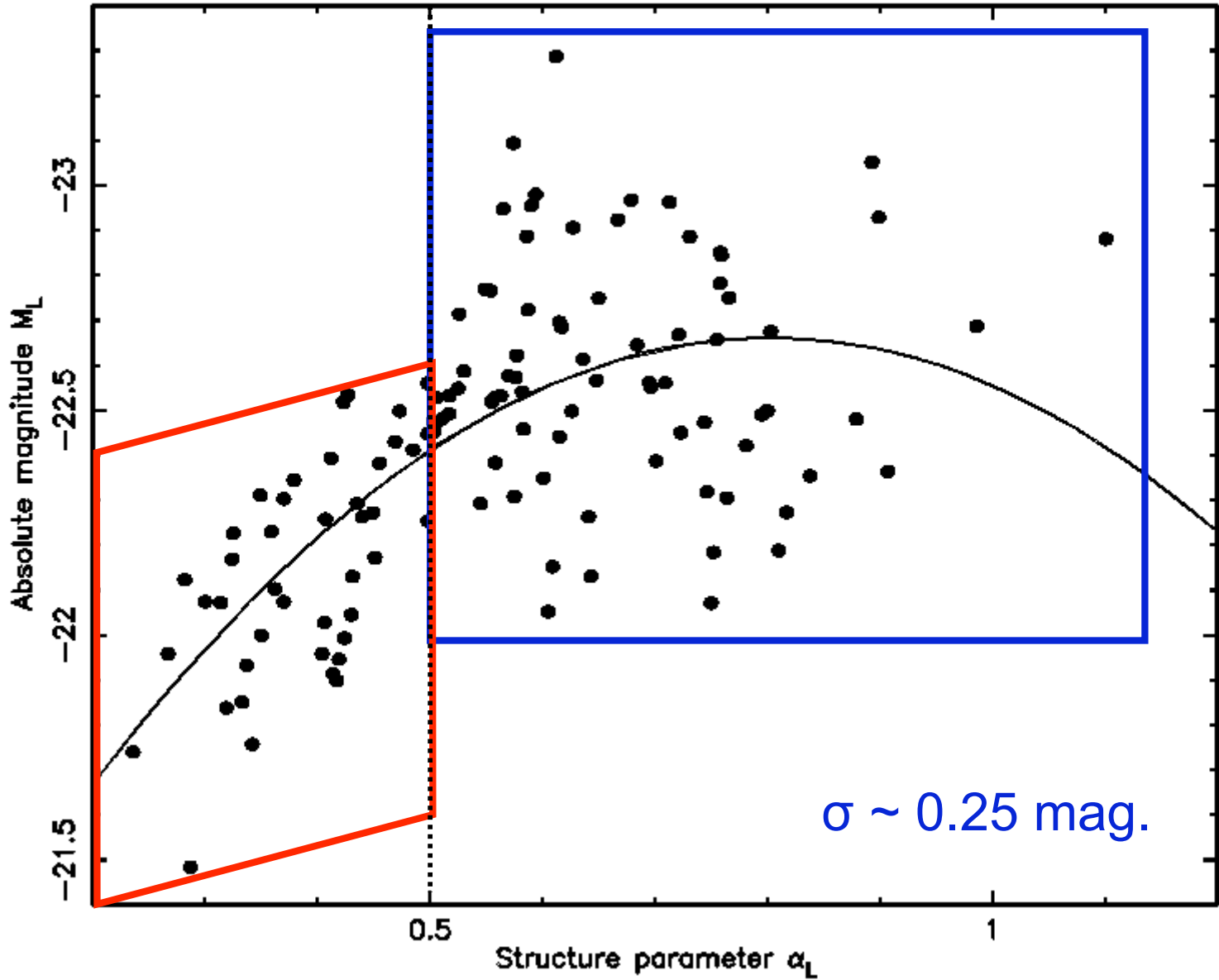
$$\alpha \sim (\partial \ln L / \partial \ln r) |_{r(lim)}$$

- No assumptions about underlying light distribution (c.f. Sersic, de Vaucouleurs)
- Avoid known departures from models (esp. BCGs/cDs: *extended amorphous haloes*)

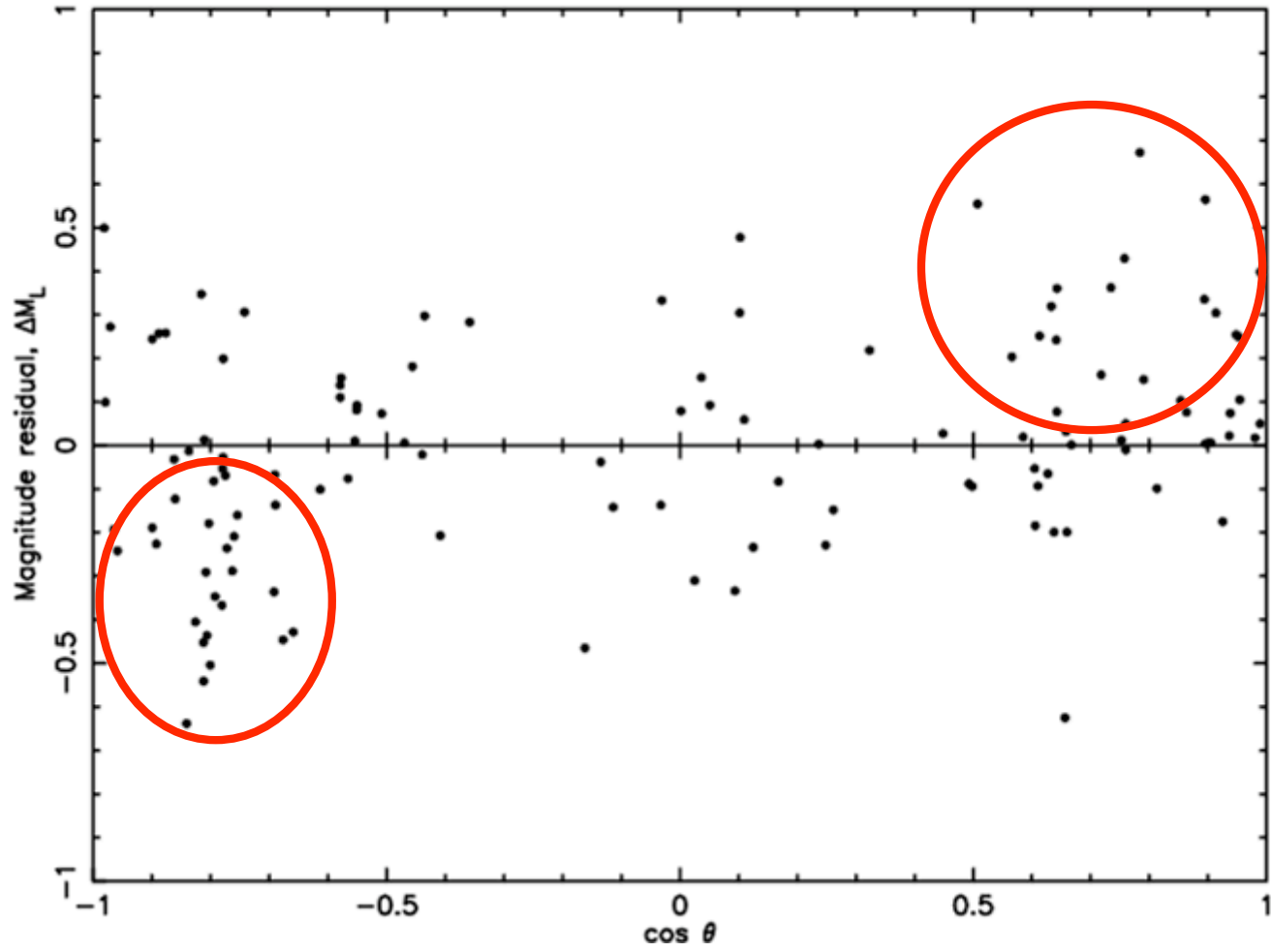
Cumulative Luminosity profile for BCG in Abell 2199, NGC 6166



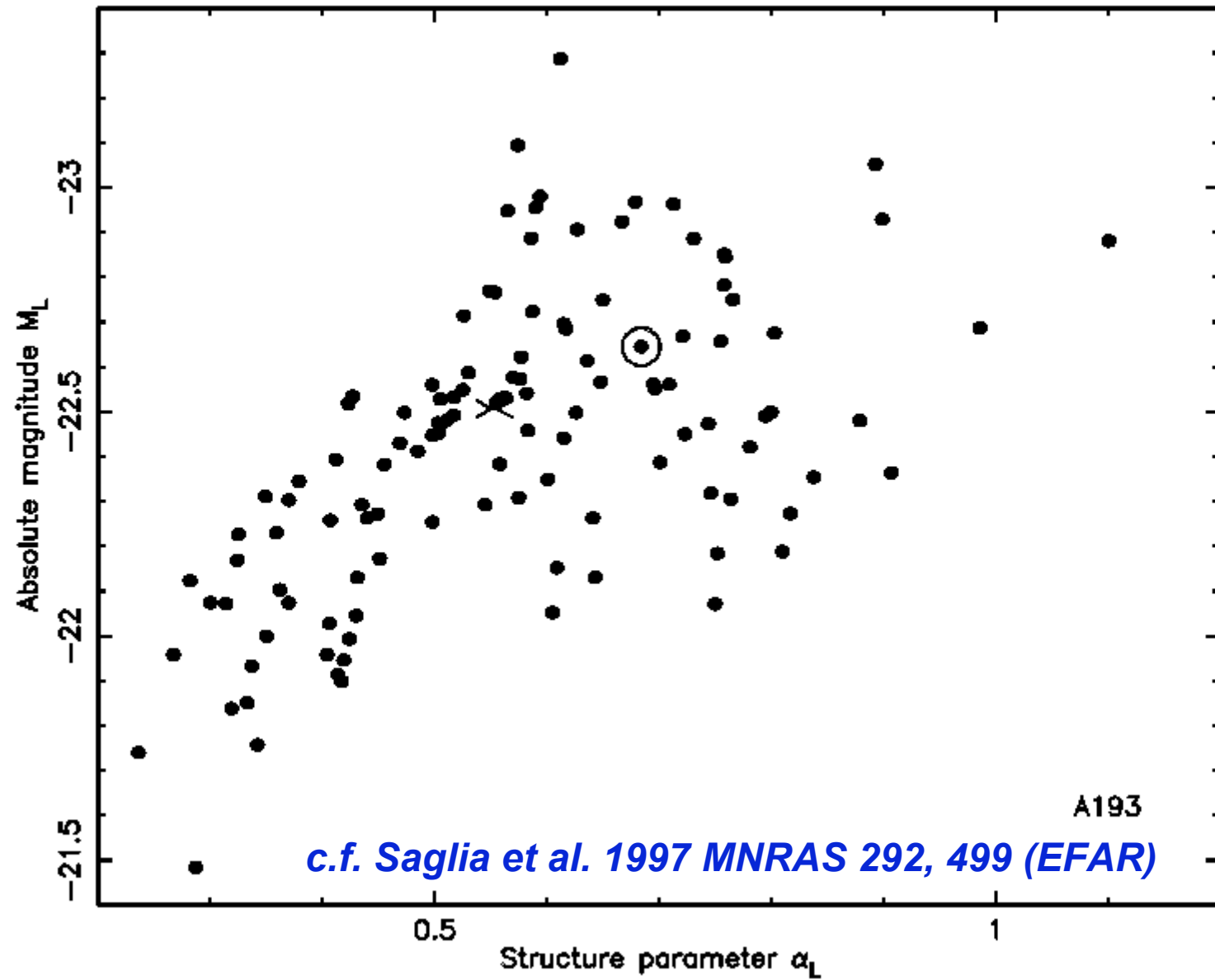


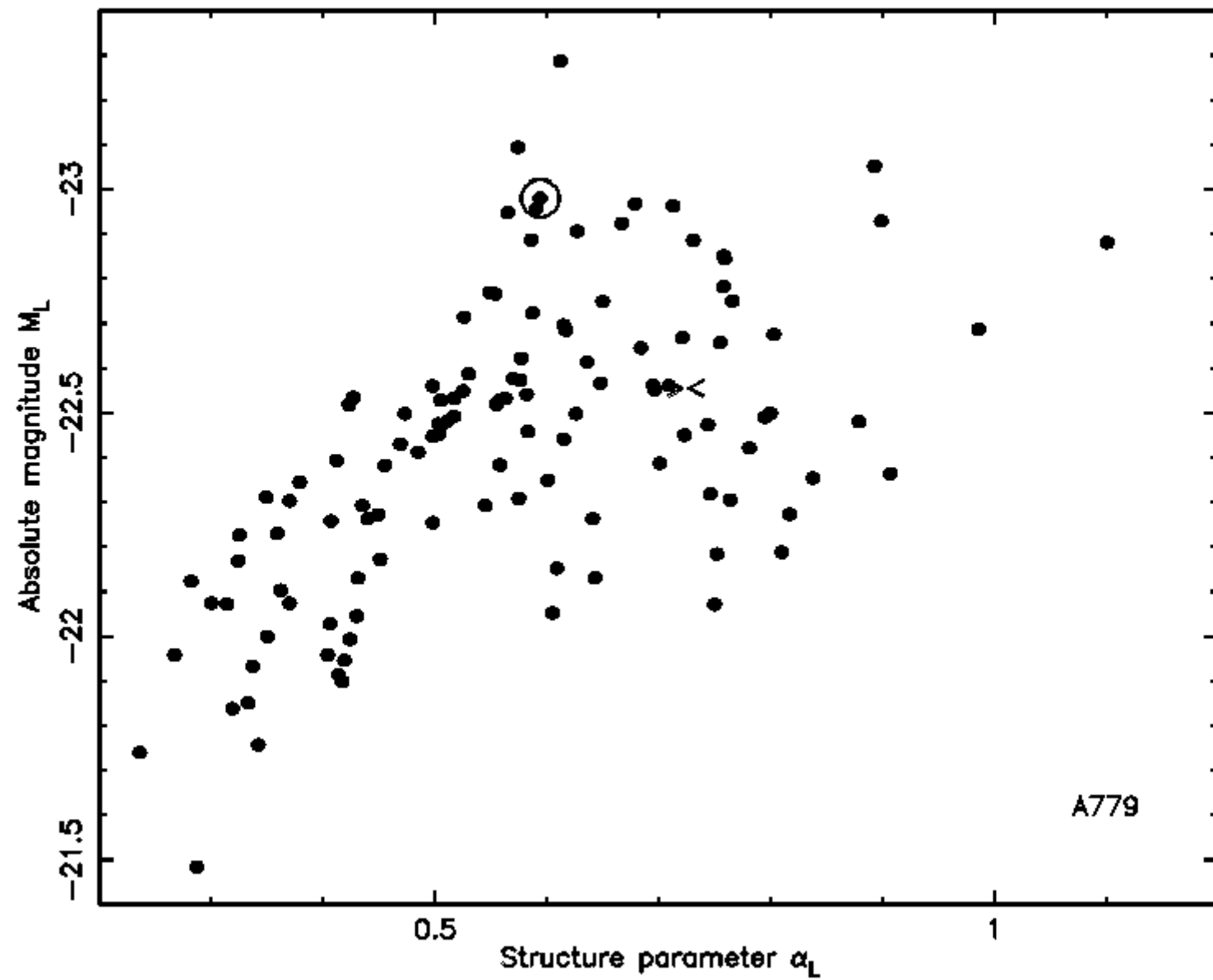


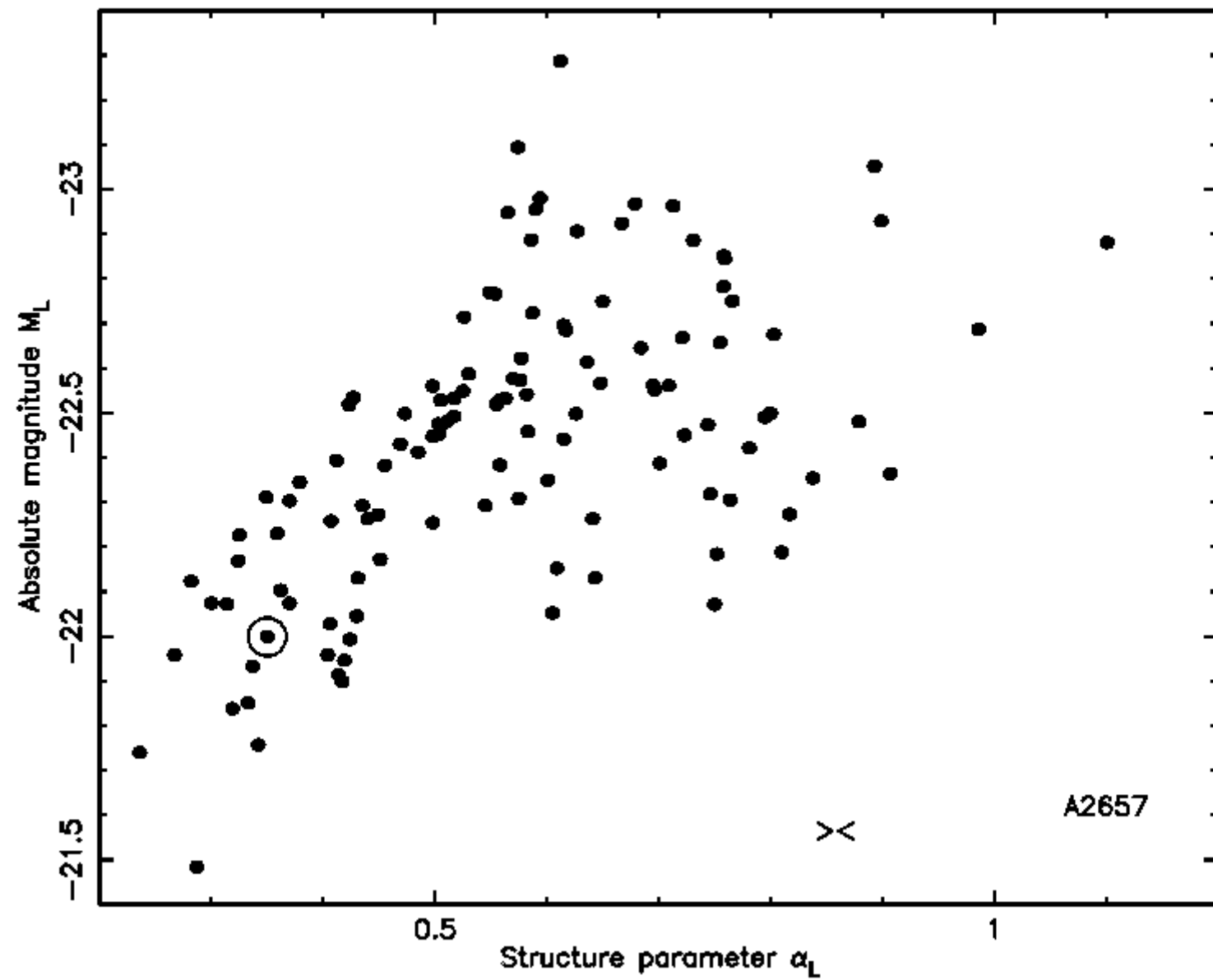
Photometric residuals as a function of position (LP94)

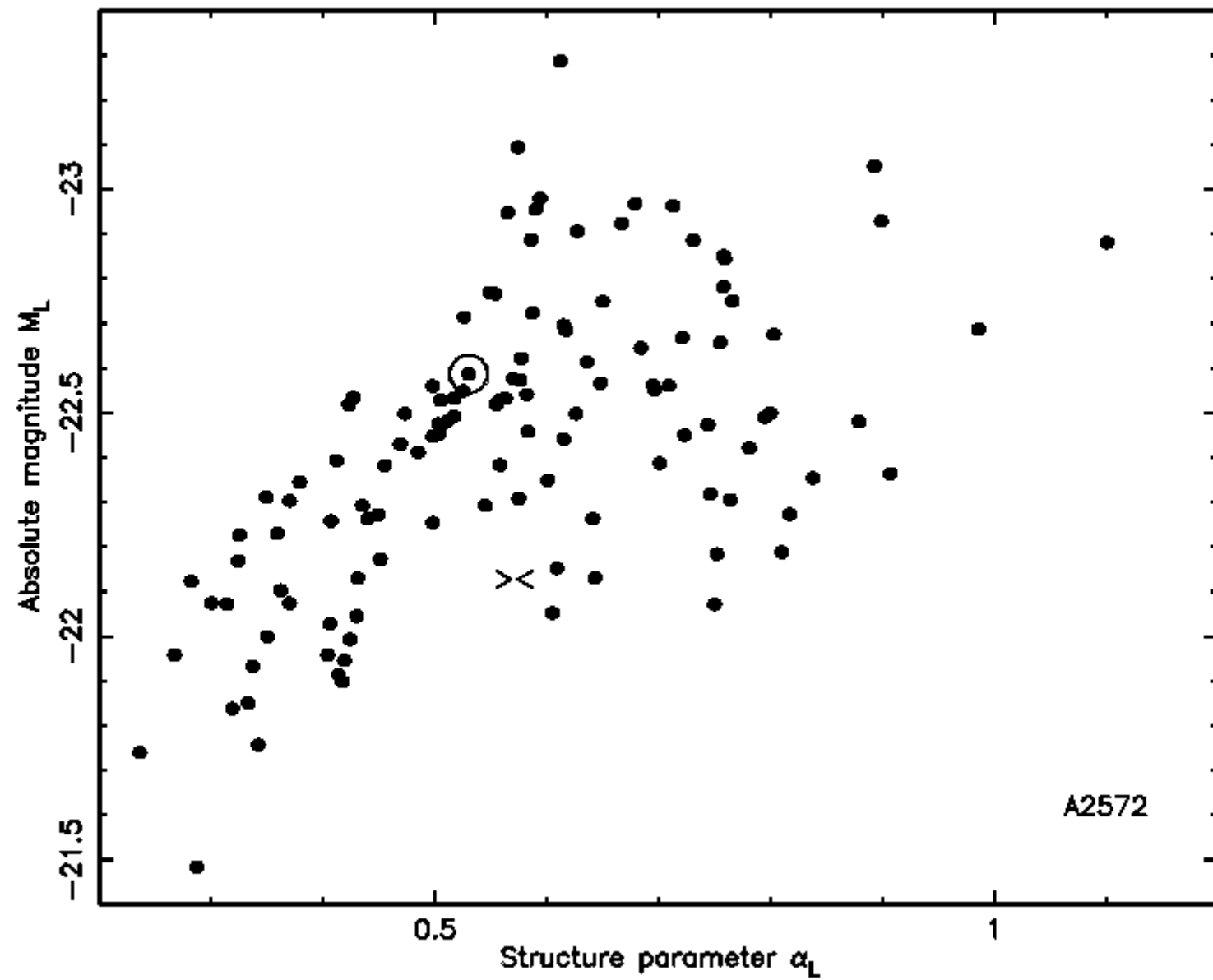


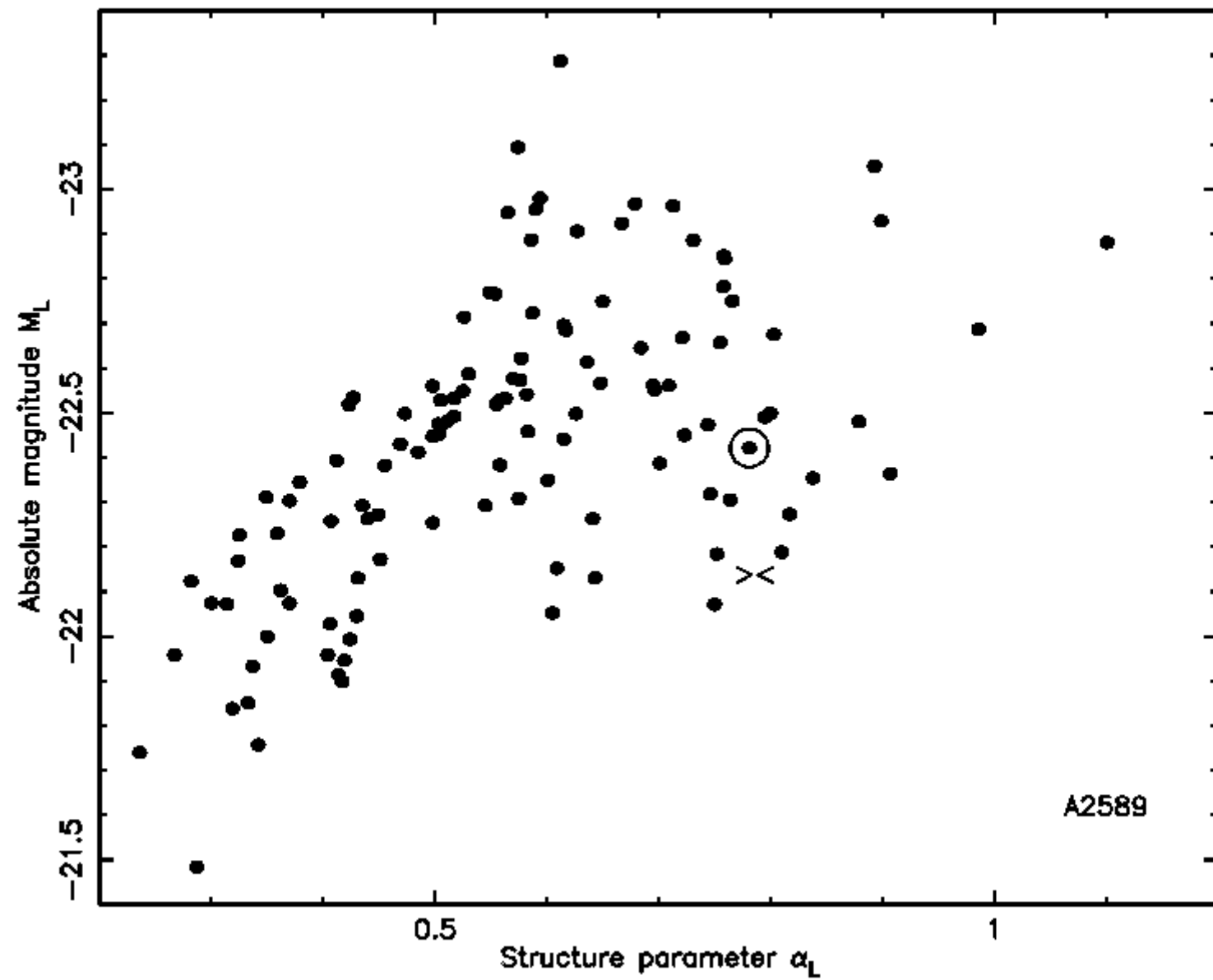
Photometry; X-ray selection & coincidence



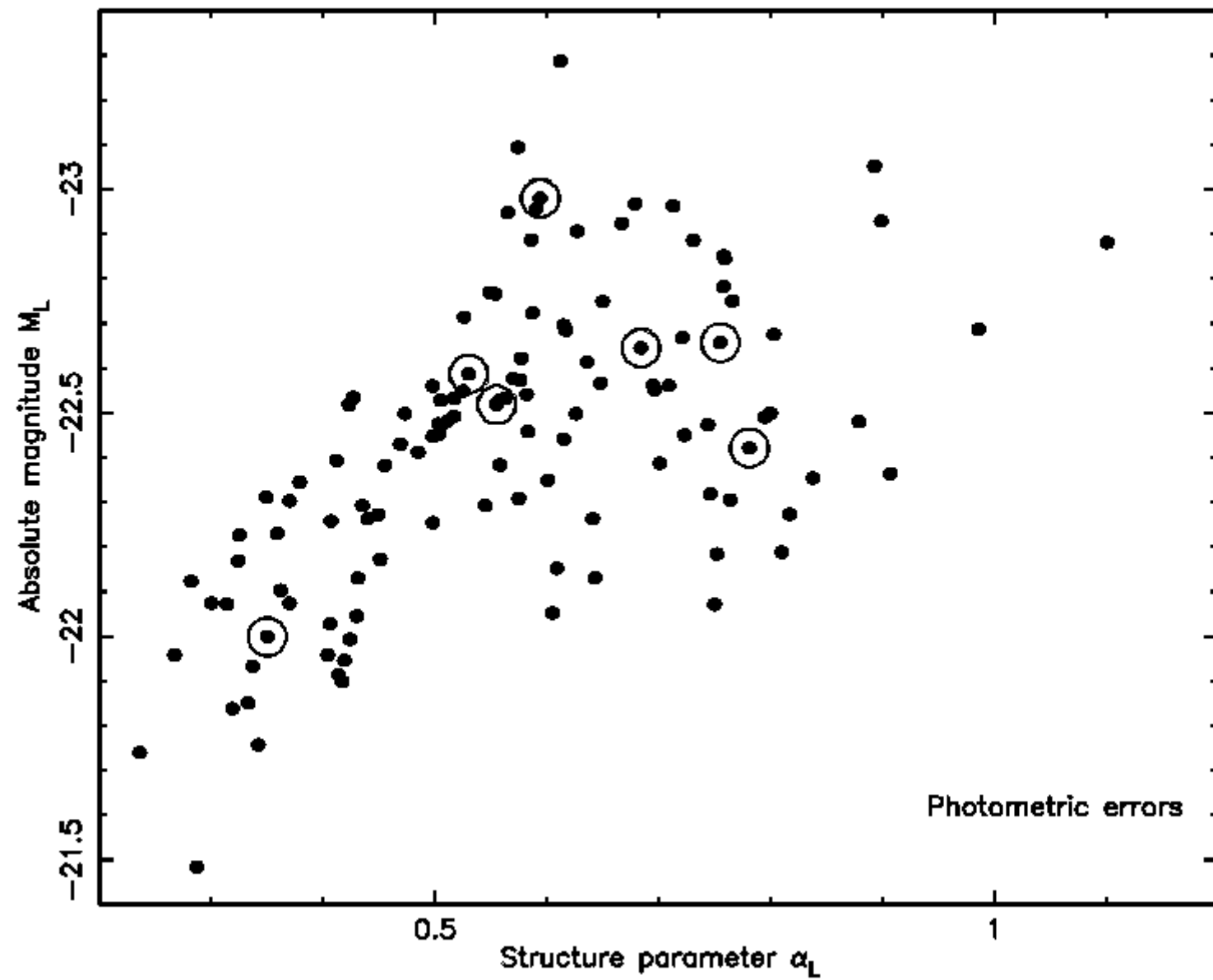






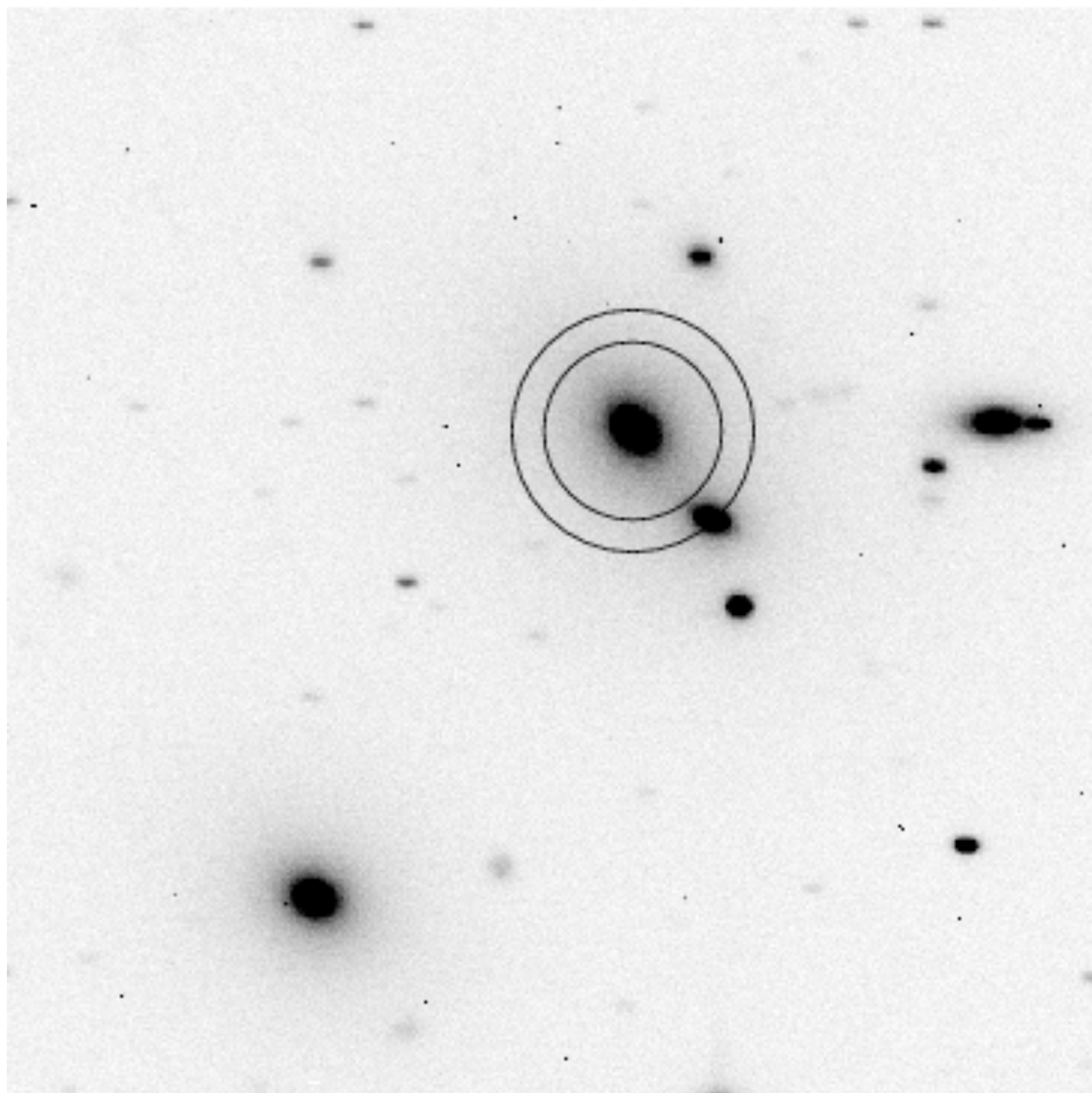


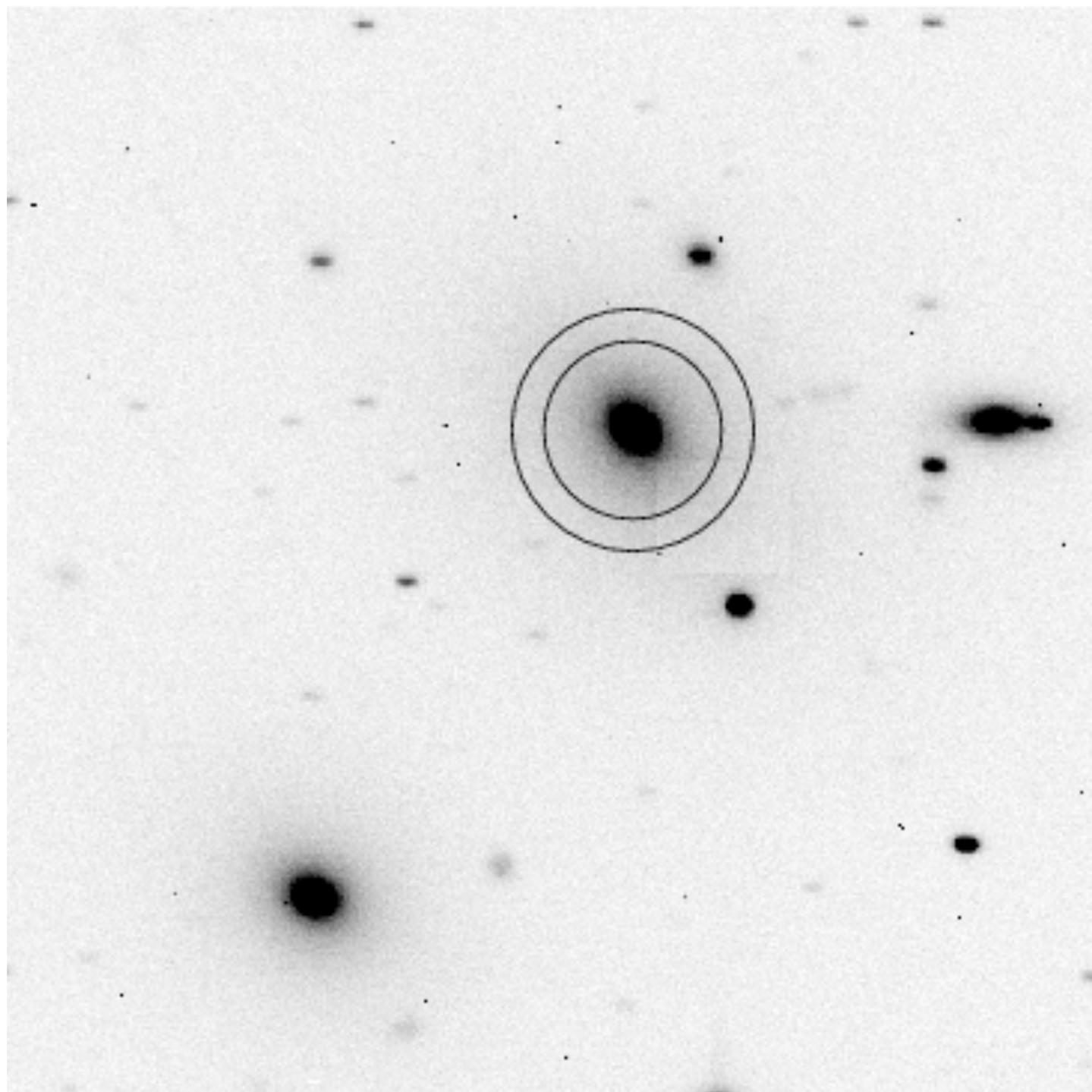
A2589

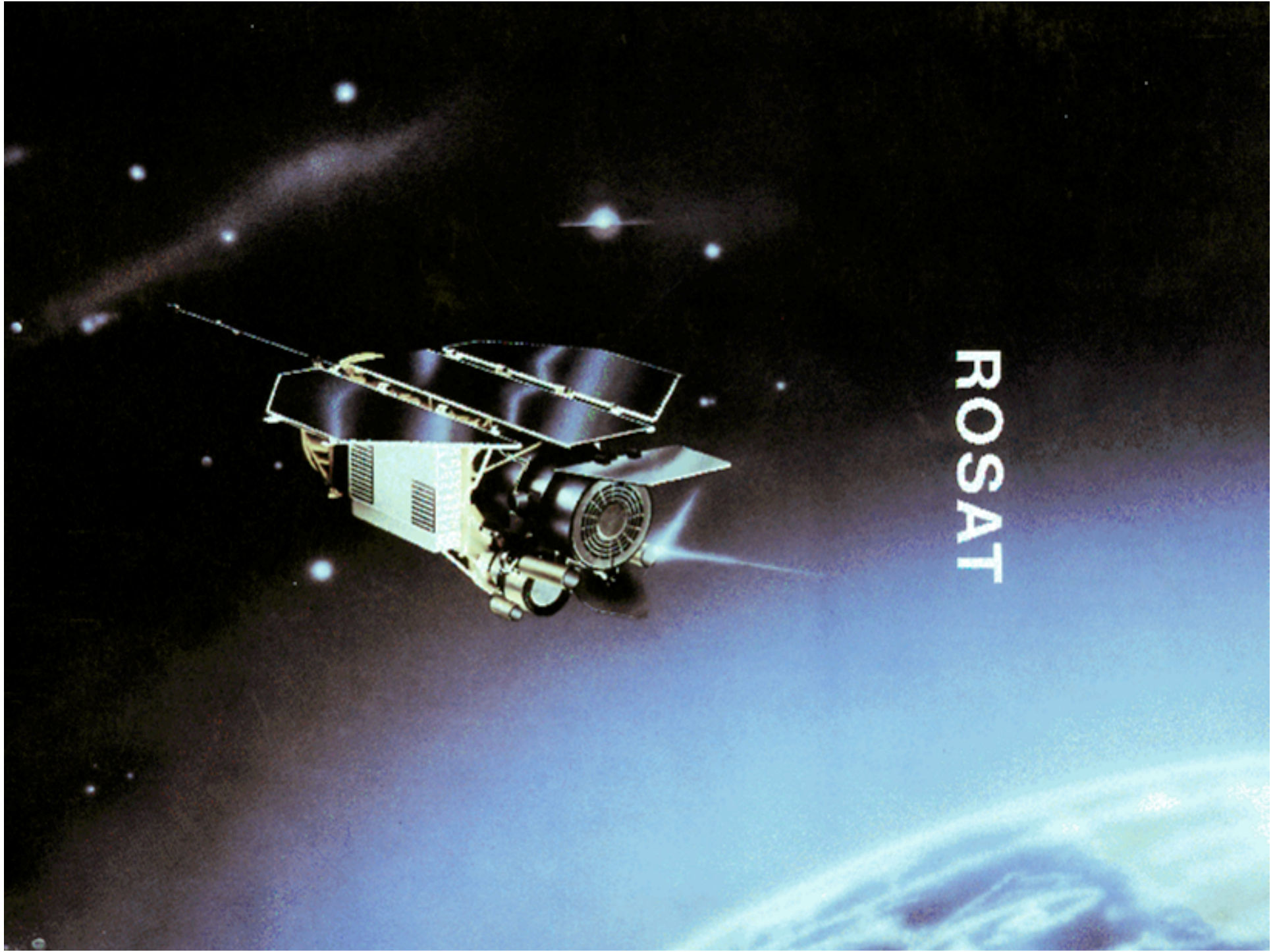


Photometric Errors

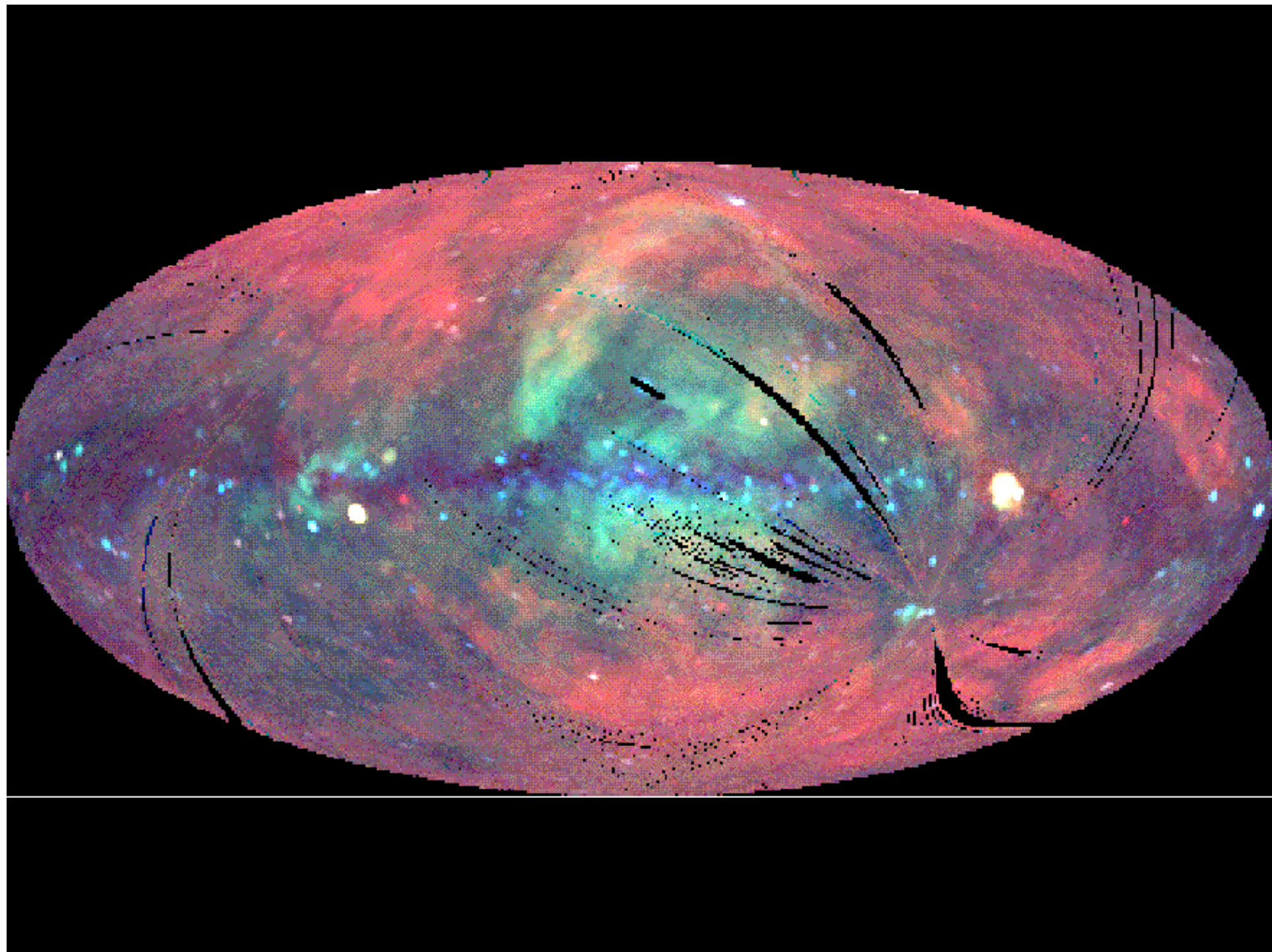
- LP claim systematics ≤ 0.01 mag.
- Comparison with EFAR \neq
- Distinction between M_1 , M_2
- Multiple contamination?
- Coherent on the sky?
- Error in sky background subtraction?
- $<30\%$ of overlap / comparison







ROSAT

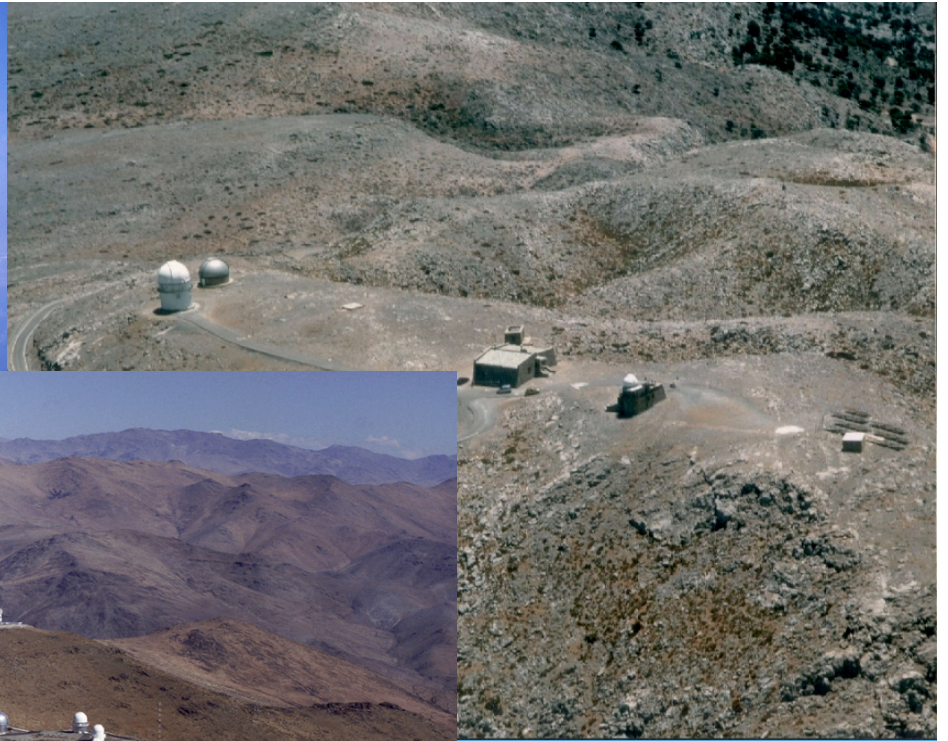
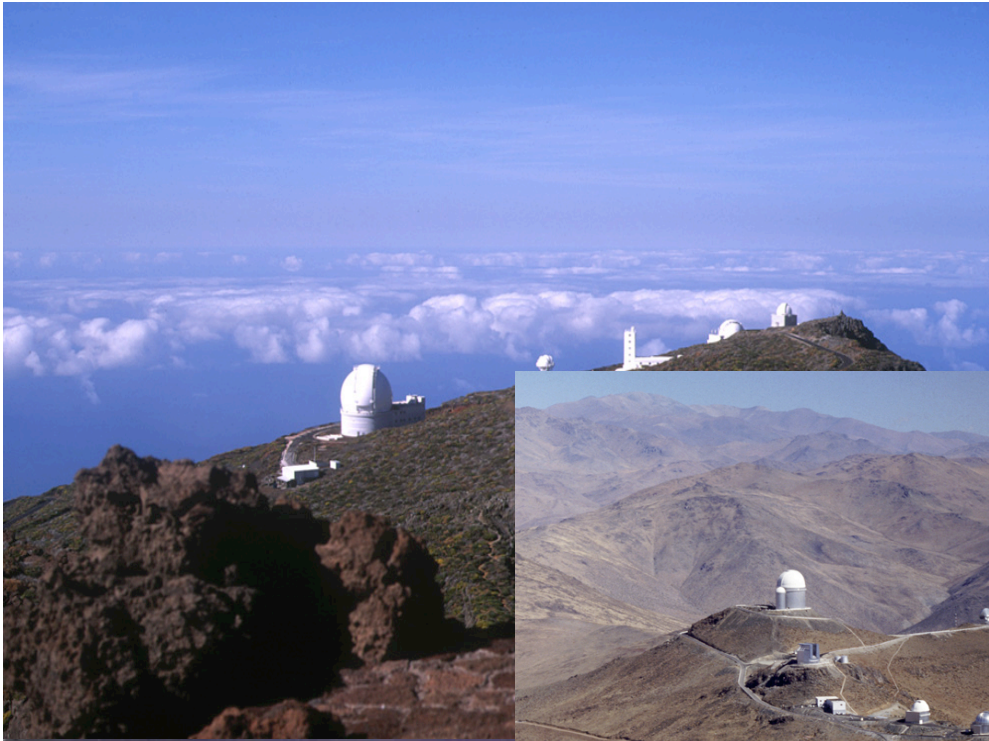


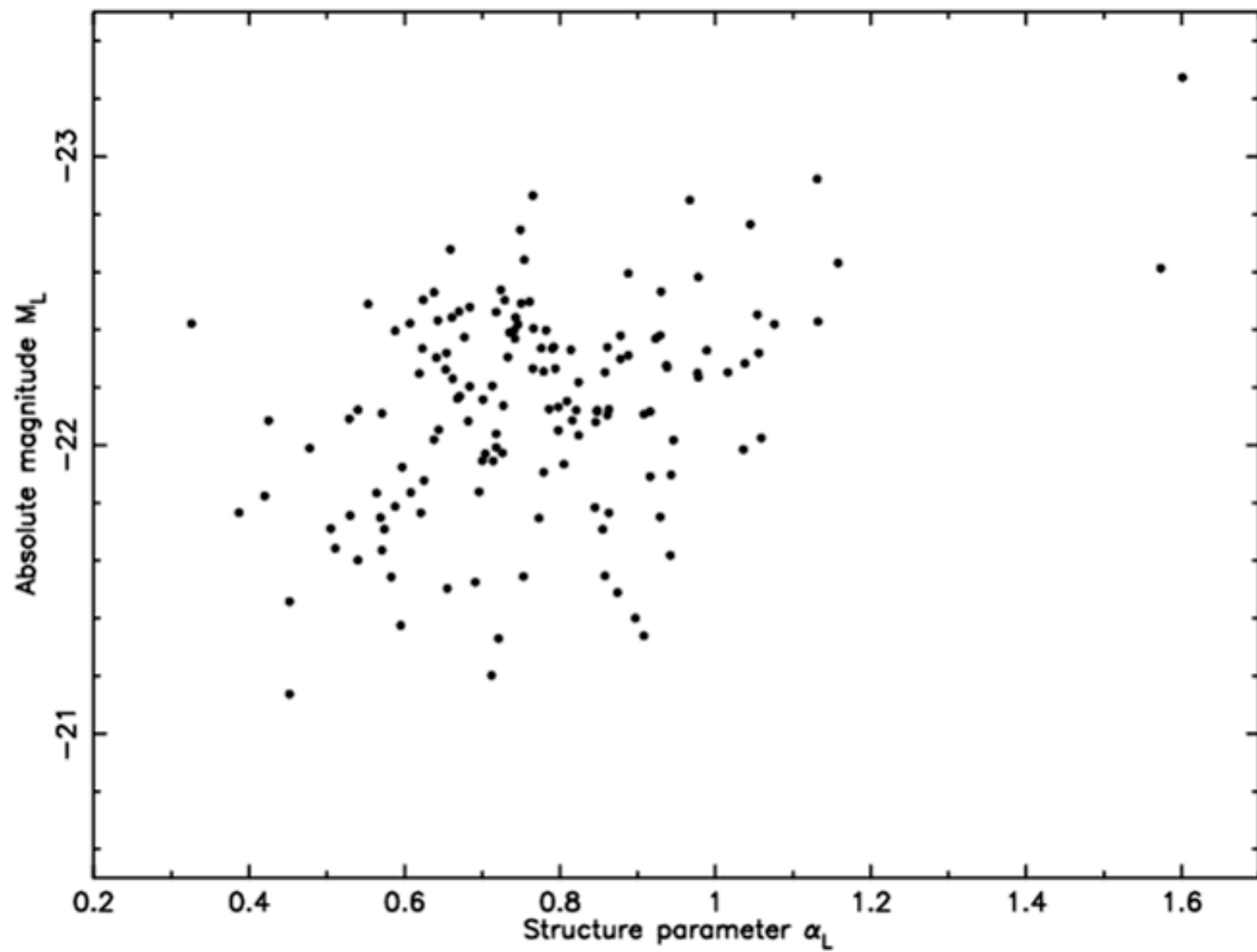
Advantages of X-ray Selection

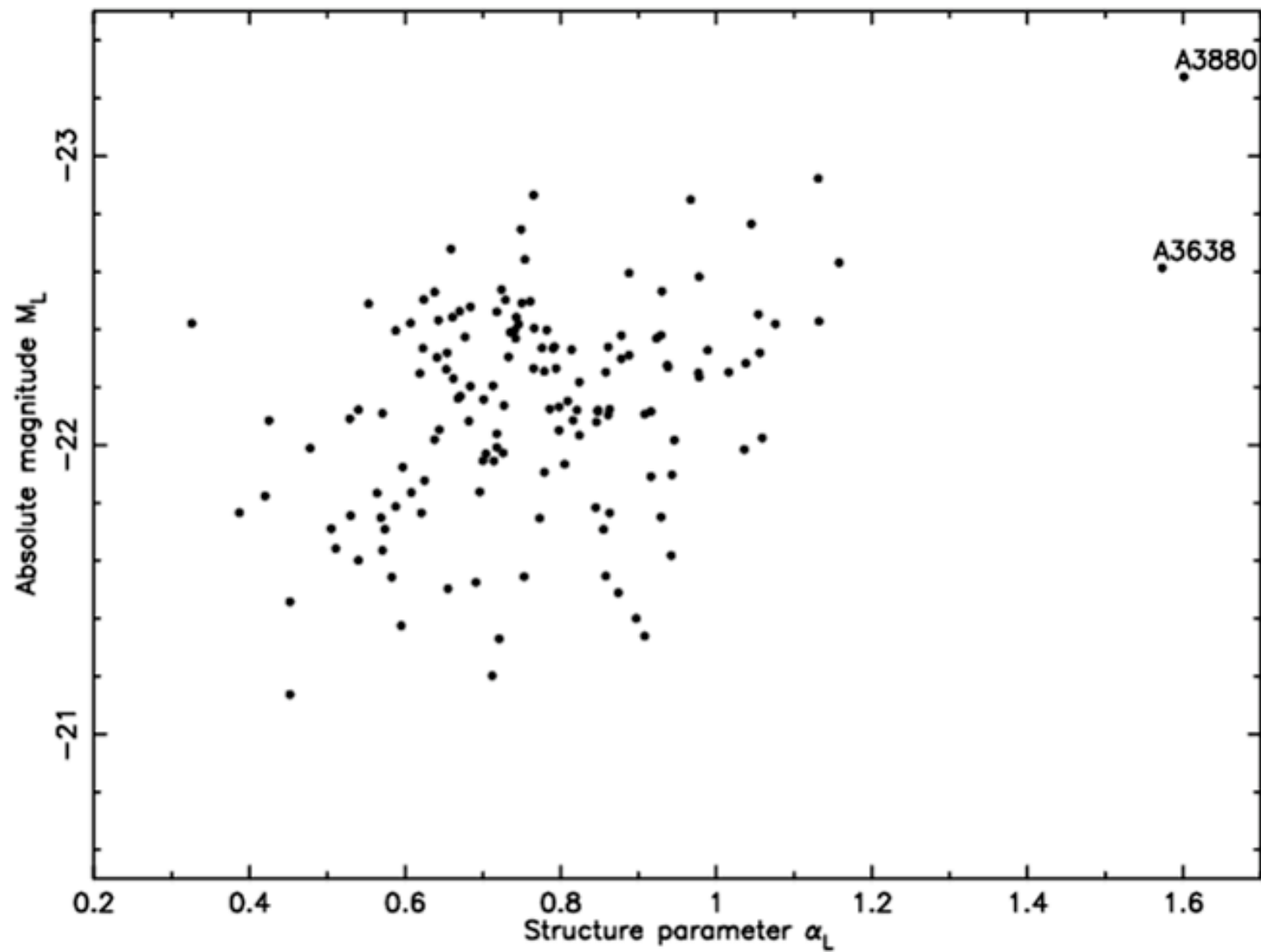
- Gas density more peaked than galaxy distribution, thus **reducing superposition effects**
- Low/No x-ray Measure **physical depth of *bona-fide* gravitational potential**
- background: **High contrast**
- Uniform, all-sky survey **eliminates systematics**

Lynam et al. Survey

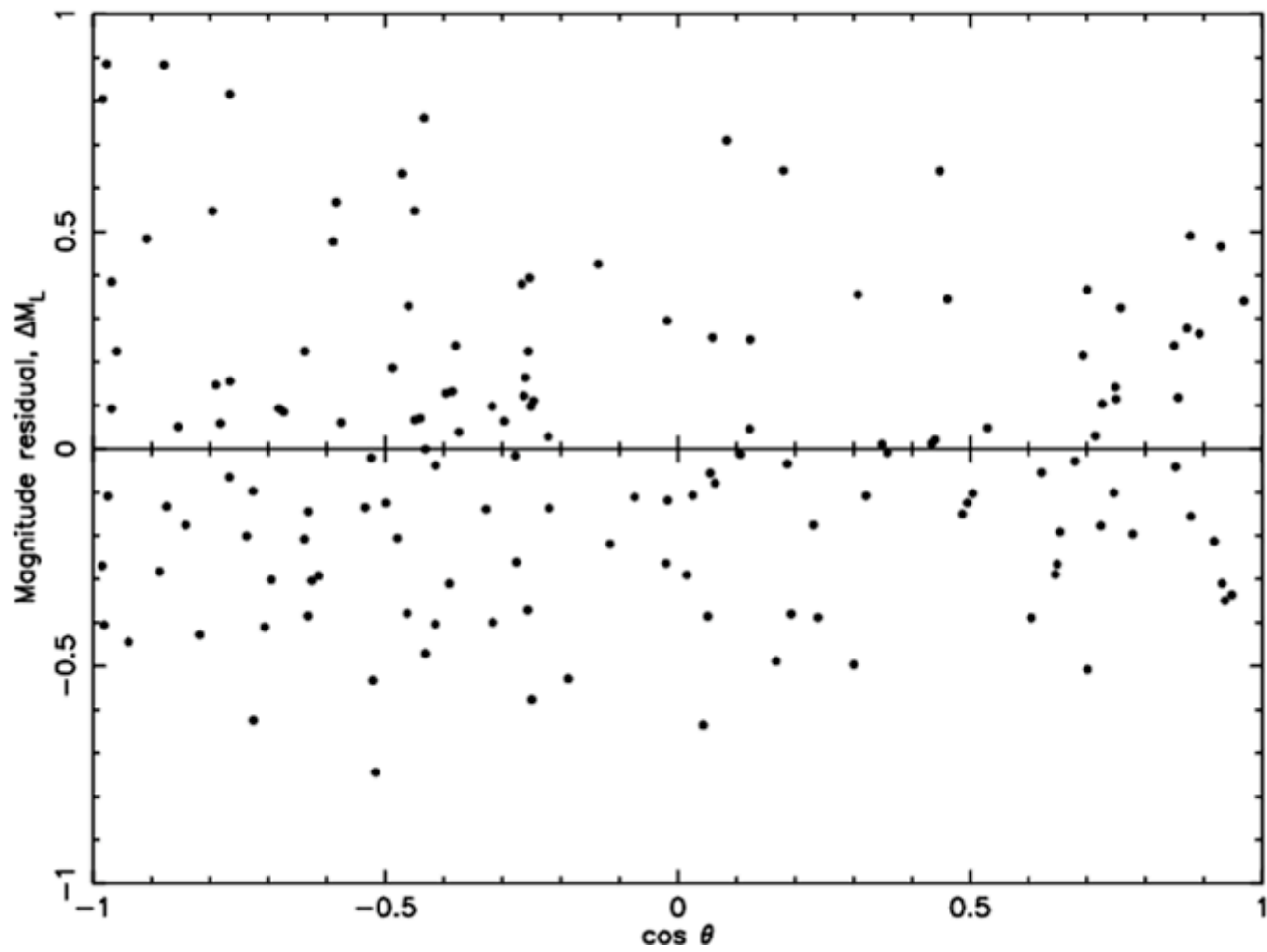
- ROSAT all-sky survey (REFLEX I (452) + NORAS), RASS II/III
- X-ray flux limit, $F_x \approx 3 \times 10^{-12} \text{ erg s}^{-1} \text{ cm}^{-2}$
- Number of clusters, $N = 145$
- Redshift limit, $z \sim 0.1$
- Photometry, $\Delta R \leq 0.03 \text{ mag.}$



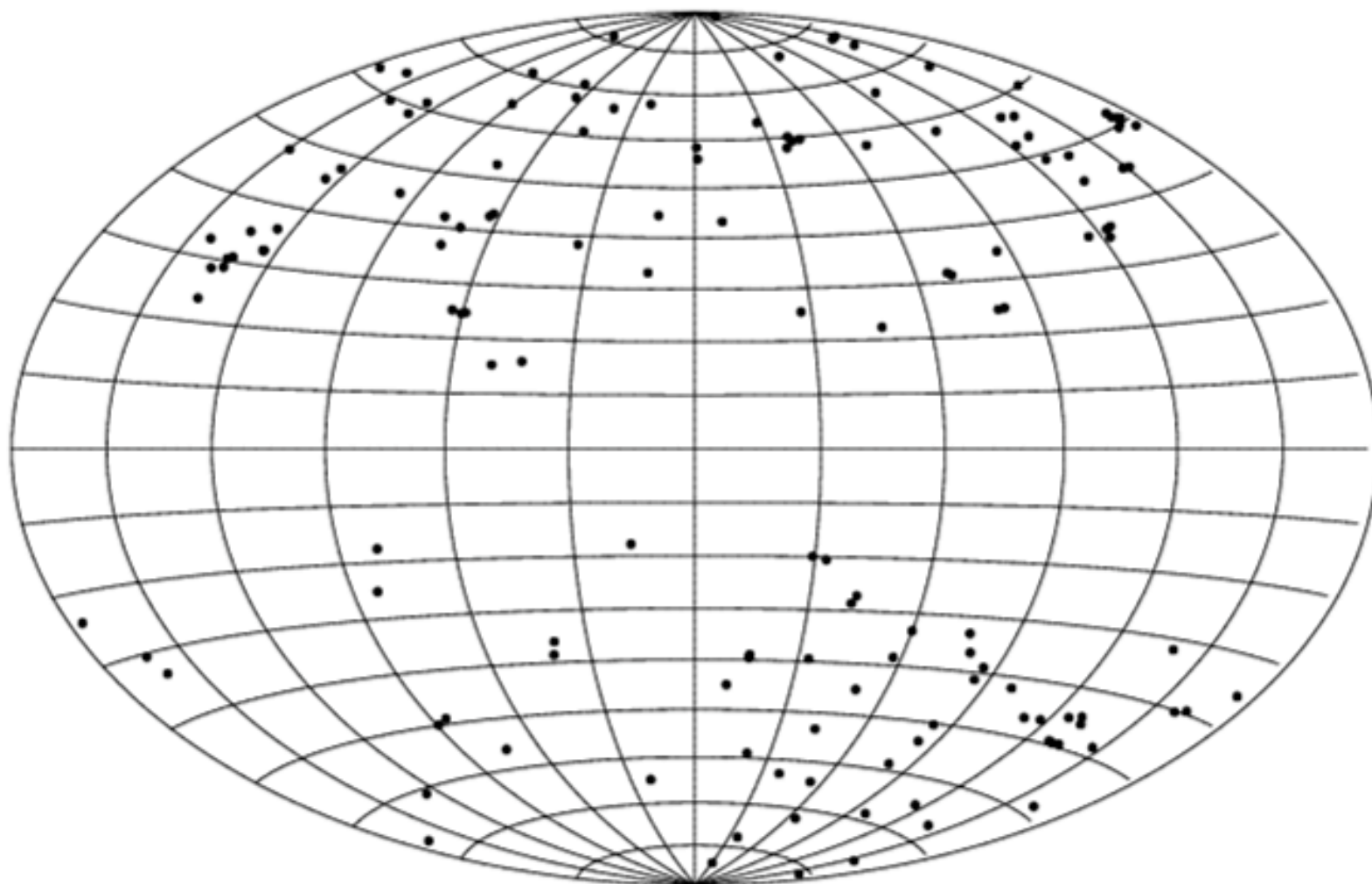




Photometric residuals as a function of position (Lynam et al. 2003)

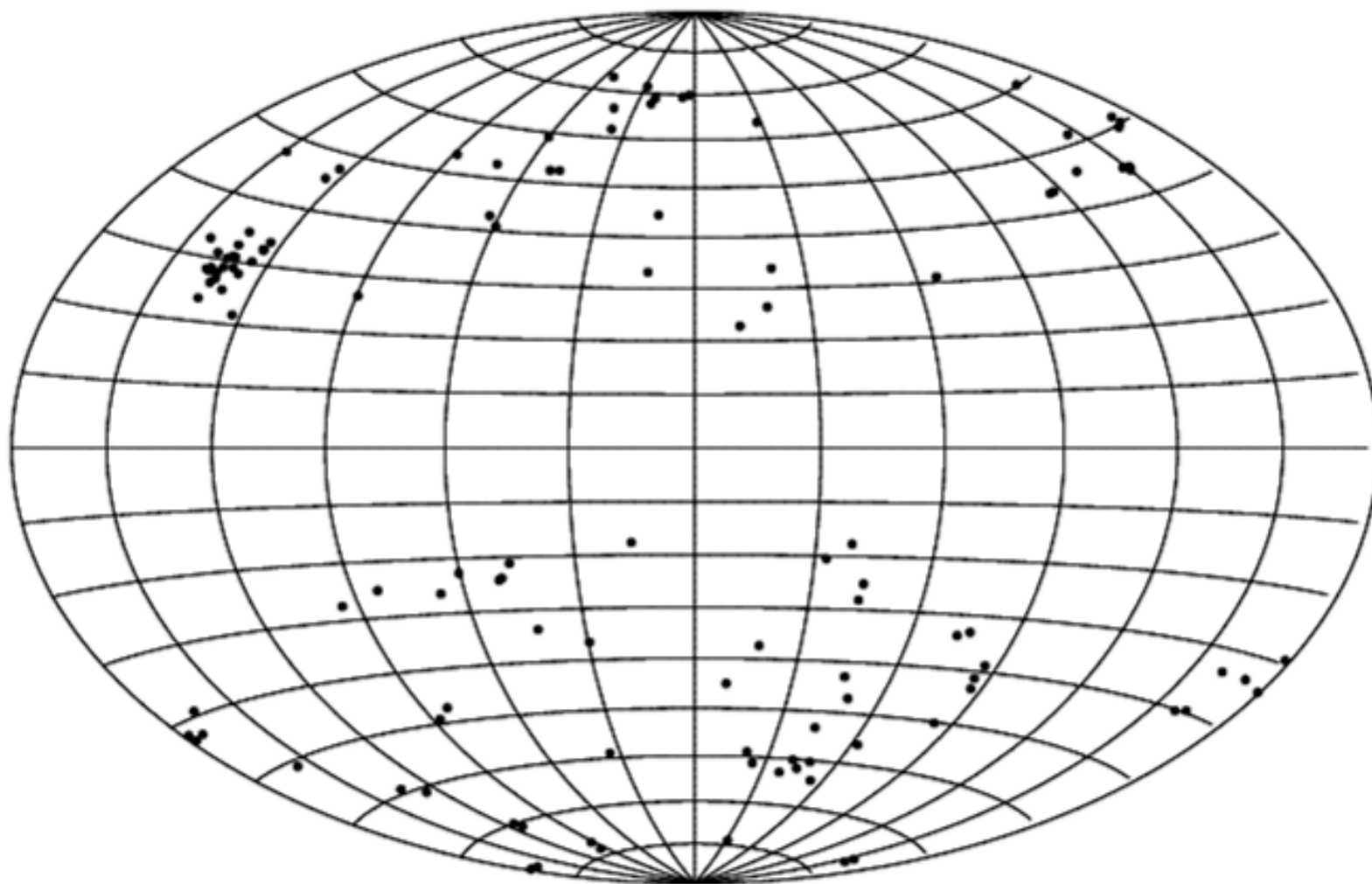


Lynam et al. X-ray Abell clusters within $z=0.1$



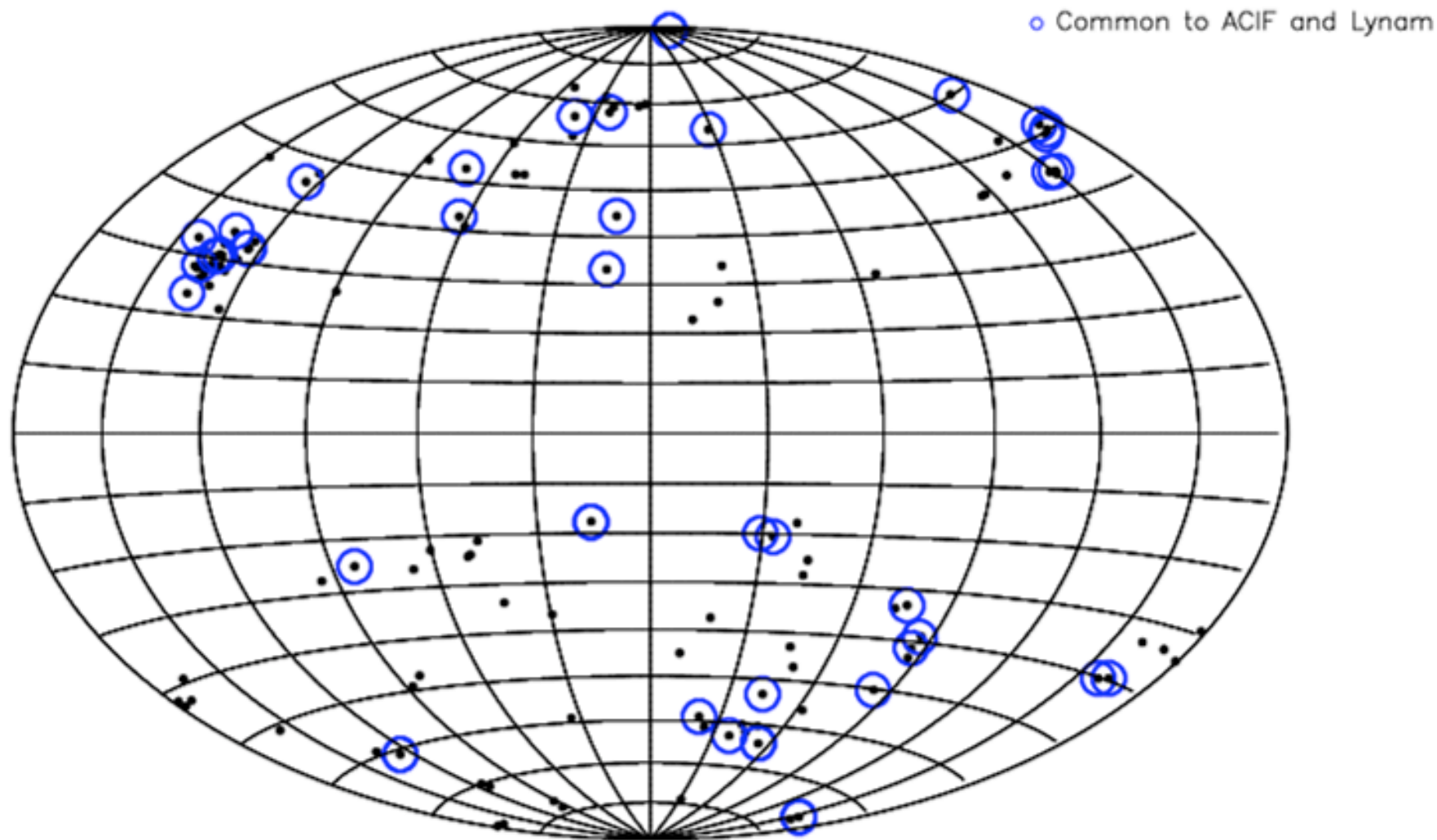
Conventional Aitoff projection, Galactic coordinates ($\alpha=12^h$ $\delta=0^\circ$)

Lauer & Postman (1994) *ACIF* clusters

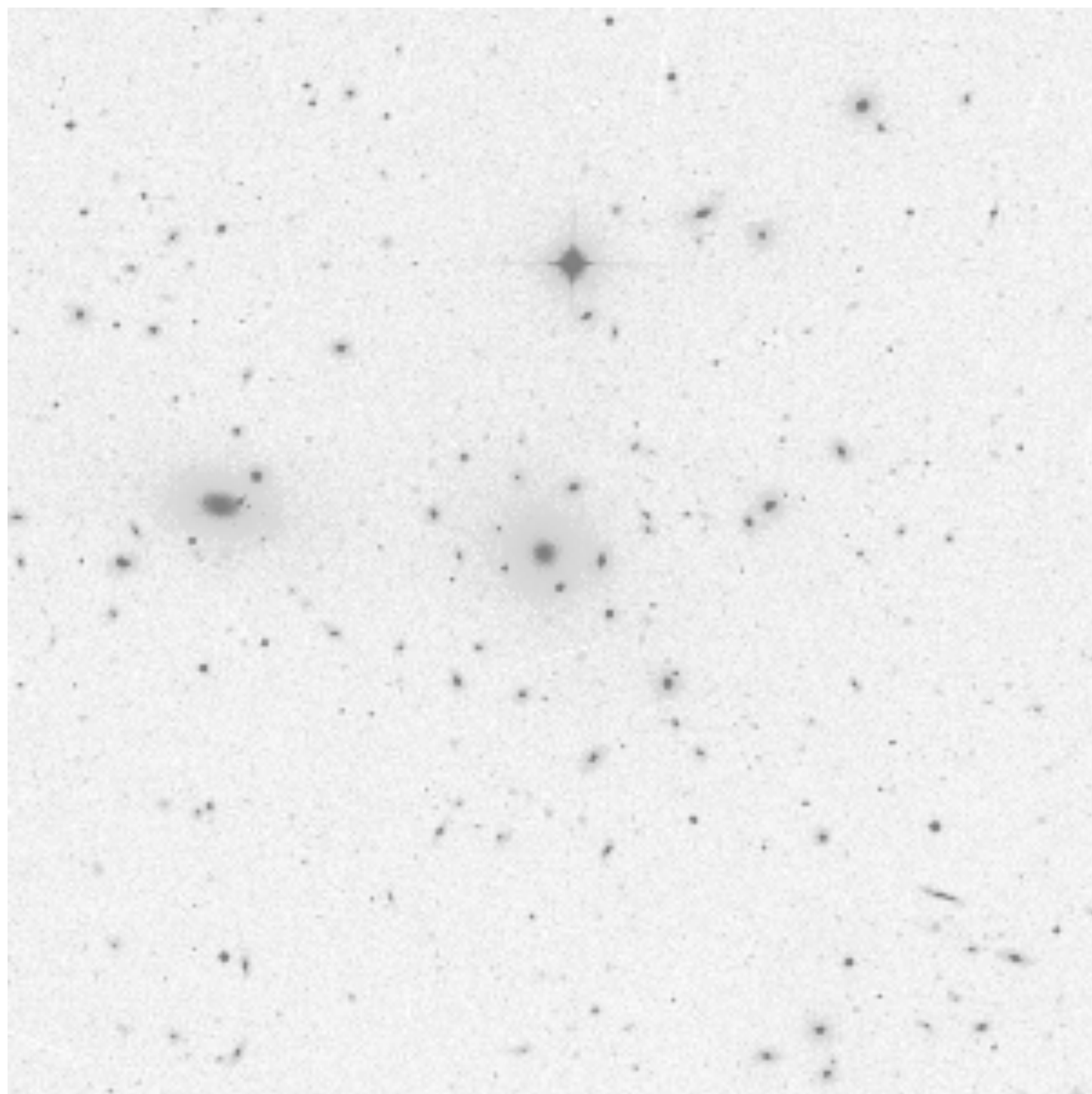


Conventional Aitoff projection, Galactic coordinates ($\alpha=12^h$ $\delta=0^\circ$)

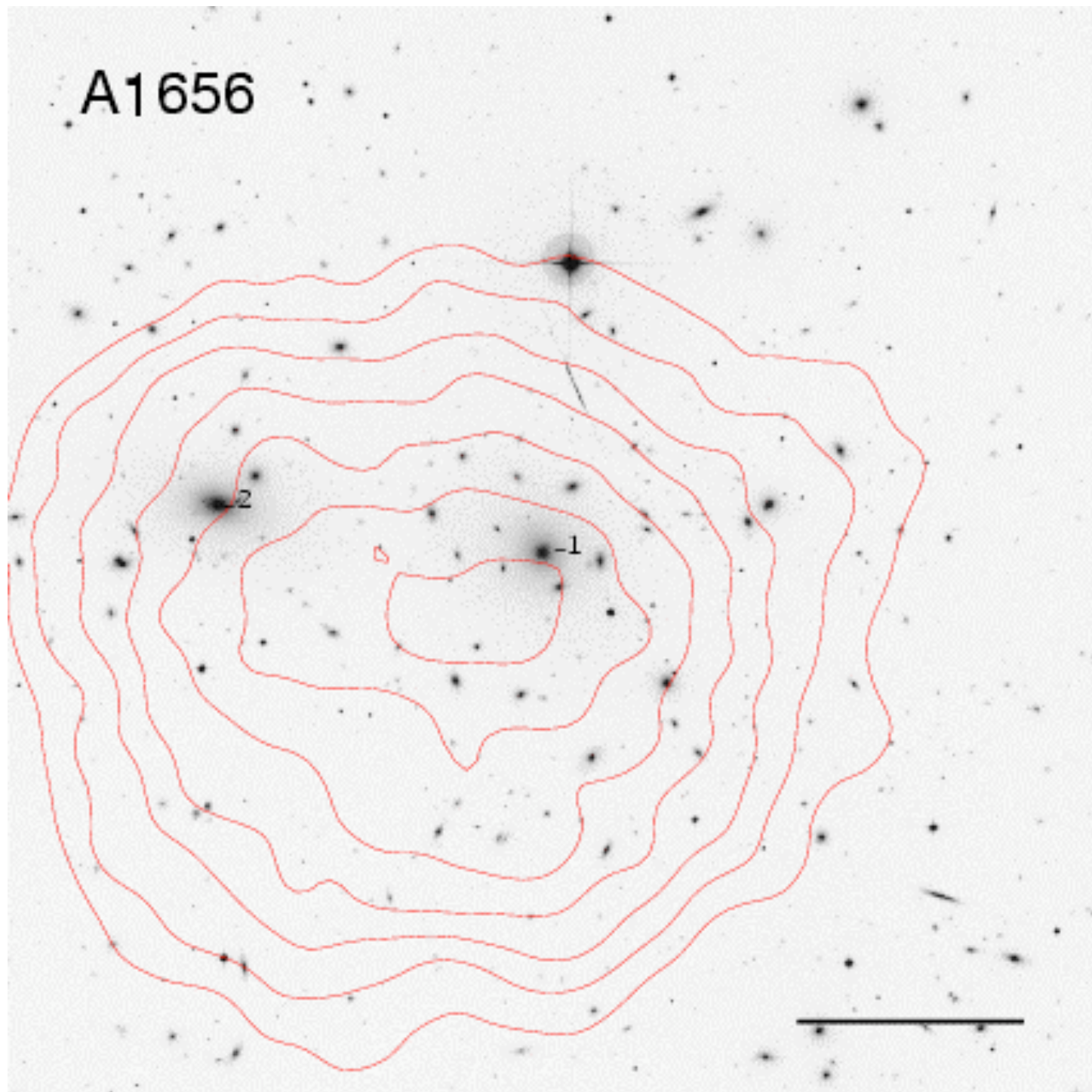
Lauer & Postman (1994) *ACIF* clusters



Conventional Aitoff projection, Galactic coordinates ($\alpha=12^h$ $\delta=0^\circ$)



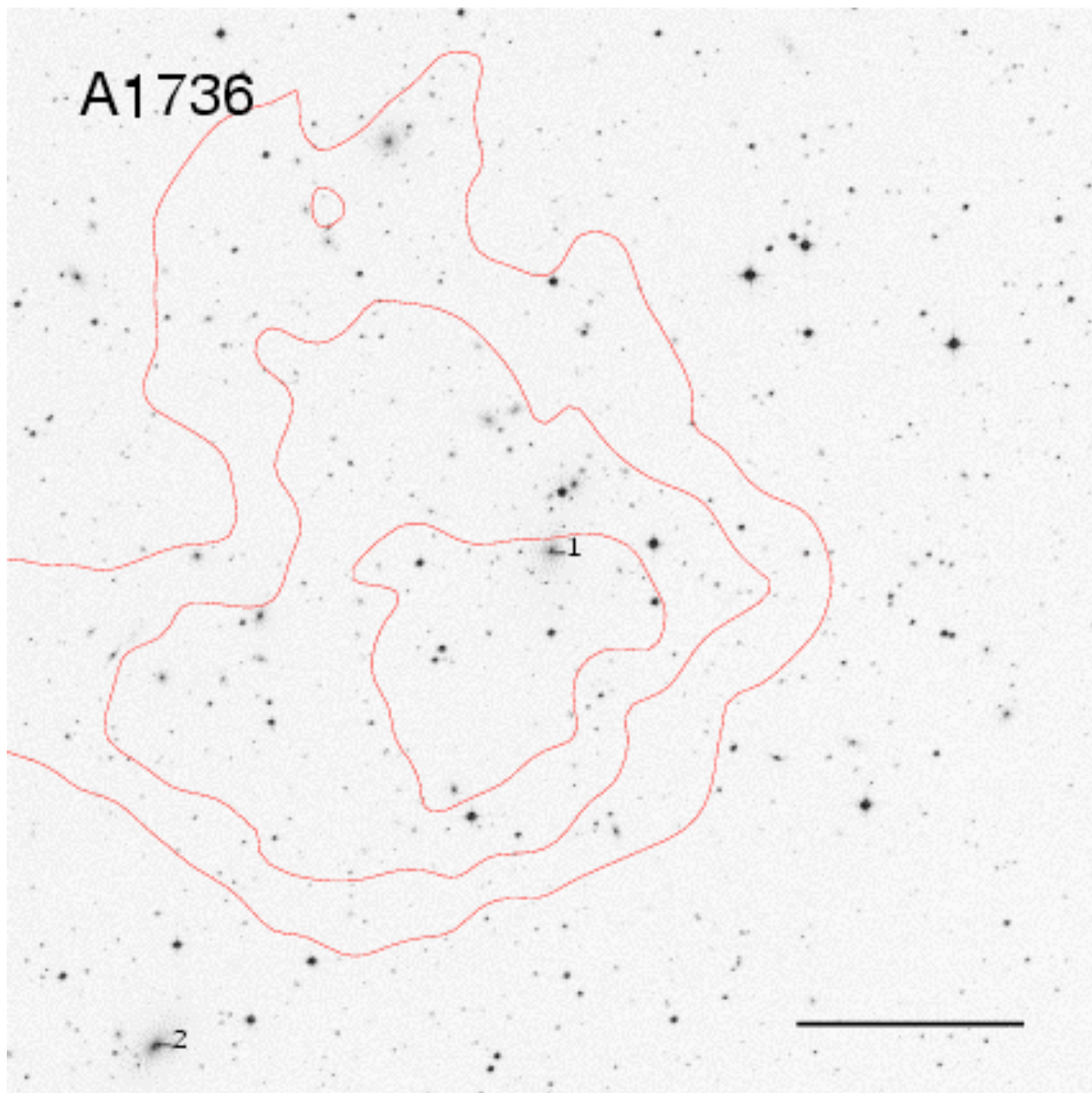
A1656



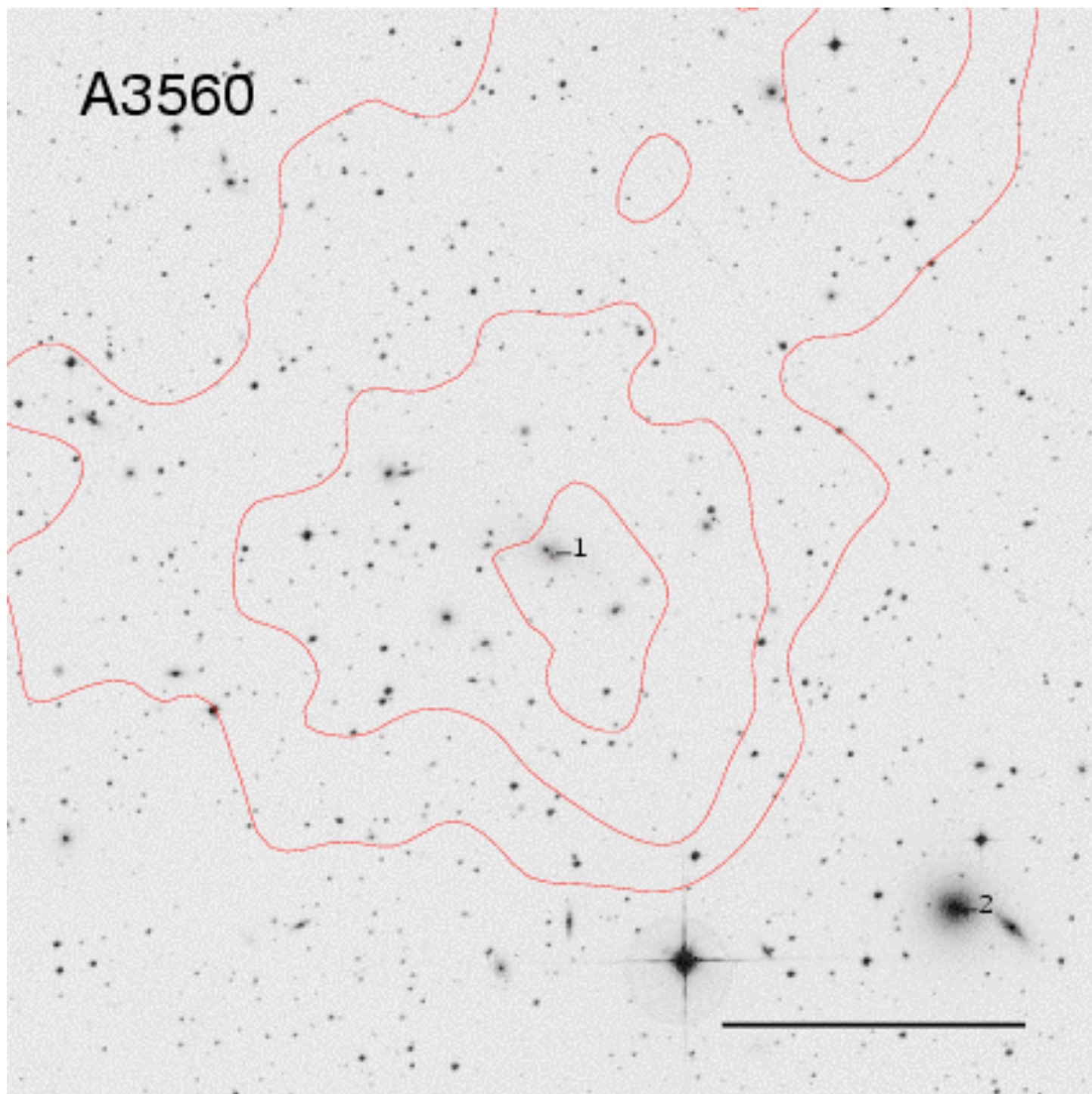
A1736

1

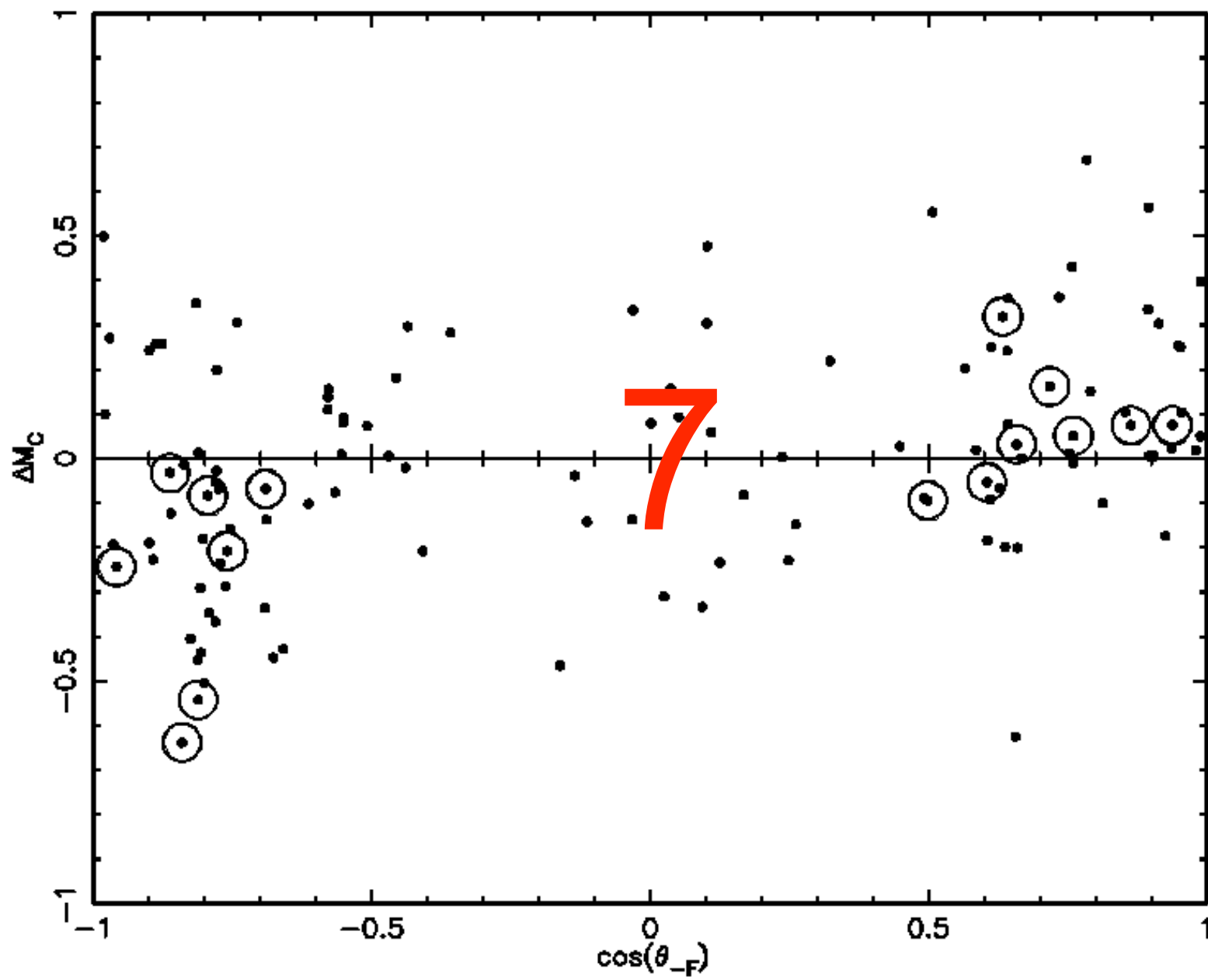
2

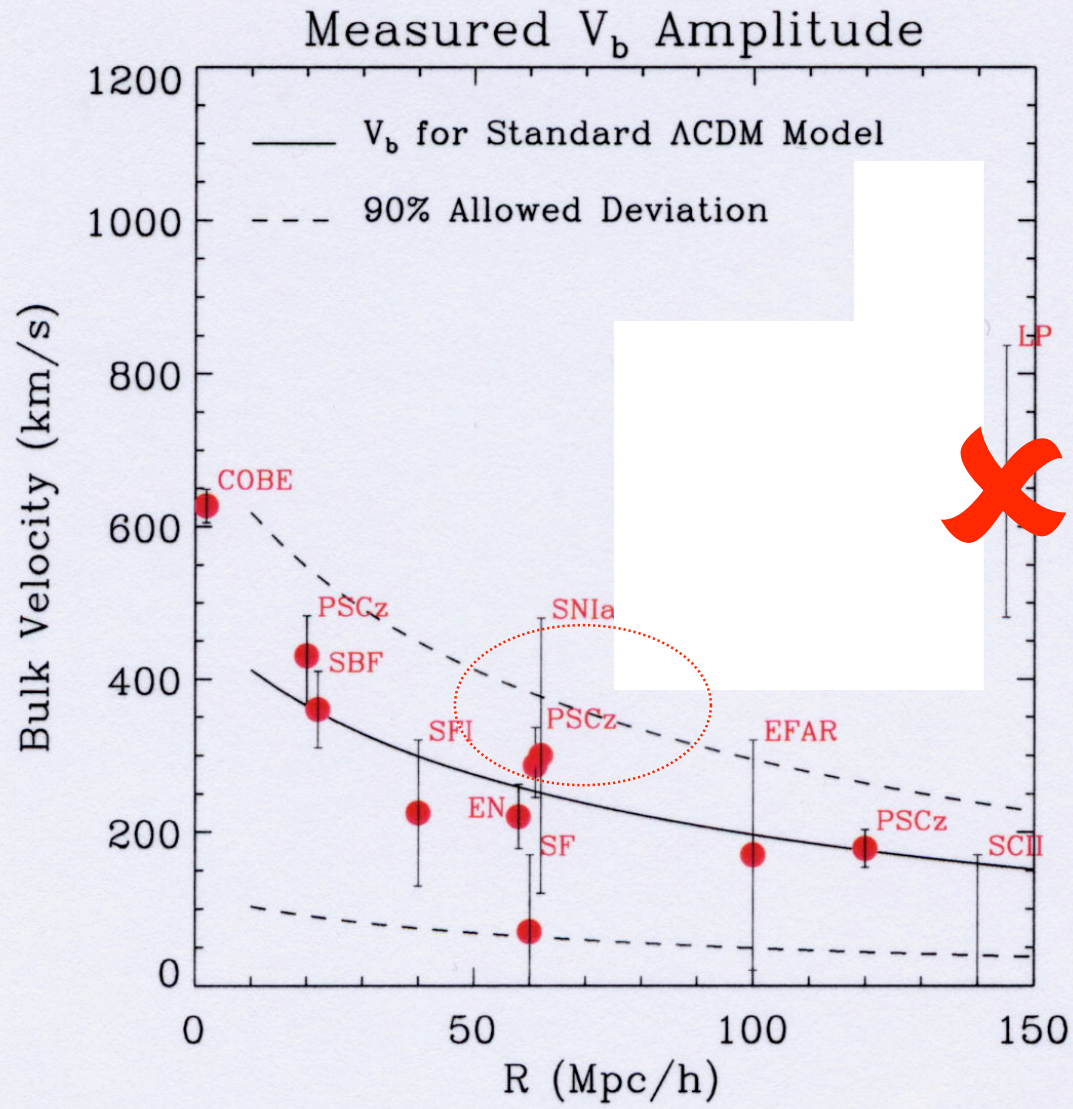


A3560



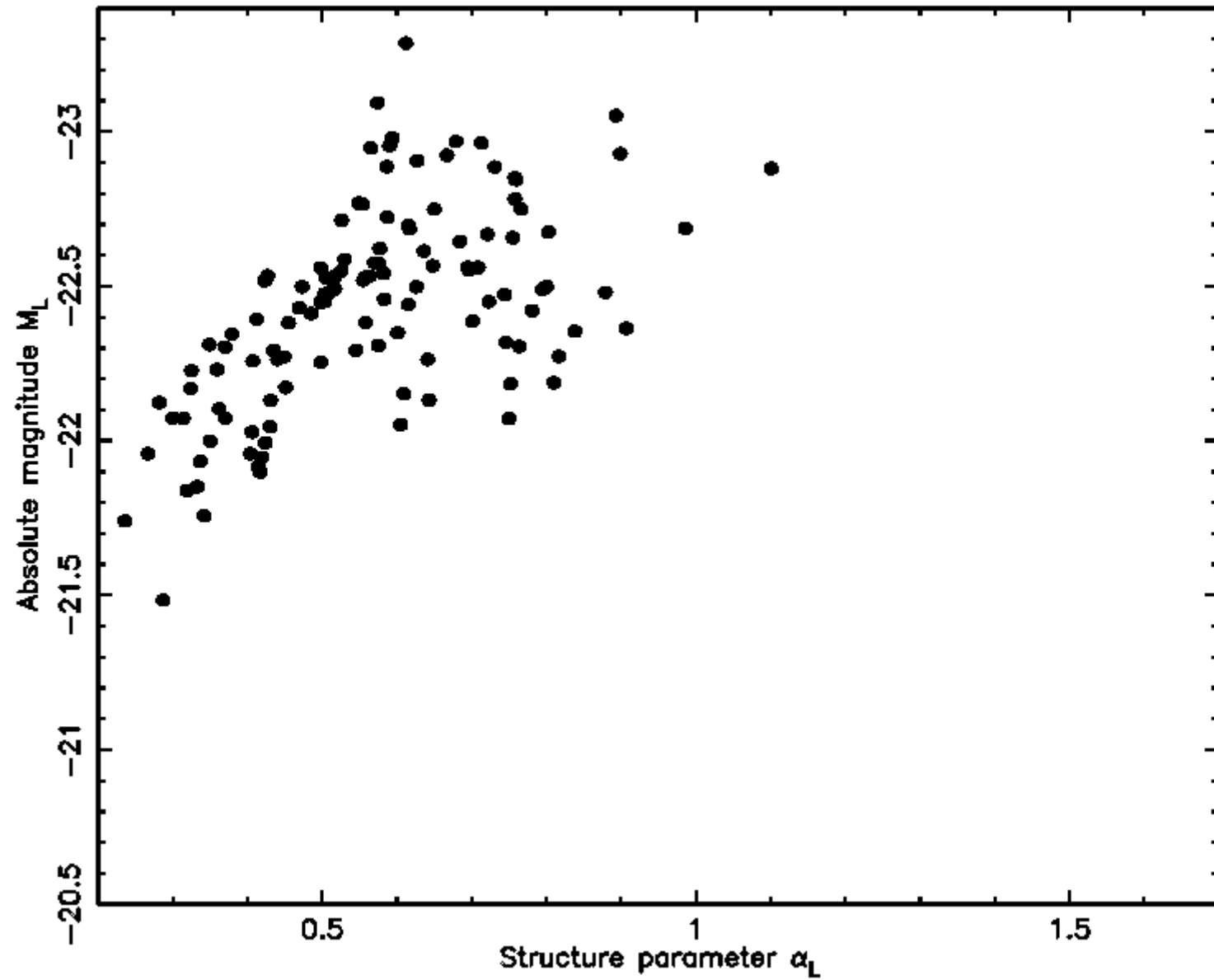
N = 119

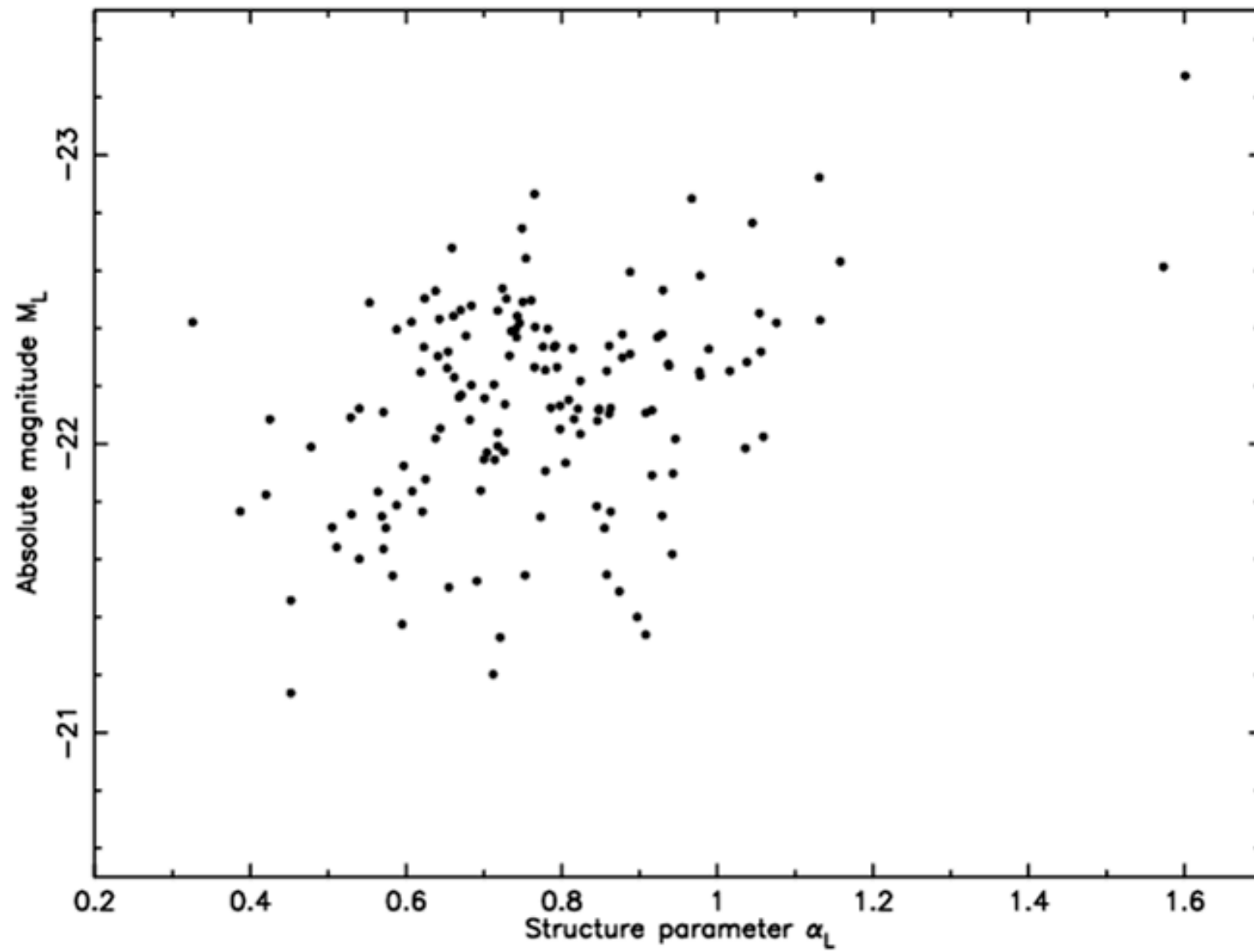




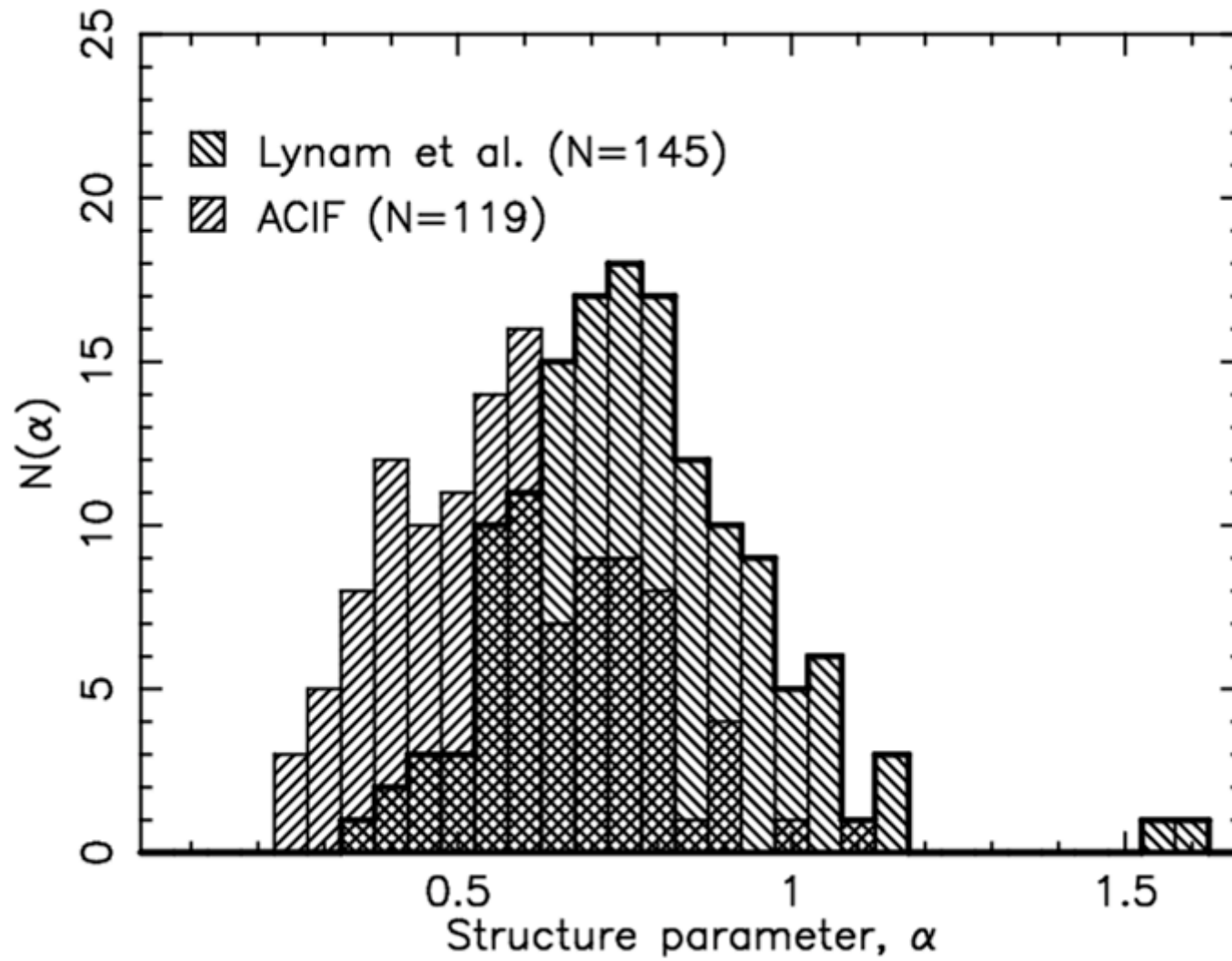
Conclusions: 1

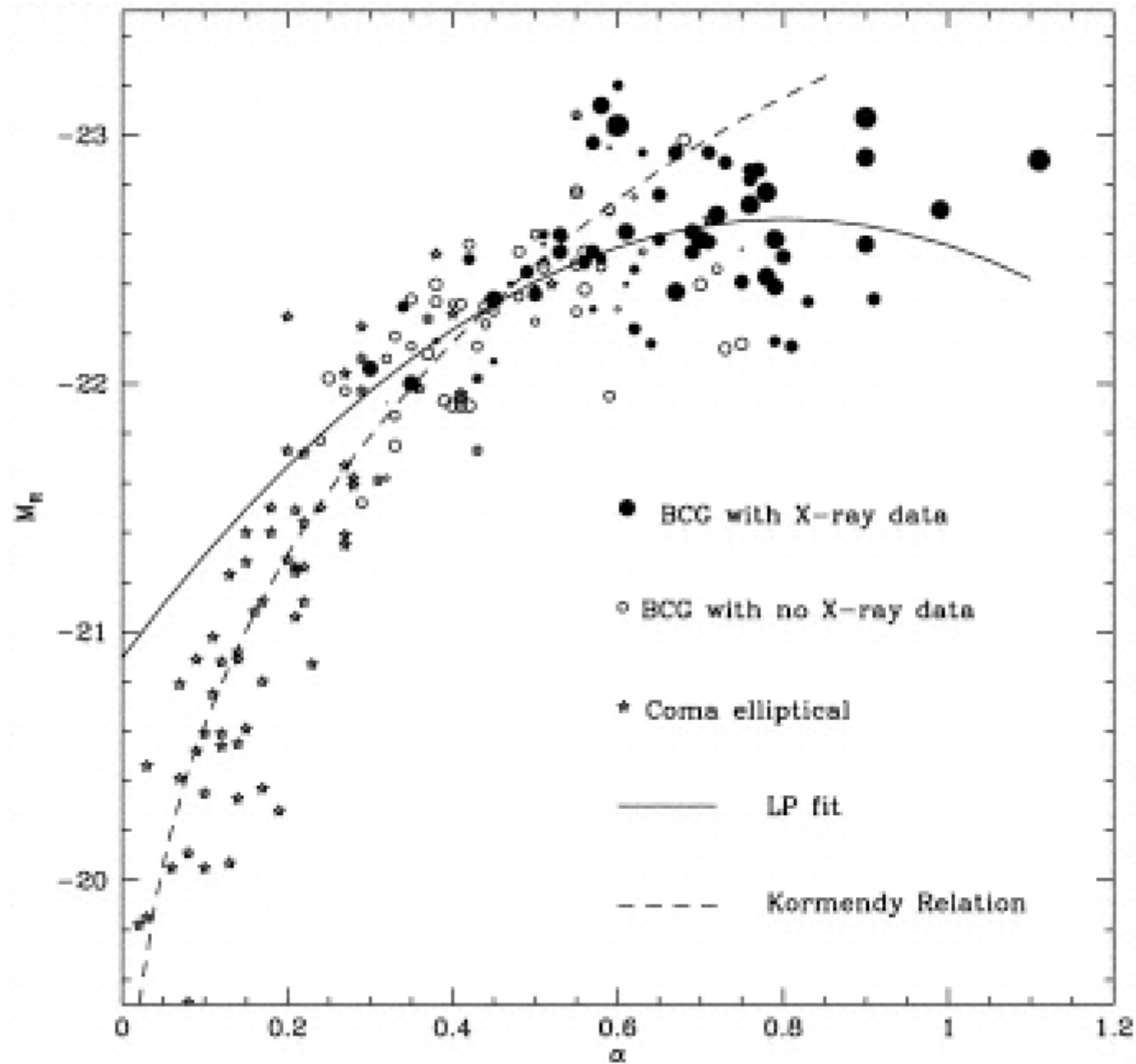
- Huge (~ 150 Mpc) pieces of material do *not* appear to be speeding around the Universe in excess of 600 km s^{-1}
- Perhaps the reliability of giant ellipticals as standard candles has been overstated





Distinguish between the 2 modes of a bimodal distribution





Hudson & Ebeling (1997) ApJ 479,621

cD Halos/ICL?

columns (1) and (2). The Rood-Sastry and Bautz-Morgan types (Struble and Rood 1987b) are listed in columns (3) and (4). The luminosities for the underlying galaxy (L_{gal}) and the cD envelope (L_{env}) are listed in columns (5) and (6) in units of solar luminosity assuming an absolute magnitude for the Sun of $M_V = 4.77$ and a $H_0 = 100 \text{ km s}^{-1} \text{ Mpc}^{-1}$. Fits of the cD envelope to the $r^{1/4}$ law (discussed in § IIIc) are listed in columns (7) and (8). The power-law slope, β , of the cD envelope is listed in column (9).

Errors resulting from the subtraction process were closely related to errors in the faint light levels between the envelopes and measured sky values. Comparisons between different templates and multiple profiles of the same cD galaxy gave an average error of ± 0.10 ($\log L$) for the envelope luminosities in Table 1. The largest error was associated with those envelopes with the shallowest slopes, where small deviations in the photometry produced large variations in calculated luminosity. A lower bound of $\log L_{env} = 9.0$ (e.g., see the profile for A779 in Paper I) was set by the impossibility of detecting such faint

ties were produced by direct subtraction ($\mu \text{ mag arcsec}^{-2}$) between the surface brightness profiles in the various bandpasses. Conversion to kiloparsecs was made using the redshifts of Struble and Rood (1987a), corrected for a Virgo infall of 300 km s^{-1} . A H_0 of $100 \text{ km s}^{-1} \text{ Mpc}^{-1}$ and a q_0 of 0 have been assumed.

III. DISCUSSION

a) Envelope Luminosities

Although extended envelopes in cD galaxies are faint in average surface brightness, they are large in area. This yields total integrated luminosities which are comparable to the luminosity of the underlying galaxy. Some of the envelopes from Paper I (e.g., A1413-G1 in Fig. 1) had no obvious cutoffs. In these cases, a pragmatic cutoff was assumed at the $30V \text{ mag arcsec}^{-2}$ level. Those profiles which do have cutoffs may have errors in their estimated sky level, thereby producing a sharp drop in the outer envelopes. Hence, the issue of how the edges

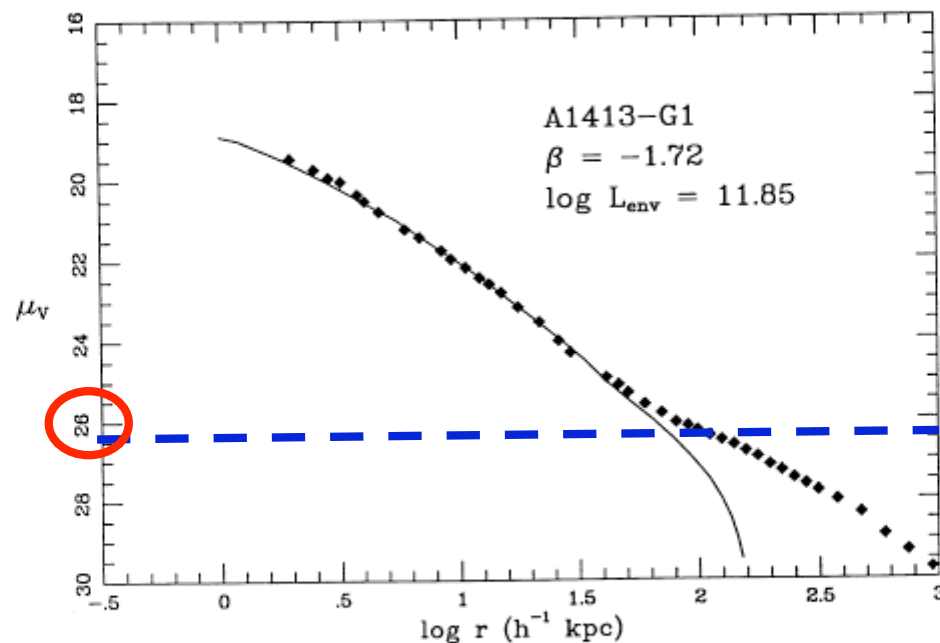


FIG. 1.—Surface brightness profile for the cD galaxy in A1413 (Oemler 1976) along with best-fit template from Paper II. Envelope luminosities in Table 1 are determined by direct subtraction of the template from the data, then summation of the remaining luminosity. This system contains one of the brighter envelopes in the sample.

It can be noted from inspection of Table 1 that, to first order, the galaxy and envelope luminosities are comparable. If the M/L of cD envelopes is similar to giant ellipticals (i.e., $M/L = 5-10$; Malumuth and Kirshner 1985) then the mass in a cD envelope contributes only as much mass to the cluster as one bright elliptical in the core. On the other hand, if the M/L values of cD envelopes are similar to the M/L envelope values for the giant D galaxy in A2029 (i.e., $M/L = 275$; Dressler 1979), then they may cause significant dynamical friction effects. If this M/L value is constant, then cD envelopes would also contain up to 15 times the mass of a first-ranked elliptical or $10^{13} M_{\odot}$.

A comparison of galaxy and envelope luminosities, $\log L_{env}$ versus $\log L_{gal}$ in solar units, is shown in Figure 2. L_{env} is weakly correlated with L_{gal} (a standard least-square correlation coefficient of $R = 0.6$), suggesting that cD envelopes share a common origin with the underlying galaxy (i.e., mergers; see Paper II). Several numerical studies (Villumsen 1982; Duncan, Farouki, and Shapiro 1983) have attempted to produce cD

envelopes of a type cD envelope. Since the luminosity of cD envelopes is often greater than the luminosity of the underlying galaxy, the possibility of a majority of the mass being heated to envelope scales by mergers or later tidal collisions is extremely unlikely. Thus, *mergers are insufficient as a source of cD envelope luminosity and scale*, but the correlation in Figure 2 is suggestive of a parallel process between the dynamical growth of a BCM and cD envelopes.

b) Envelope Colors

Stripping theory would propose that cD envelopes are predominantly blue because low luminosity and disk systems are more numerous and easier to strip than giant ellipticals (White 1982). Strom and Strom (1977) discovered evidence of this process in several nearby clusters by detecting a difference in the mean structure of galaxies in the cores versus galaxies with orbits in the outer regions. Furthermore, they also determined that galaxies with strong blue color gradients are less common centrally than in the outer cluster regions. This is interpreted as the blue halos having stripped from low-luminosity objects.

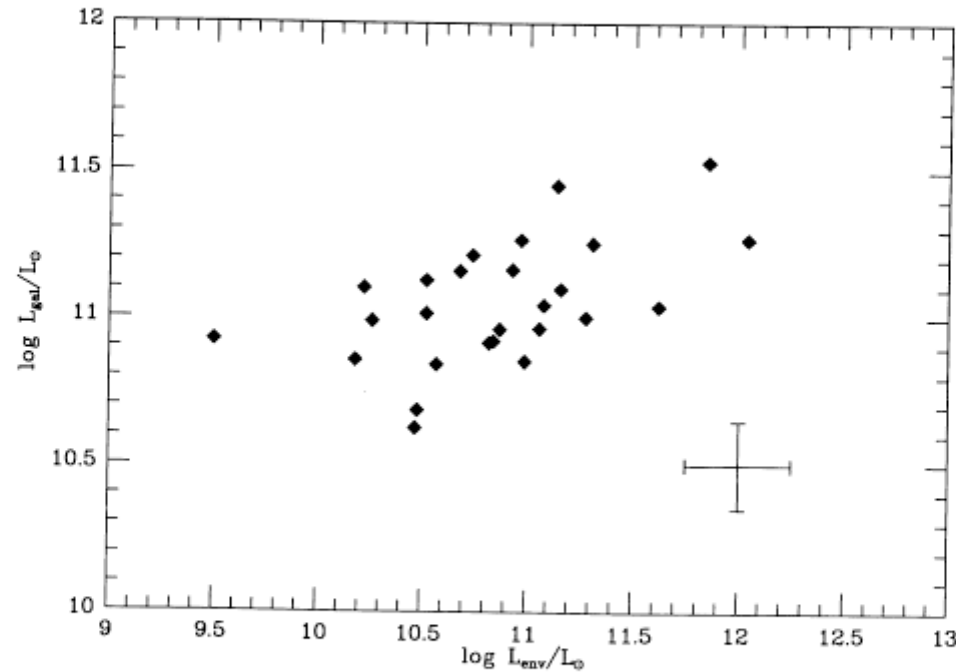


FIG. 2.—Luminosity of underlying galaxy, L_{gal} , vs. the luminosity of the cD envelope, L_{env} , in solar units. The weak correlation suggests a parallel process between cD envelope formation and the growth of the parent elliptical. Typical error bars are indicated.

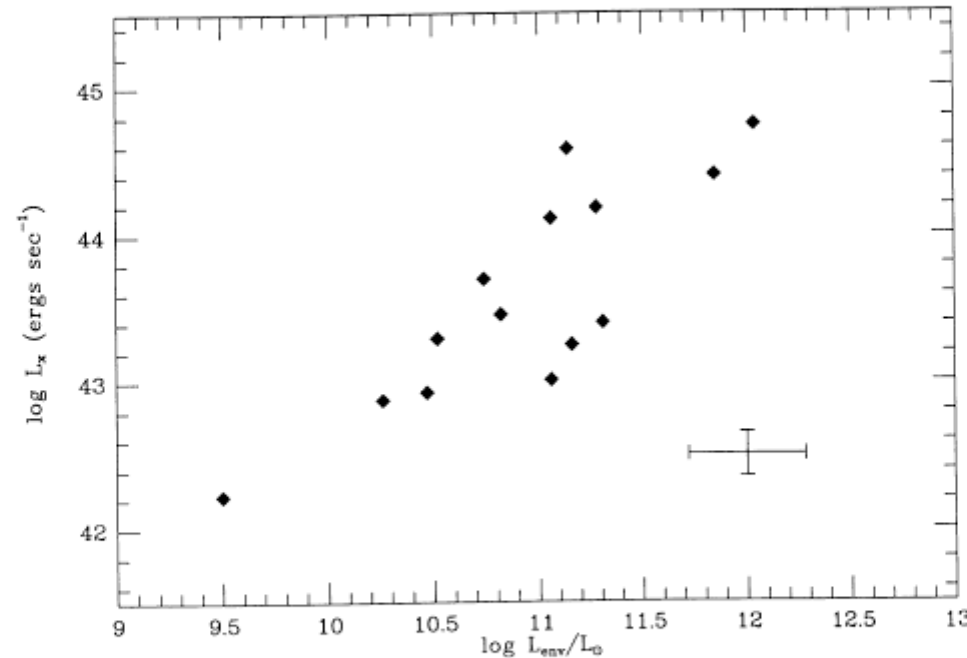


FIG. 10.—Total cluster X-ray luminosity (Valentijn and Bijleveld 1983) vs. envelope luminosity. This correlation ($R = 0.72$) is the strongest evidence in this study for a link between the dynamical state of a cluster and the luminosity of the cD envelope.

ticals such as NGC 4839 in Coma (Oemler 1976) and NGC 6034 in Hercules (Schombert 1984). However, all envelopes were found at local cluster density maxima (see also Beers and Geller 1983) and none was discovered in the field.

5. The envelope colors of three cD galaxies display no large deviations from the red color of the parent galaxy. This observation is a direct contradiction with the blue colors in cD envelopes found by Valentijn (1983).

6. The surface brightness profiles of cD envelopes are well fitted by the $r^{1/4}$ law extending the relationship of characteristic surface brightness and radii for BCMs from Paper II to cluster scale lengths. The power-law slopes of cD envelopes follow the same form as other luminous material in clusters (i.e., galaxies and globular clusters; $\rho \propto r^{-2.6}$), but do not conform to the distribution of hot X-ray gas ($\rho \propto r^{-2.1}$; Jones and Forman 1984).

7. A two-component model combining an underlying

measure of the depth of the cluster potential, and a strong indicator that cD envelopes are directly linked to the evolution of the cluster potential. Of course, the reverse causality situation must also be considered; cD envelopes induce more rapid cluster evolution and, thus, the envelope itself may be responsible for the high X-ray luminosity and deeper potential.

Although the data present here cannot definitively determine which formation theory for cD envelopes is correct, the observations can discriminate between various predictions and provide more information for speculation. For example, based on the red envelope colors it is clear that recent star formation has not occurred in cD envelopes. In fact, since the colors of the envelopes are so similar to the colors of the parent galaxy, it is unlikely that even the biased star formation proposed by Fabian, Nulsen, and Canizares (1984) for cooling flows can reproduce the expected mass and M/L suggested by the two component model. While this process may result in an

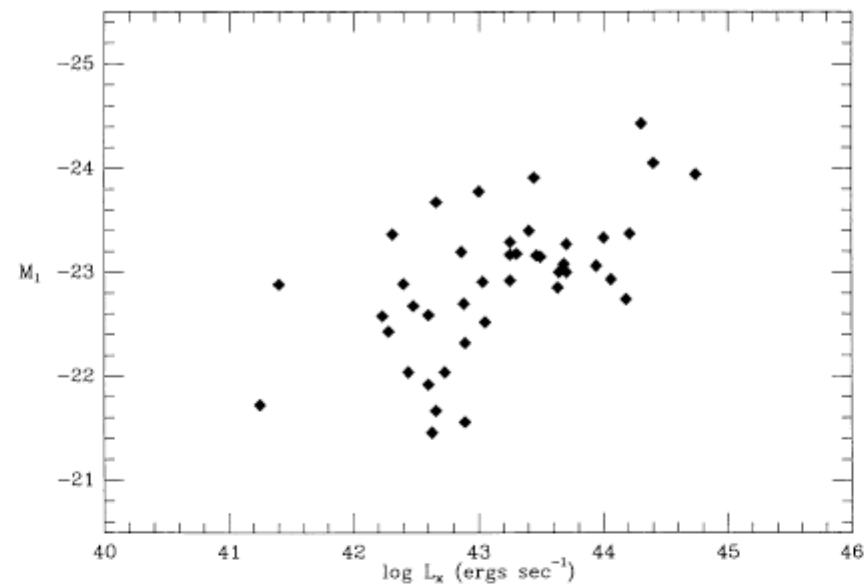


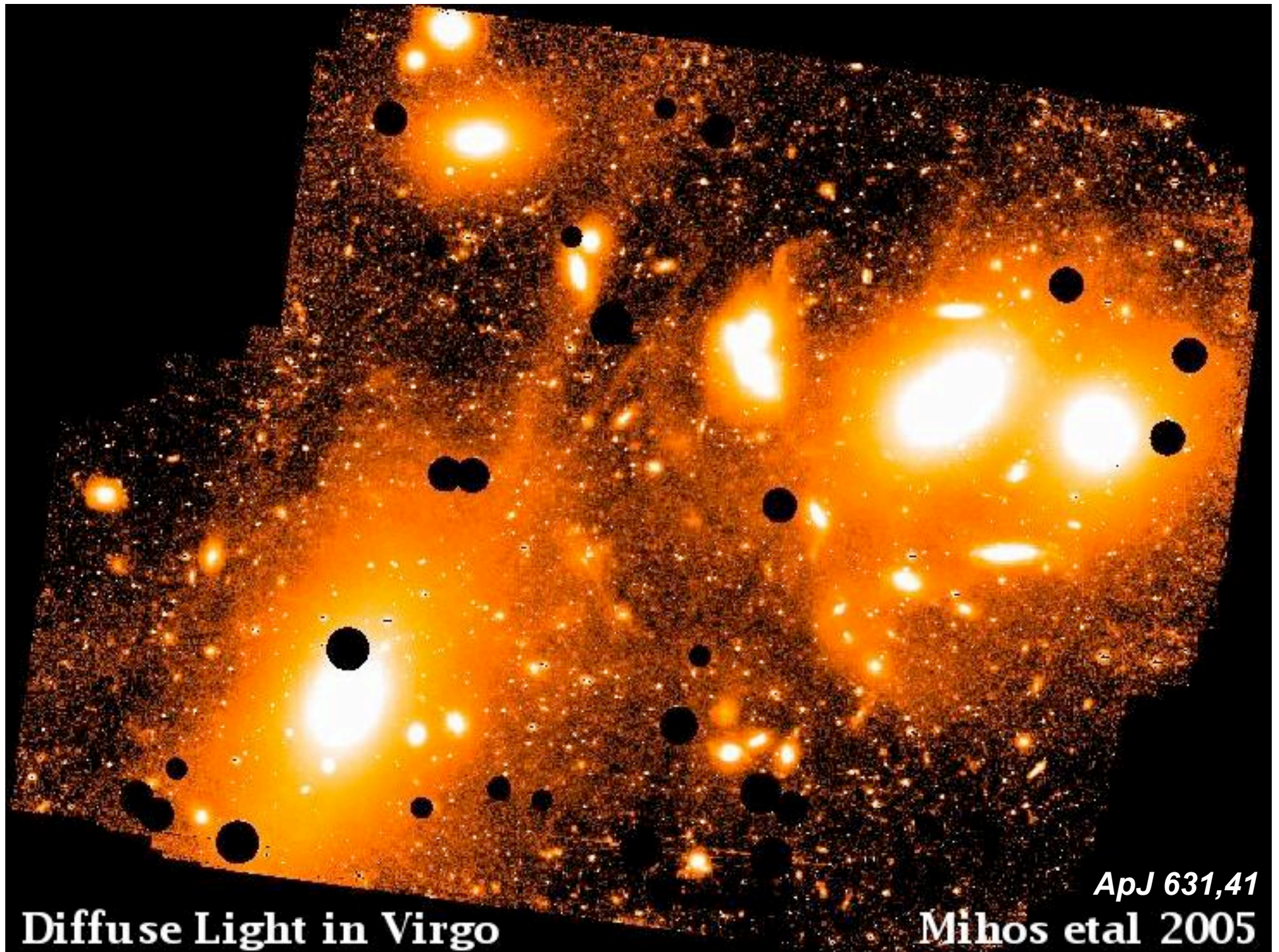
FIG. 13.— M_1 vs. total cluster X-ray luminosity. Another weak correlation with a global parameter that measures the dynamic state of the cluster argues that the dynamical growth of BCMs must have been an early process as proposed by Merritt (1984); see discussion in text.

correlation (coefficient = 0.67) is present, with brighter BCMs occupying clusters with high velocity dispersions. The underlying physics is not clear in this situation. It is expected from a simple theory of cannibalism that a cluster with a lower velocity dispersion would have a higher rate of mergers and, hence, a brighter BCM. The average velocity dispersion of the bound population to a BCM is expected to be similar to the internal velocity dispersion of the galaxy, on the order of $200\text{--}300\text{ km s}^{-1}$ (Cowie and Hu 1986). On the other hand, it has been argued by Tonry (1985) that the low-velocity members are missing in evolved clusters because they have already merged with the central members. With this low-velocity population disappearing, the average cluster velocity dispersion would increase. It is this second scenario that is supported by Figure 12. Figure 13 displays BCM luminosity versus cluster X-ray luminosity from Valentijn and Bijleveld (1983). Although there is a slight tendency for brighter BCMs to be associated with X-ray-luminous clusters, this correla-

tion is weak. It is possible that the BCMs are part of a bound population of accreting galaxies, but it remains unclear whether BCMs are still undergoing mergers with the multinucleus companions.

IV. CONCLUSIONS

The main purpose of this paper is to support the idea that BCMs have particular structural deviations, as seen in surface photometry profiles, which are best explained by comparisons with merger simulations. These special properties are enlarged characteristic radii, shallow profile slopes, and high inner surface brightnesses. From the appearance of the profiles, it is possible to outline the morphological types gE, D, and cD ellipticals: gE galaxies are typified by their large size, D galaxies are a gE type with a very shallow slope ($\beta < -1.7$) and cD galaxies are a D type with a large, faint extended envelope.

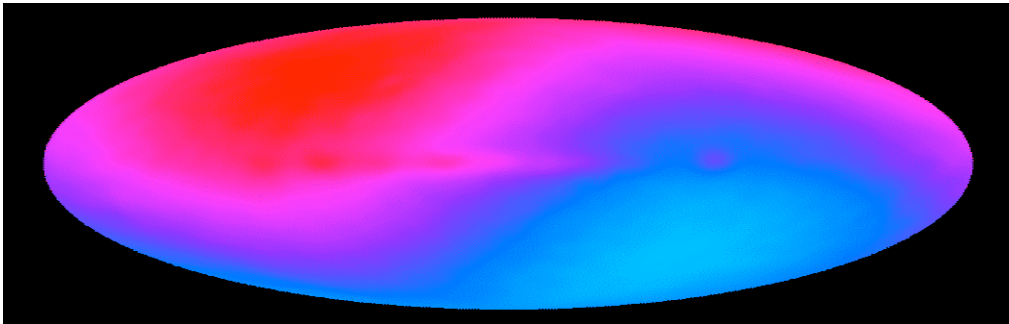


Diffuse Light in Virgo

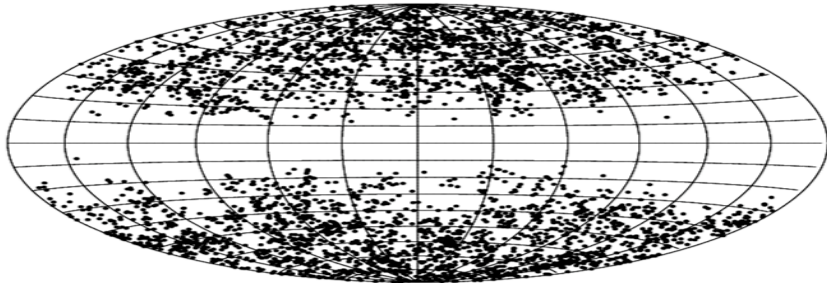
ApJ 631,41
Mihos et al 2005

Conclusions: 2

- Evidence suggesting the underlying distribution of cluster giant ellipticals is bimodal (M , α , L_x)
- The properties of the modes are moderated by the location of the galaxy within the cluster, the depth of the gravitational potential & may reflect evolution
- Since they appear to respond to global cluster properties, evolution in the giant elliptical may reflect evolution of the cluster as a whole



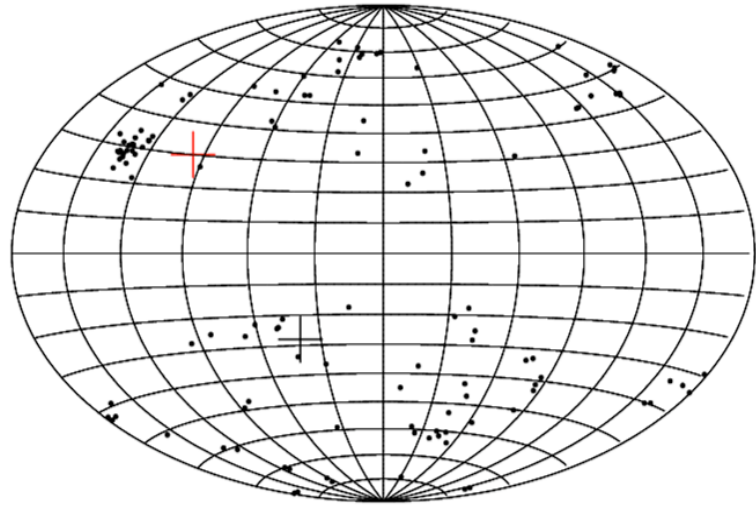
Abell (1958) and Abell, Corwin and Olowin (1989) clusters



Conventional Aitoff projection, Galactic coordinates ($\alpha=12^h$ $\delta=0^\circ$)

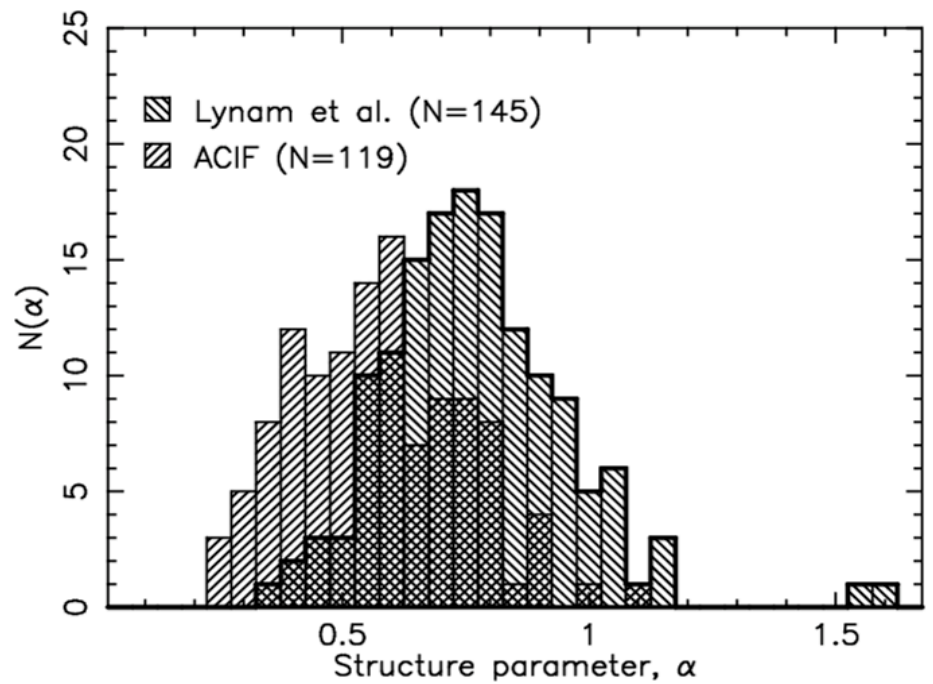
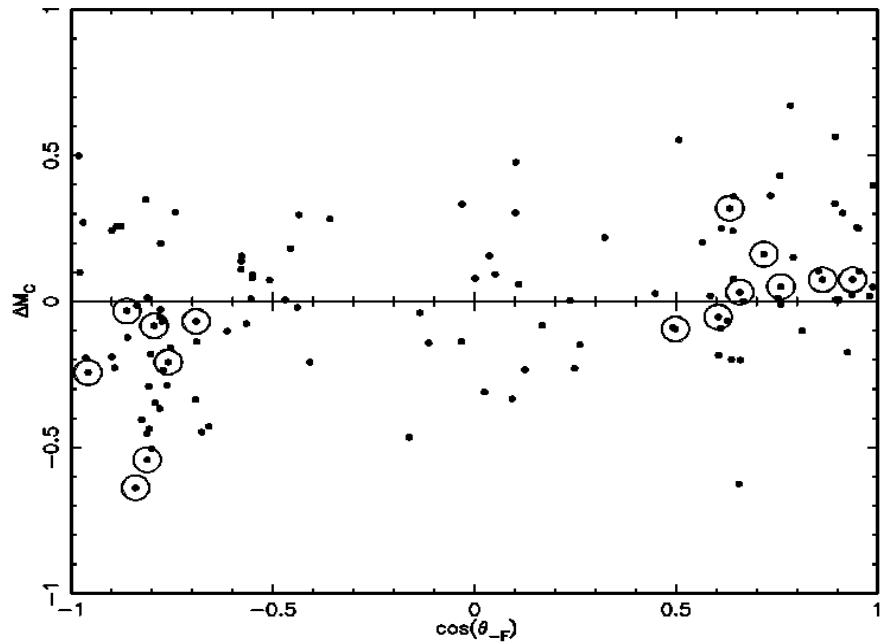
Lauer & Postman (1994) *ACIF* clusters

- + CMB Hot Pole
- + Apex of LG w.r.t *ACIF*

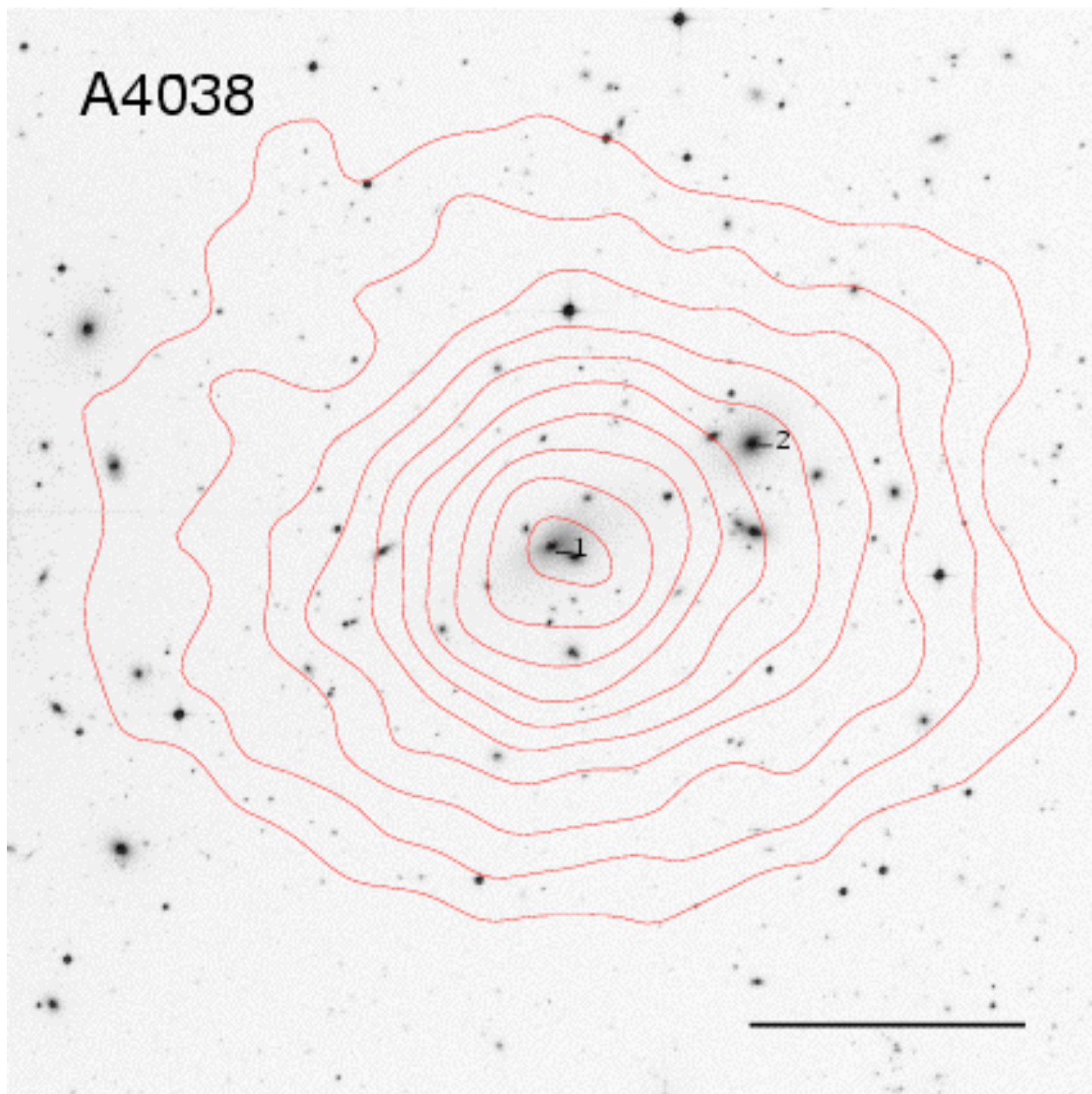


Conventional Aitoff projection, Galactic coordinates ($\alpha=12^h$ $\delta=0^\circ$)

N = 119



A4038



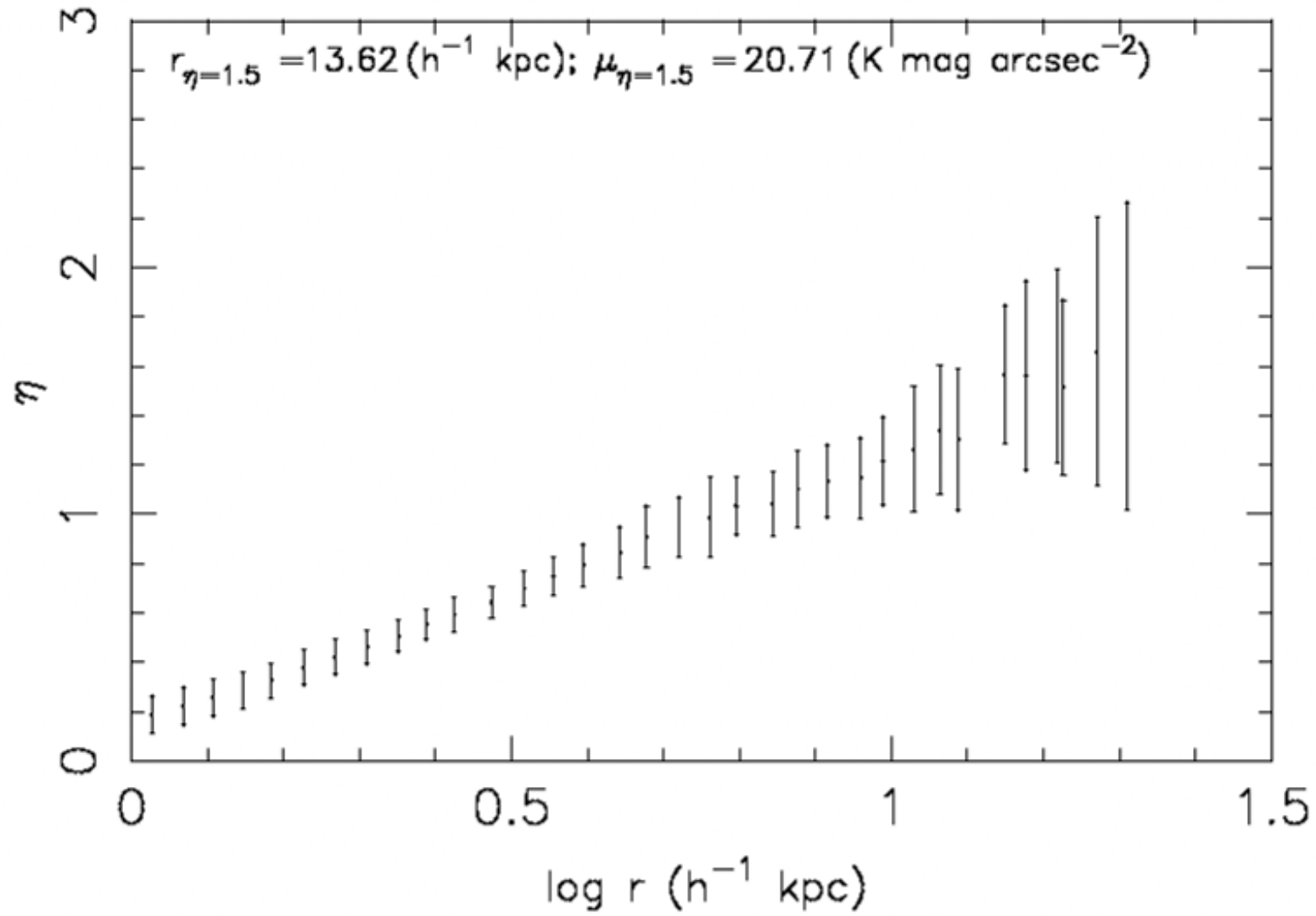
Petrosian Radius

- Petrosian Radius (Petrosian 1976 ApJ 209, L1):

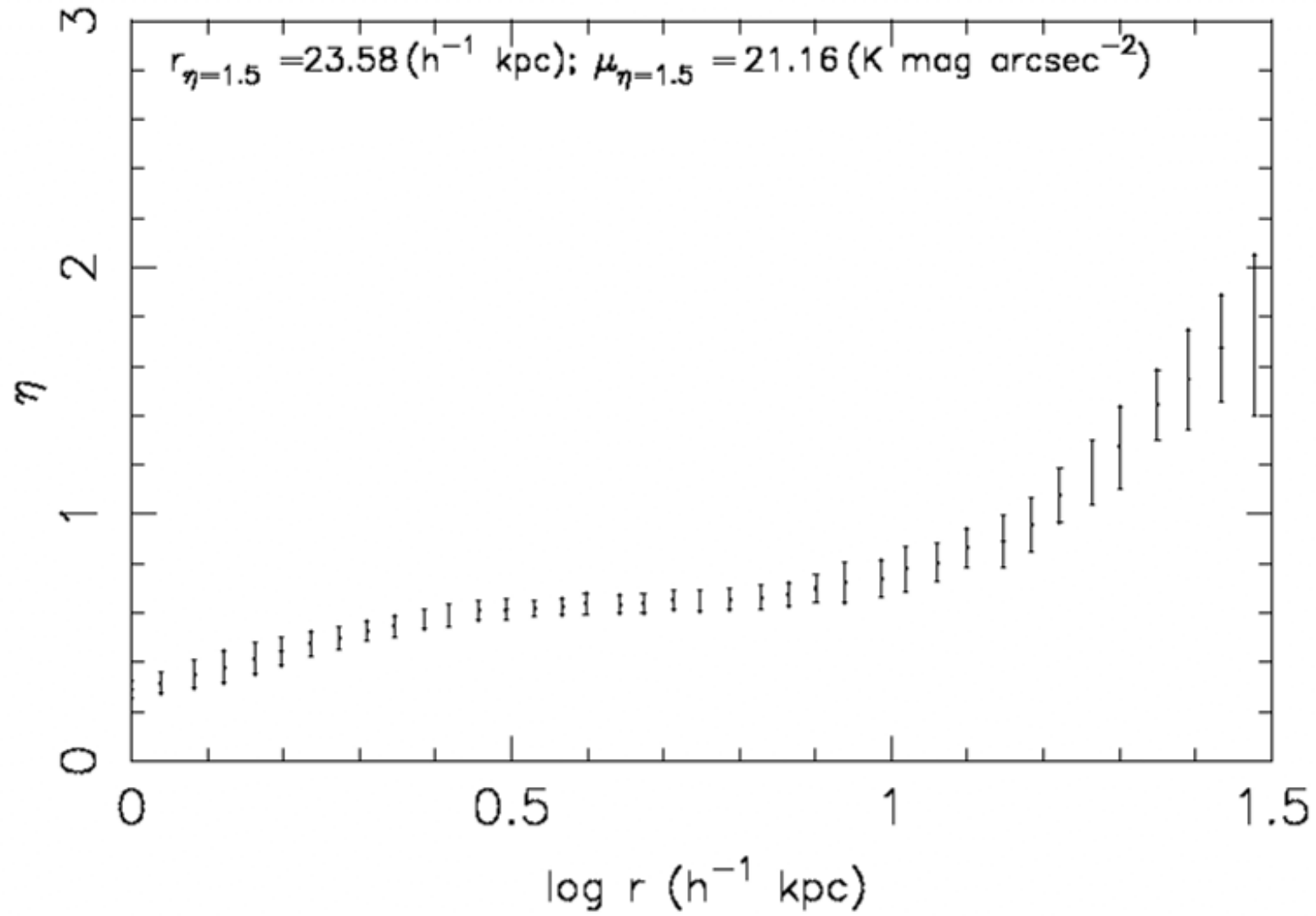
$$\eta(r) = \mu(r) - \langle \mu(r) \rangle$$

- No assumptions about underlying light distribution (c.f. Sersic, de Vaucouleurs)
- Relatively insensitive to zero-point & extinction correction errors

a566_r

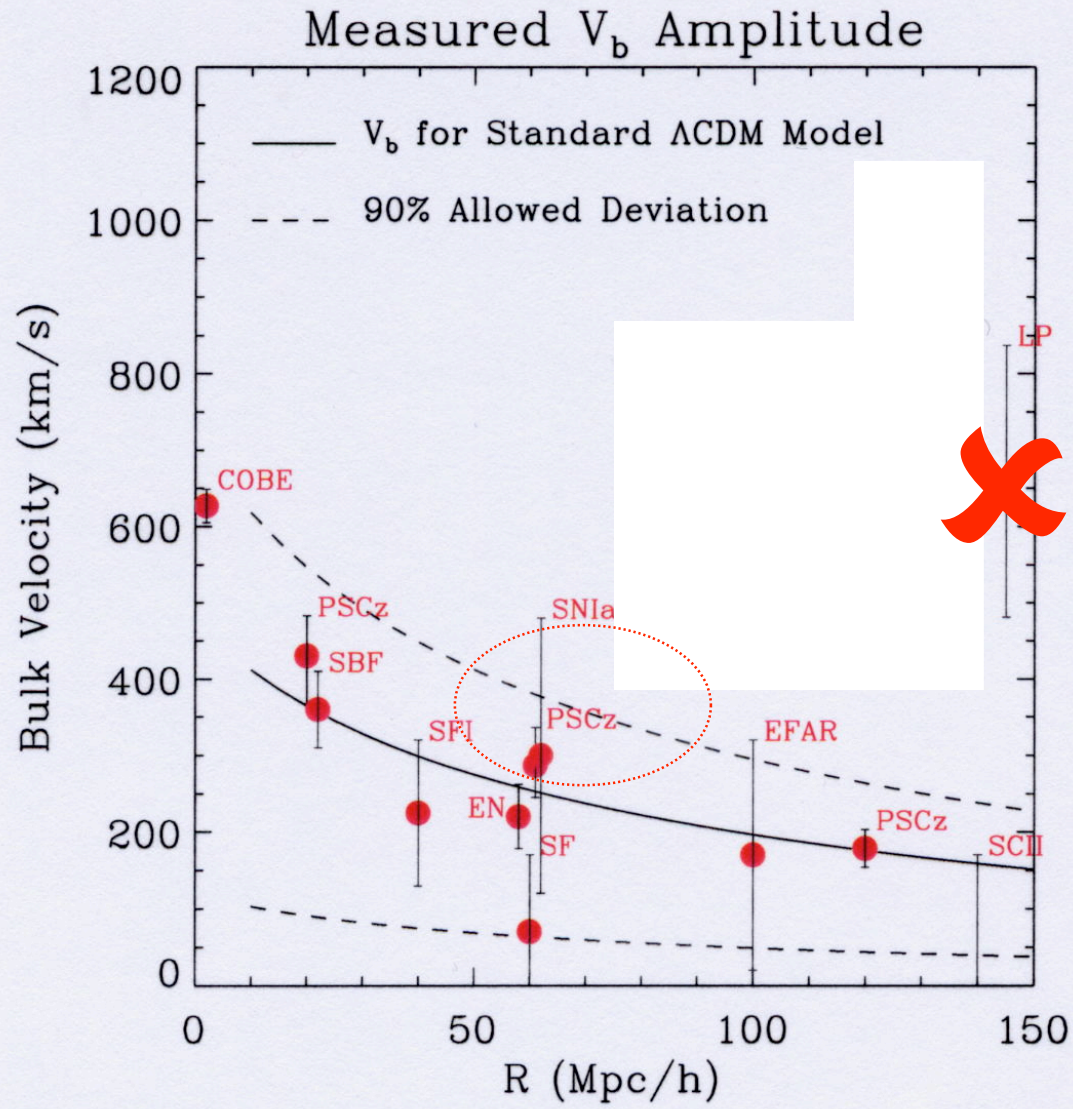


α1644_r



On Large Scales, Universe is
Homogeneous & Isotropic

...What is the Convergence Scale?



TBD!

Questions

the measure of the steepness of the luminosity function of galaxies at the tail end; (4) M_{ex} , the mean of the absolute magnitude of the statistical extremes, we shall instead use the parameter $b = M_{sp} - M_{ex}$, the difference in the means of the magnitudes of special galaxies and statistical brightest galaxies; and (4) d , the fraction of clusters that have a special galaxy.

$$b = M_{sp} - M_{ex} = -0.48 \text{ mag}, \quad (10)$$

$$a = 4.01, \quad (11)$$

$$d = 0.63. \quad (12)$$

Figure 2 shows the comparison of the data with the model (eq.

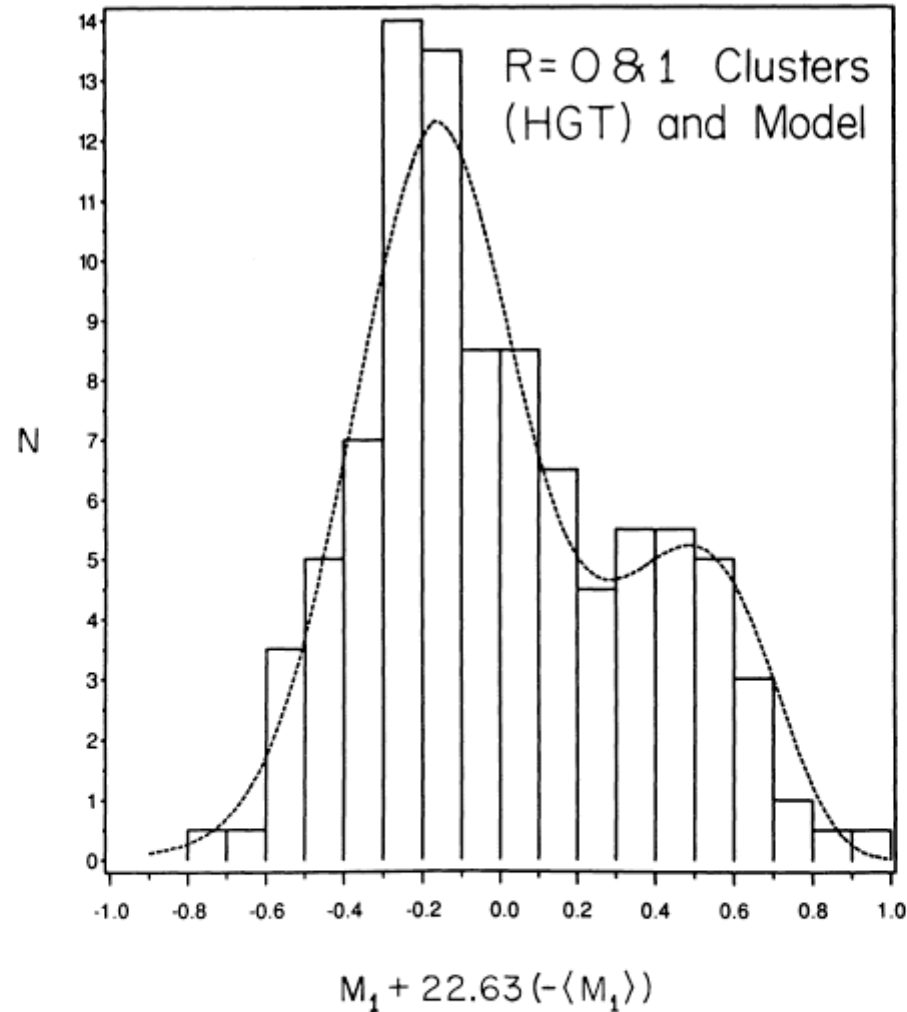
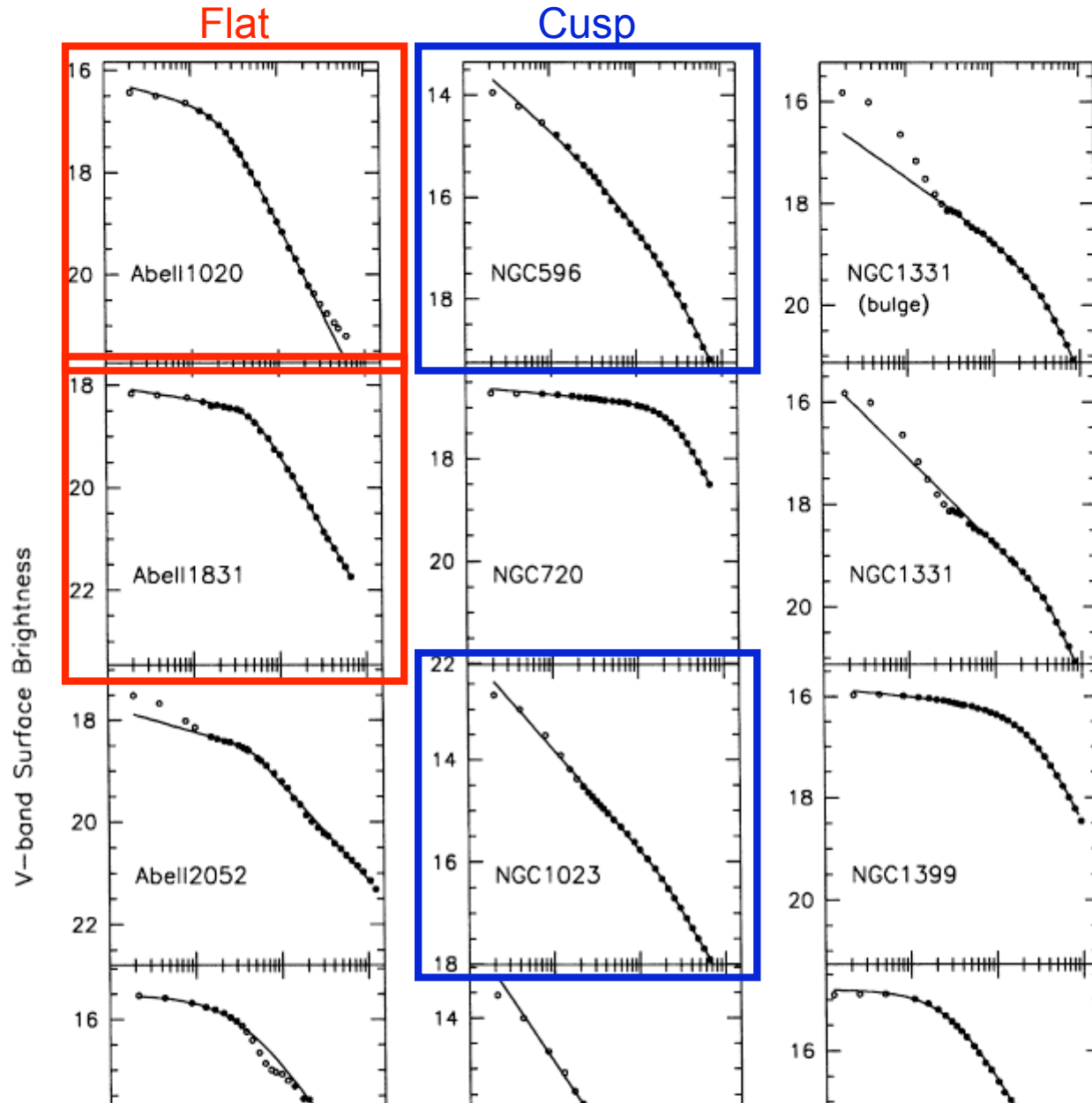
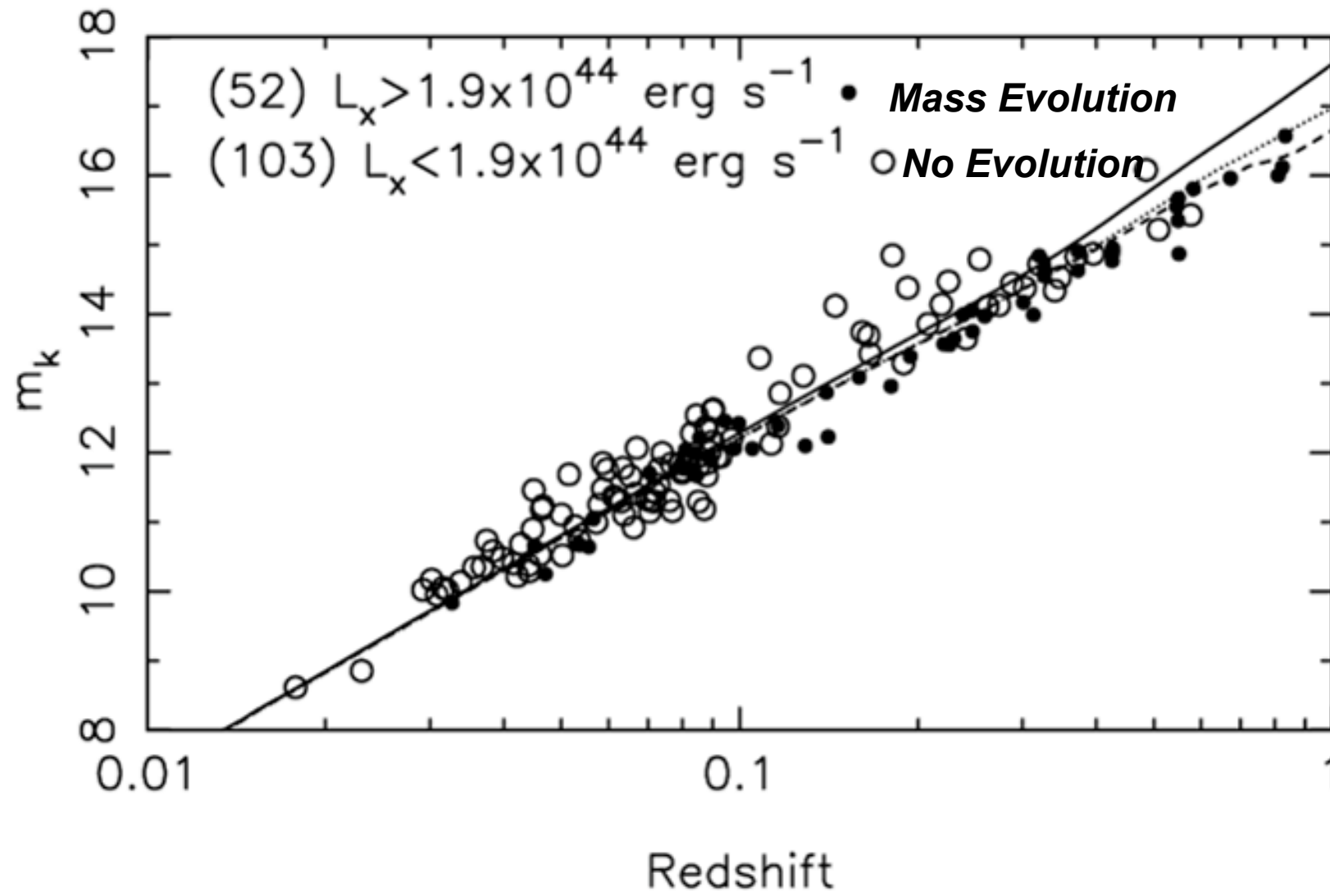


FIG. 2.—The same histogram of the data as shown in Fig. 1, compared to the model. The parameters in the model have not been evaluated to fit this particular histogram, but are determined by the maximum-likelihood method, using all 93 data points.





Conclusions/Summary: 1

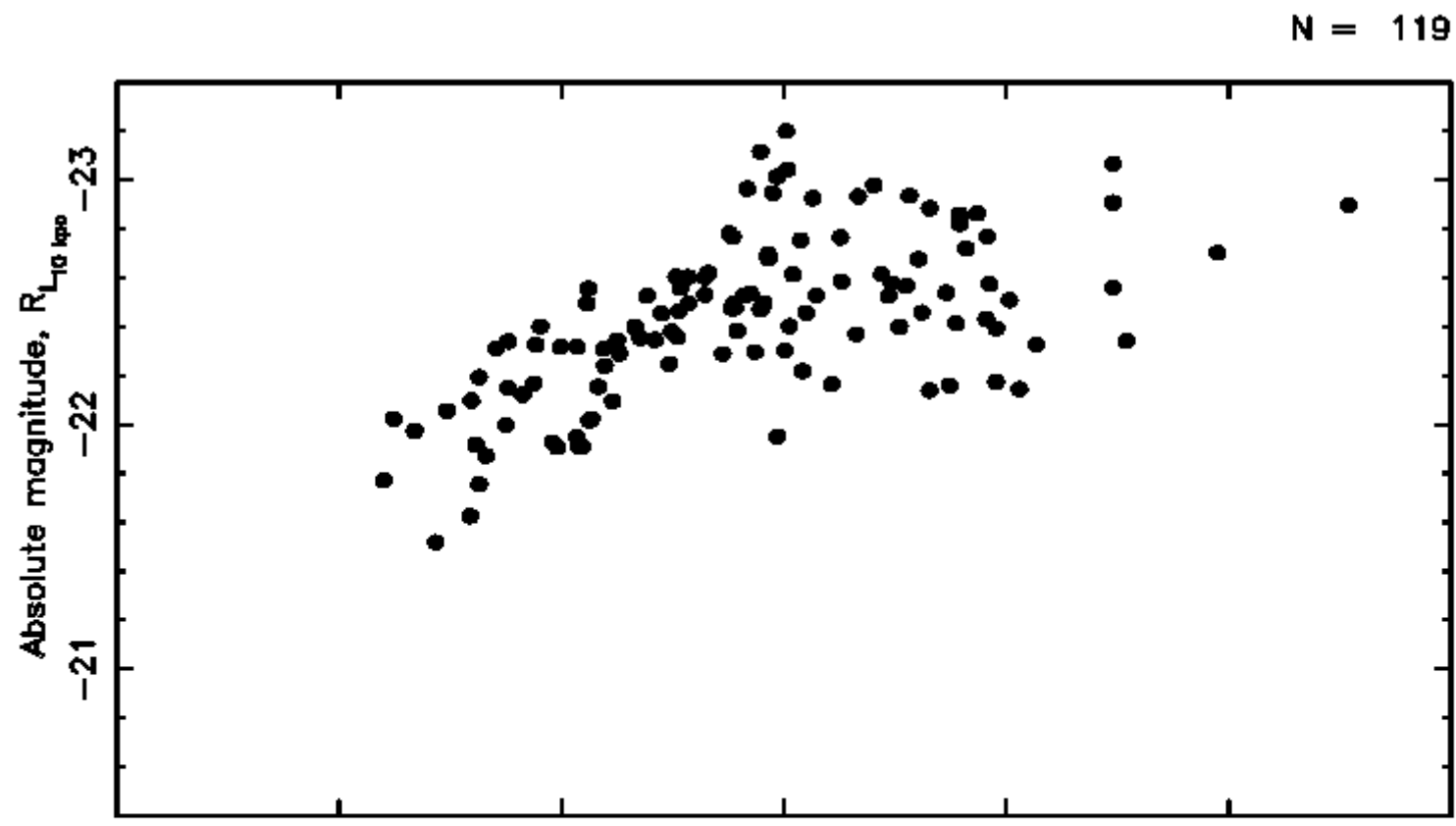
- X-ray selection avoids biases present in optically compiled samples, which can propagate to generate spurious cosmological results (e.g. large bulk flows, strong merger evolution).
- Giant cluster ellipticals exhibit a number of properties that indicate them to be physically distinct from other galaxies
- X-ray selection provides a major advantage over previous optical studies: ~30% of clusters found in optical samples yield alternative BCG candidates under our objective criteria
- This selection technique yields a population of BCG candidates which, on average, have higher (>0.5) values of structure parameter, α when compared to optically selected data sets.
- Huge (~150 Mpc) pieces of material do not appear to be speeding around the Universe at 600 km s⁻¹
- The Lauer & Postman (1994) signal arises due to biases introduced by low- α optical contaminant galaxies
- Consistent with all literature addressing the Lauer & Postman signal
- Perhaps the reliability of giant ellipticals as standard candles has been overstated

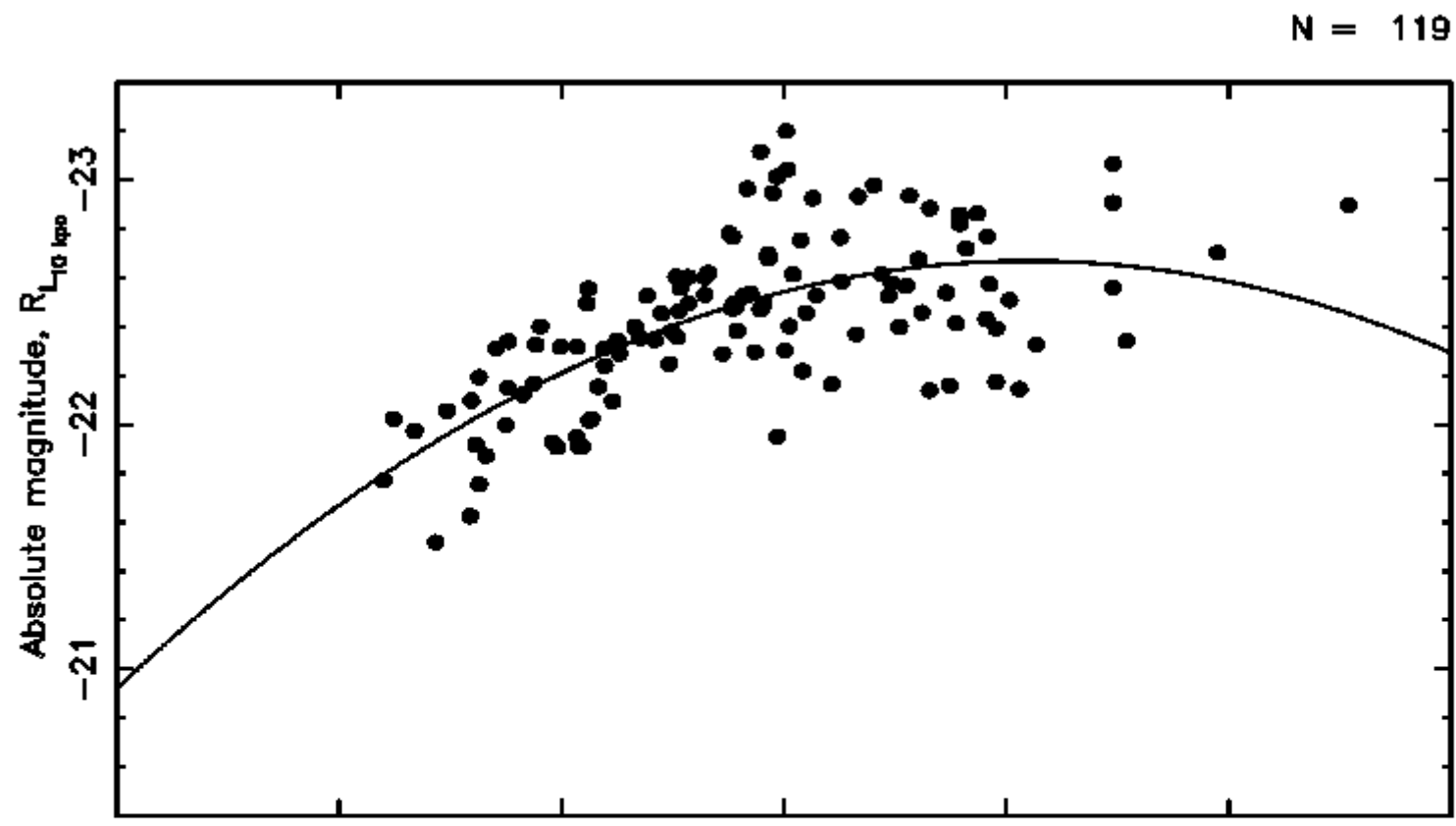
Conclusions/Summary: 2

- Evidence suggesting the underlying distribution of cluster giant ellipticals is bimodal (M , α , L_x)
- The properties of the modes are moderated by the location of the galaxy within the cluster, the depth of the gravitational potential & may reflect evolution
- Giant ellipticals in low- L_x (therefore low mass) clusters appear to evolve through a process of mergers, while those in more luminous clusters seem to be evolving passively
- Since they appear to respond to global cluster properties, evolution in the giant elliptical may reflect evolution of the cluster as a whole

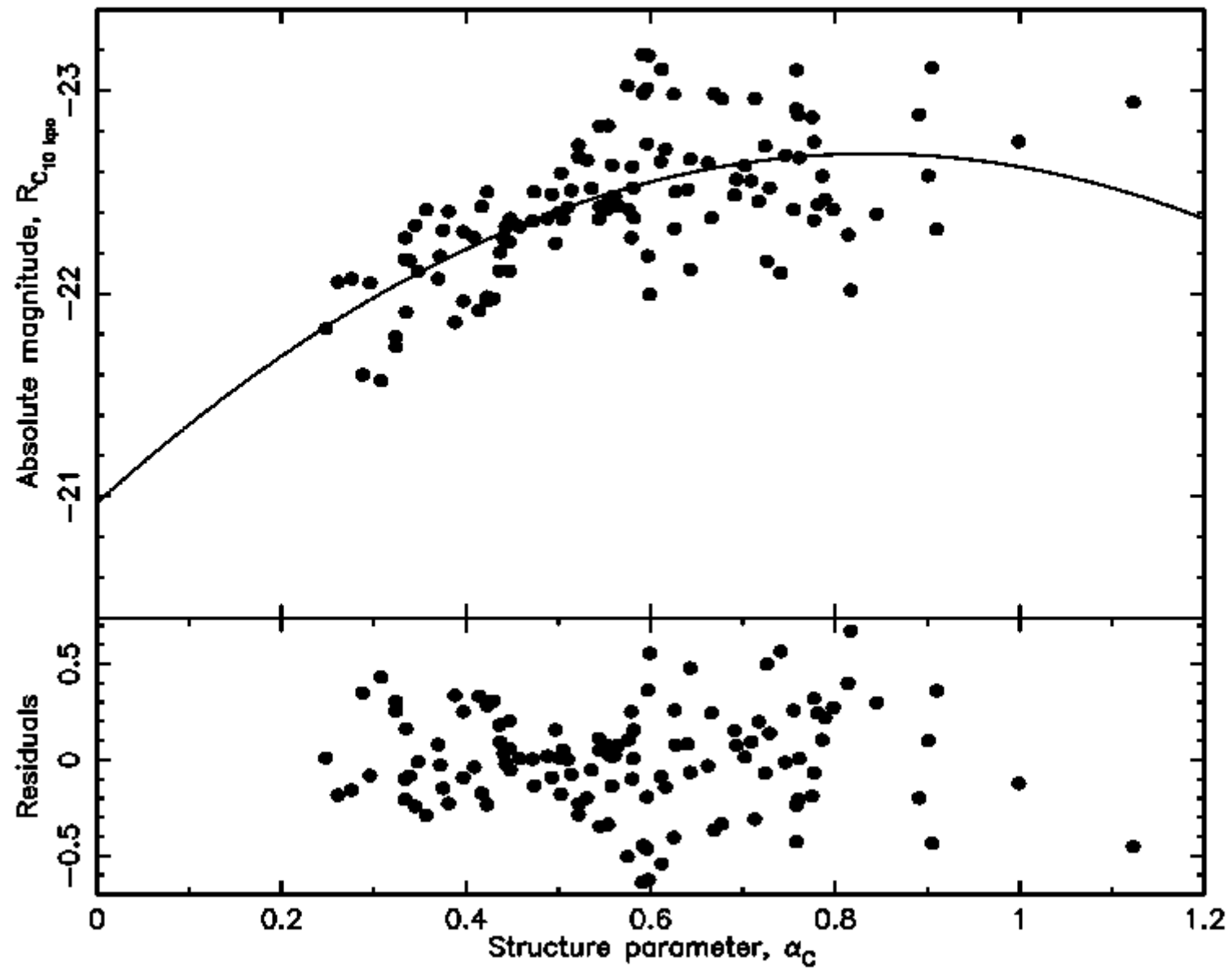
Further investigations

- Search for comparative ($z \sim 0.15$; $z \sim 0.30$; $z \sim 0.45$) evolutionary signals in Colour-Magnitude diagrams (CMD) of a well-defined sample of X-ray selected clusters
- Investigation of relationship between giant elliptical nuclear properties (multiplicity, cuspy versus flat core profiles) and location in cluster potential
- The dependence of diffuse cD halos on location of the giant elliptical

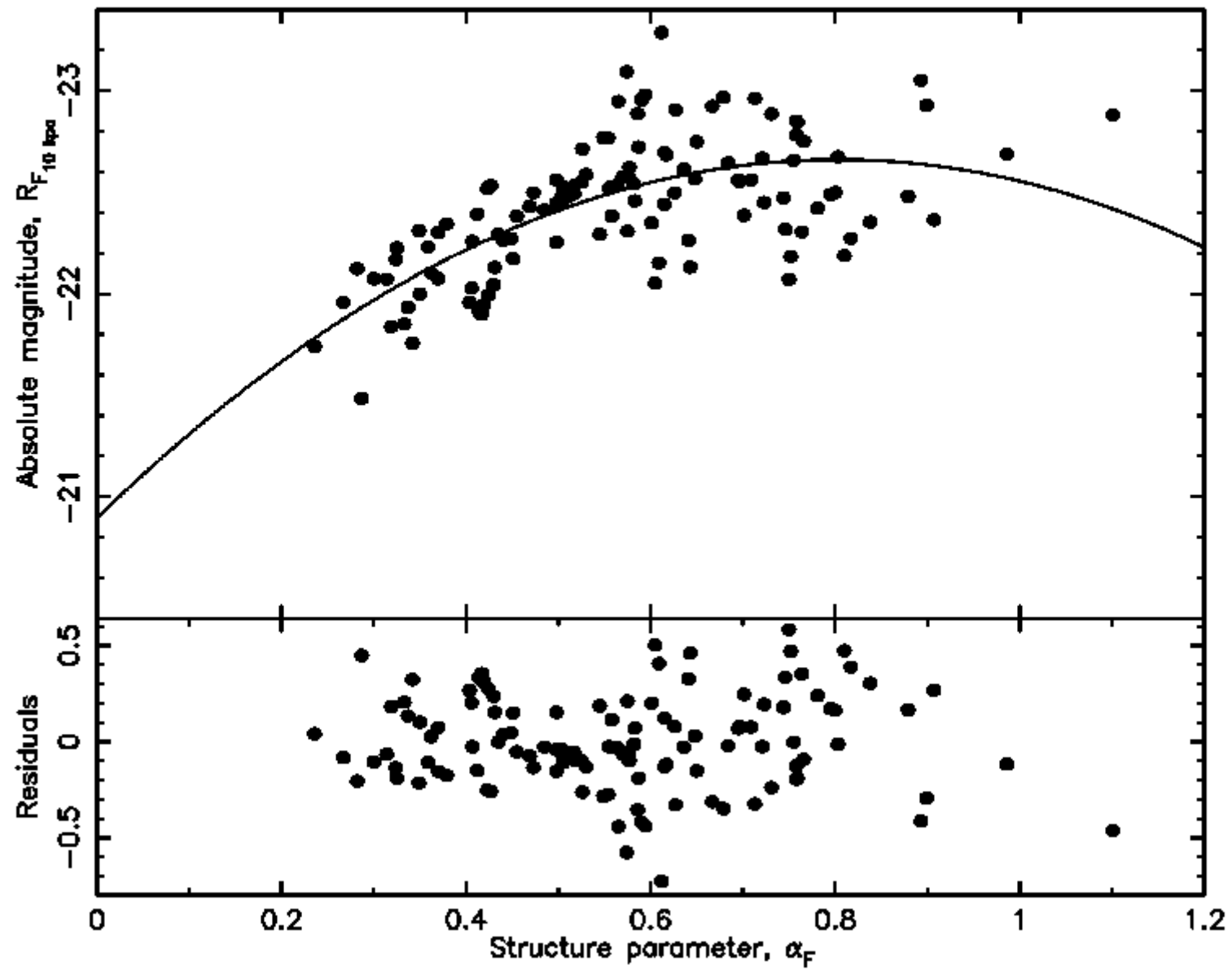




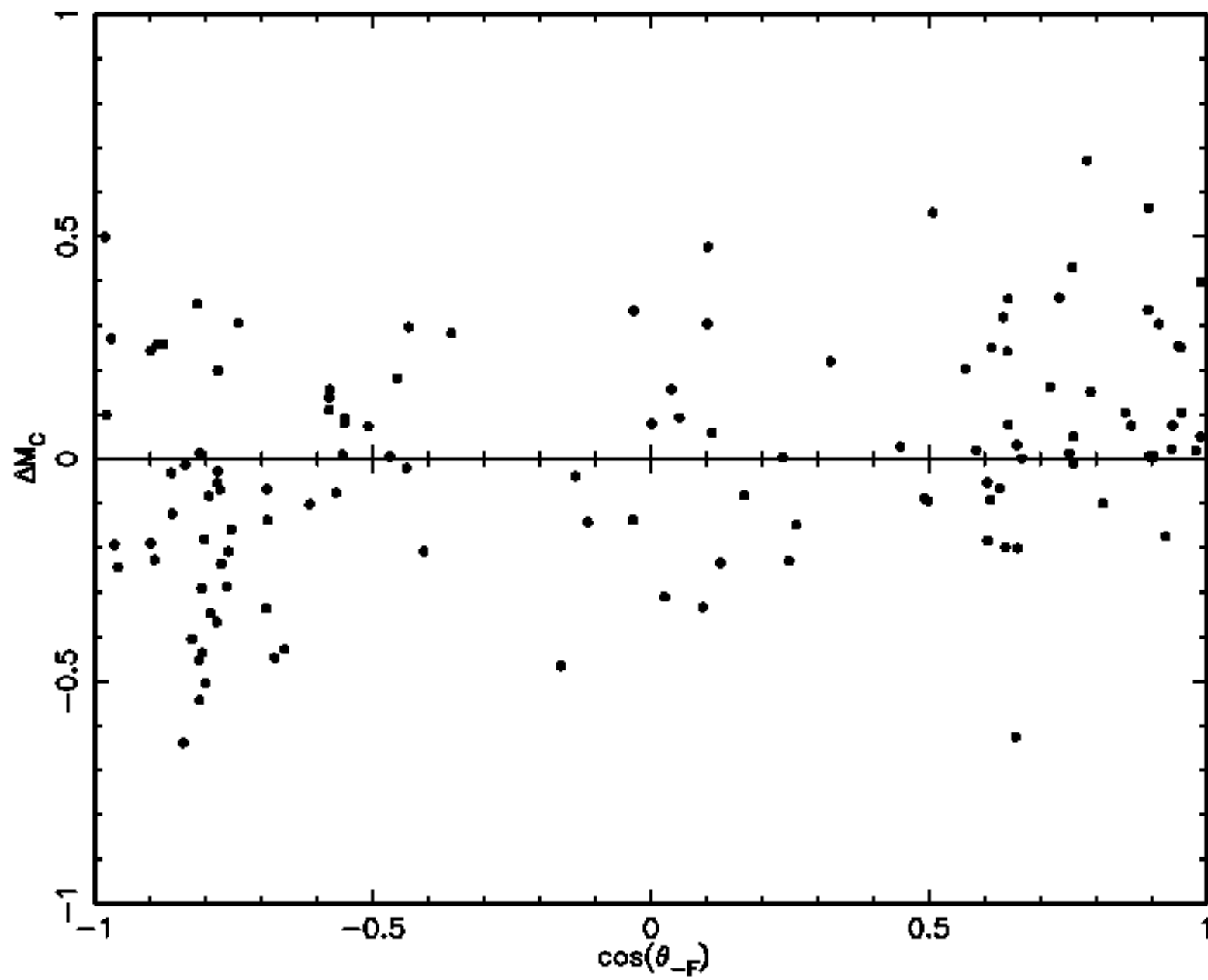
N = 119

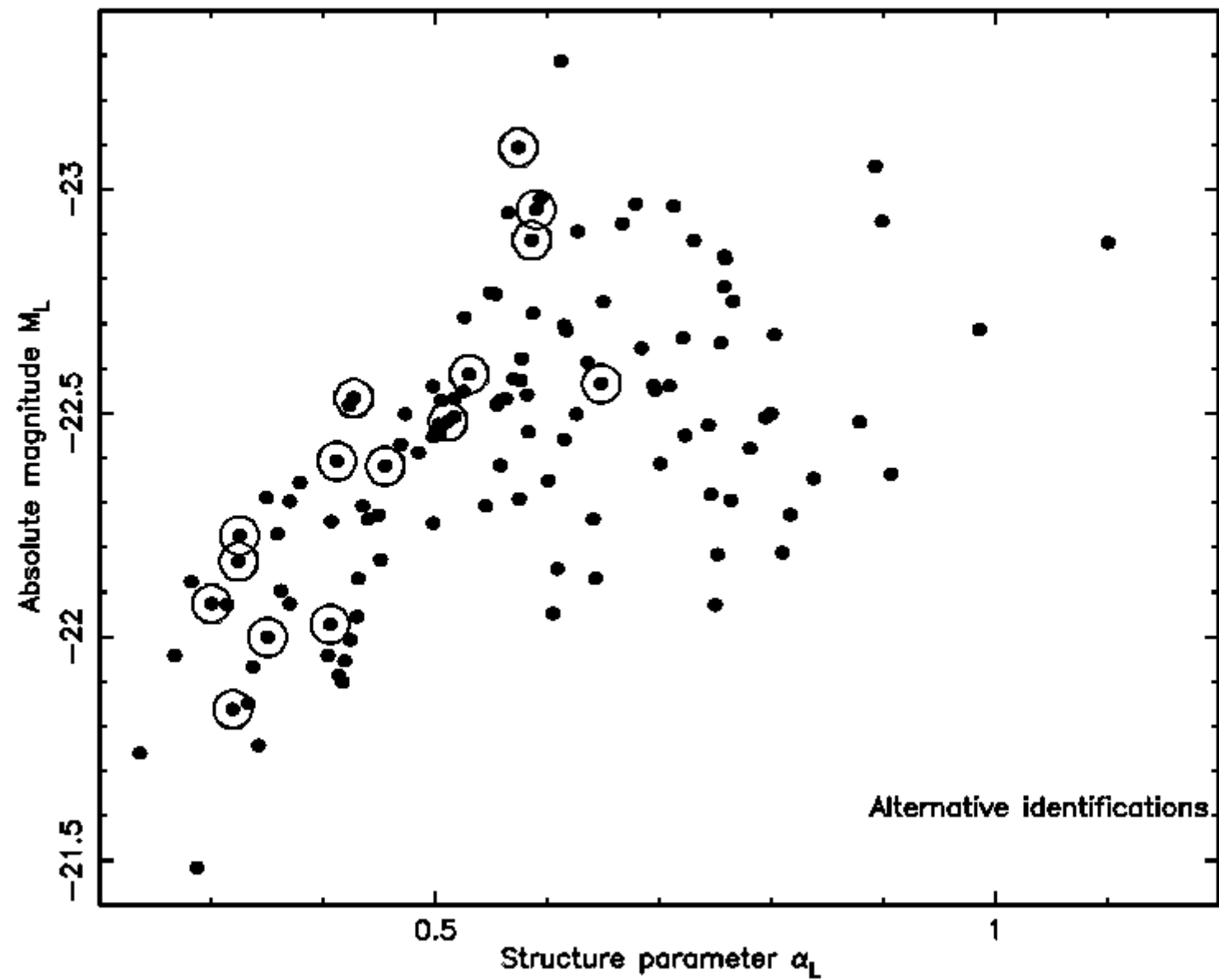


N = 119

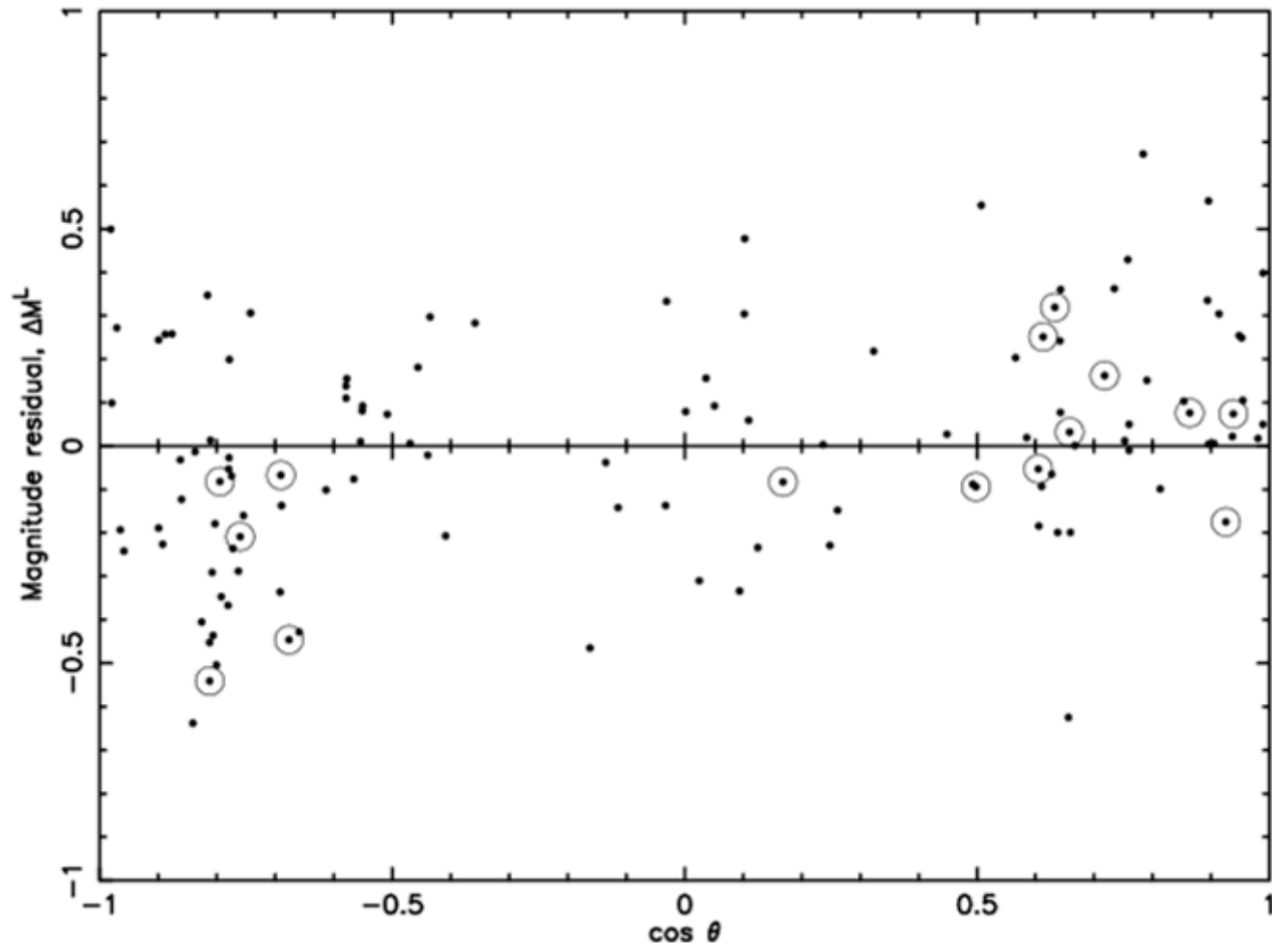


N = 119

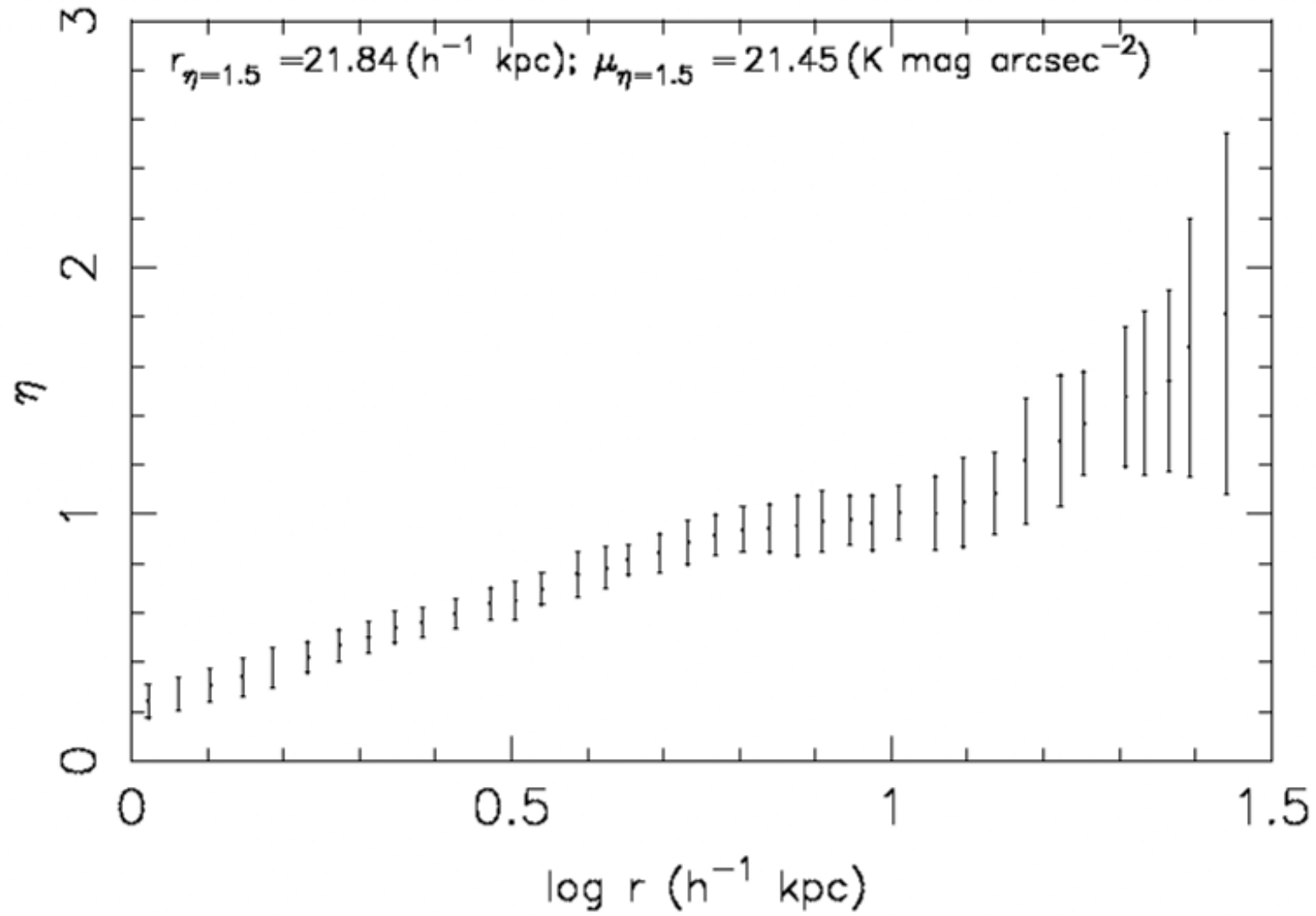




Photometric residuals as a function of position (LP94)



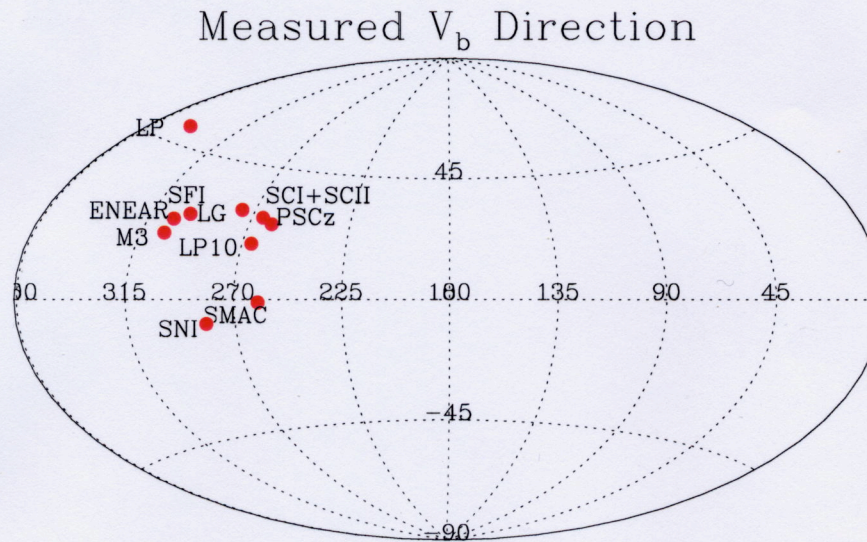
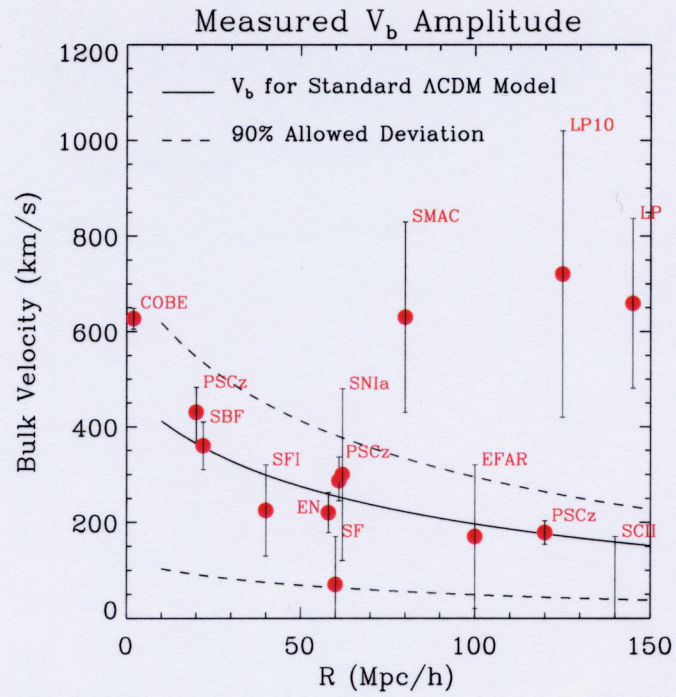
a644_r

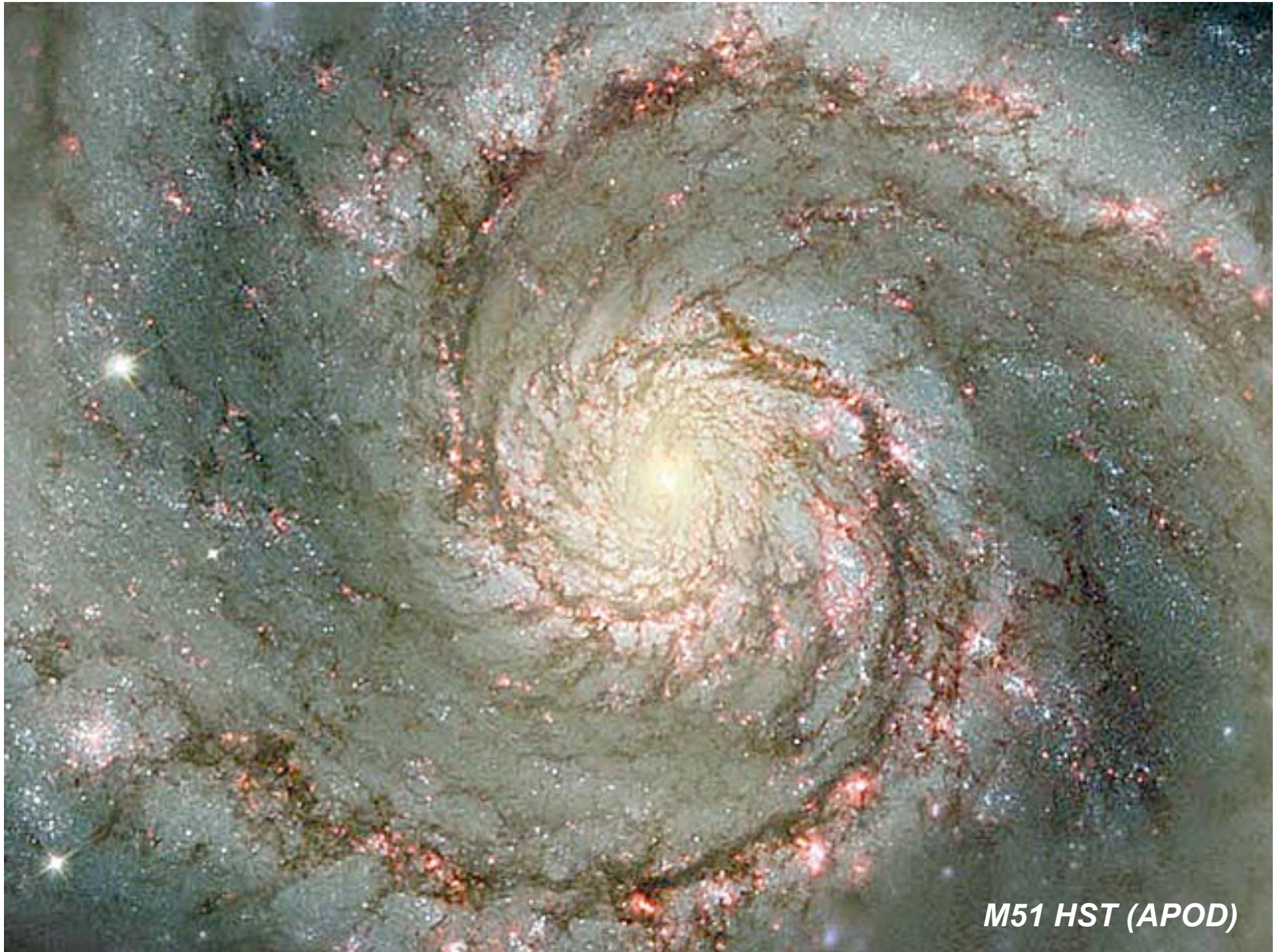


Evolution?

Questions

- Deep Imaging & detection of GCs in the environs of gEs at $z \leq 0.1$?
- IR studies?





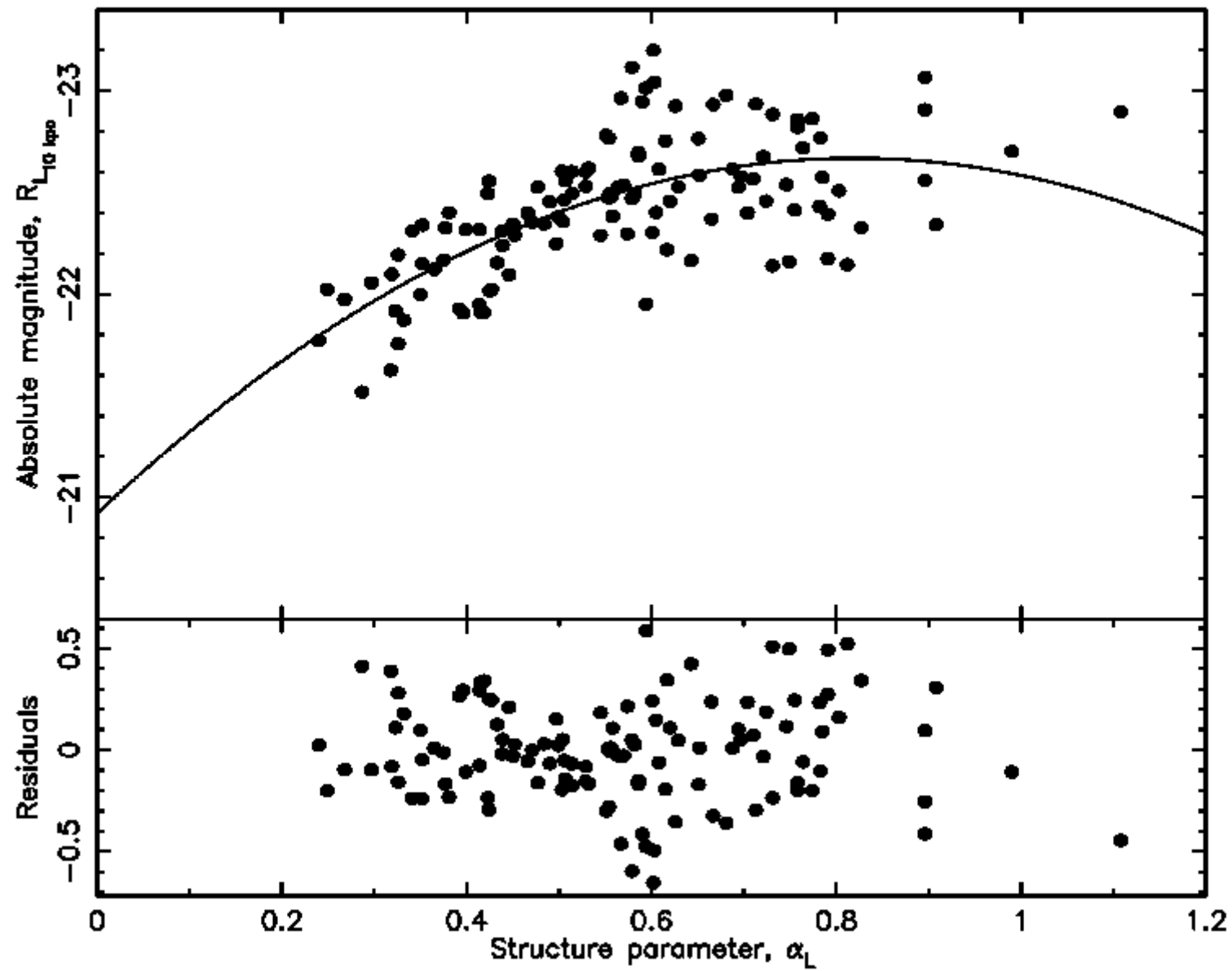
Properties of Giant Ellipticals: 1

- Most luminous objects emitting photospheric light
- $M_V \sim -23.5$ within ~ 10 kpc (c.f. $M_* \sim -20$).
- Depart from the tip of the Schechter LF. (Tremaine & Richstone 1997; Bernstein & Bhavsar 1980)
- $\sim 50\%$ exhibit diffuse envelopes extending upto ~ 1 Mpc (Hoessel & Schneider 1985)

Properties of Giant Ellipticals: 2

- Flatter profiles than de Vaucouleurs; larger r_e than “normal” ellipticals (Schombert 1986); Overluminous for their velocity dispersions (Malumuth & Kirschener 1981, 1985)
- Occupy distinct region on FP (Hoessel 1987, Schombert Oegerle & Hoessel 1991)

N = 119



Properties of Giant Ellipticals: 3

- Axial alignments with host cluster & LSS (Binggelli 1982, West 1994; Kim et al. 2002)
- Increased incidence (25-50%) of nuclear multiplicity (Geller & Beers 1988; Ryden et al. 1989)
- Small dispersion in absolute aperture magnitudes: r_e , σ , $\langle\mu\rangle_e \rightarrow 21\%$ (Oegerle & Hoessel 1991); $M-\alpha \rightarrow 17\%$ (Hoessel 1980; Lauer & Postman 1994; Collins & Mann 1997)

c.f. SN $\sim 16\%$

Misidentifications

N = 119

